STUDIES OF NOVEL GLYCINE-CONTAINING LIPIDS THAT DIFFER GREATLY IN TYPE 2 DIABETES

by

Autumn Brooke White

A thesis submitted in partial fulfillment
of the requirements for the degree

of

Master of Science

in

Biochemistry

MONTANA STATE UNIVERSITY
Bozeman, Montana

July 2014

©COPYRIGHT

by

Autumn Brooke White

2014

All Rights Reserved

TABLE OF CONTENTS

TABLE OF CONTENTS – CONTINUED

TABLE OF CONTENTS – CONTINUED

LIST OF TABLES

LIST OF FIGURES

Figure Page

LIST OF FIGURES – CONTINUED

Figure Page

LIST OF FIGURES – CONTINUED

Figure Page

GLOSSARY

^{1}H-NMR	Proton nuclear magnetic resonance
^{31}P-NMR	Phosphorus nuclear magnetic resonance
ACN	Acetonitrile
ADA	American Diabetes Association
AGE	Advance-glycation end products
AHA	American Heart Association
ALA	5-aminolevulinic acid
ALAS-1	Delta-aminolevulinate synthase 1
AQ	Aqueous
ATCUN	N-terminal copper and nickel binding motif
ATP	Adenosine triphosphate
BHT	Butylated hydroxytoluene
C15:0	Pentadecanoic acid
C16:0	Palmitic acid
CaH_2	Calcium hydride
CD_3OD	Deuterated methanol
CDC	Center for Disease Control
$CDCl_3$	Deuterated chloroform
CH_3I	Methyl iodide
$CHCl_3$	Chloroform
CID-MS/MS	Collision induced dissociation tandem mass spectrometry
D_2O	Deuterium oxide
DAD	Diode array detector
Dansyl-Cl	5-(dimethylamino)naphthalene-1-sulfonyl chloride
DCC	Dicyclohexylcarbodiimide
DCM	Dichloromethane
DCM2	Methanol depleted dichloromethane layer
DCU	Dicyclohexyl urea
DIA	Diisopropyl amine
DNS-gly	Dansyl-glycine
EI	Electron ionization
EDTA	Ethylenediaminetetraacetic acid
ESI	Electrospray ionization
eV	Electron volts
FA	Fatty acid
FA1-FA7	Fatty acid site 1 – Fatty acid site 7
FFA	Free fatty acids
F-HC	Fasting healthy control
FSH	Framingham Heart Study
F-T2D	Fasting Type 2 Diabetes
GCMS	Gas chromatography mass spectrometry
GCS	Glycine cleavage system

GLOSSARY CONTINUED

GLP-1	Glucagon-like peptide
GLUT-2	Glucose transporter-2
GSH	glutathione
H_3PO_4	Phosphoric acid
HbA_{1c}	Glycated hemoglobin
HC	Healthy control
HCl	Hydrochloric acid
HSA	Human serum albumin
IFG	Impaired fasting glucose
IGT	Impaired glucose tolerance
IPA	Isopropanol
IR	Insulin resistance
IS	Insulin sensitivity
K_2CO_3	Potassium carbonate
K_{ATP}	ATP sensitive potassium channel
KCl	Potassium chloride
KORA	Cooperative Health Research in the Region of Augsburg
LC-MS	Liquid chromatography mass spectrometry
LPC (18:2)	Lysophosphatidyl chloine 18:2
m/z	Mass-to-charge
MBS	Multiple-binding site
MEK	Methylethylketone
MeOH	Methanol
MetS	Metabolic syndrome
MS	Mass spectrometry
MS/MS	Tandem-mass spectrometry
MTHF	5,10-Methylenetetrahydrofolate
NADH	Nicotinamide adenine dinucleotide
NADPH	Nicotinamide adenine dinucleotide phosphate
NAGly	N-arachidonyl glycine
NaI	Sodium iodide
N-boc	N-(tert-butoxycarbonyl)
N-boc glycine	N-(tert-butoxycarbonyl)-L-glycine
NEFA	Non-esterified fatty acids
NF-HC	Non-fasting healthy control
N-Fmoc	9-Fluorenylmethoxycarbonyl
NGT	Normal glucose tolerance
NICI	Negative ion chemical ionization
NL	Neutral loss
NMR	Nuclear magnetic resonance
OAA	Oxaloacetate
OGTT	Oral glucose tolerance test

GLOSSARY CONTINUED

OS	Oxidative stress
PFB-Br	Pentafluorobenzyl bromide
PLP	Pyridoxal phosphate
Qtof	Quadrupole time-of-flight
RBC	Red blood cell
RBF	Round bottom flask
R_f	Retardation factor
RISC	Relationship between insulin sensitivity and cardiovascular disease
ROS	Reactive oxygen species
RP-HPLC	Reverse phase high pressure liquid chromatography
RT	Retention time
SHMT	Serine hydroxyl methyl transferase
$SOCl_2$	Thionyl chloride
TAG	Triacylglycerol
T2D	Type 2 Diabetes
TCA	Tricarboxylic acid
THF1	Tetrahydrofolate
THF2	Tetrahydrofuran
TLC	Thin-layer chromatography
α-HB	α-hydroxybutyrate

ABSTRACT

Type 2 Diabetes (T2D) is a growing problem that affects hundreds of millions of people. This work focused on understanding the pathogenesis of T2D by studying novel glycine-containing lipids found greatly changed in T2D with glycine linked via the carboxyl end to a hydrophobic moiety (Bowden, 2011). Different forms of these novel lipids were found in fasting Type 2 Diabetes (F-T2D), fasting healthy control (F-HC), and non-fasting healthy control (NF-HC) plasma by separation on Reverse Phase-High Performance Liquid Chromatography (RP-HPLC). The ratio in F-T2D/F-HC differed by approximately fifty-fold, but both were present in NF-HC plasma, along with several additional forms with different RP retention. We isolated compounds of interest from the plasma from NF-HC volunteers and pooled enough plasma in hopes for structural elucidation using Nuclear Magnetic Resonance (NMR). Since these compounds were found to be carried by Human Serum Albumin (HSA), HSA was purified from human plasma. A 2:1 Dichloromethane (DCM):Methanol (MeOH) modified Folch-extraction (Folch, 1957) was used to extract the hydrophobic metabolites from HSA. The lipid mixture was separated by RP-HPLC and a small portion of each fraction was derivatized by pentafluorobenzyl-bromide (PFB-Br) and analyzed by LC-MS. A portion of each underivatized fraction, based on the results of the PFB-Br reaction, was analyzed by LC-MS. Each prominent peak was fragmented using collision-induced dissociation tandem mass spectrometry (CID-MS/MS). Peaks of the most interest showed neutral loss masses corresponding to glycine and phosphate. This evidence led to the hypothesis that the glycine moiety is attached to a phosphate via a mixed acyl-phospho anhydride linkage. This linkage is thought to be consistent with the rapid hydrolysis of the compounds of interest under mild conditions during sample preparation. Compounds were synthesized that could be followed in the HSA work-up procedure to determine the stability of the anhydride linkages at different steps of the work-up. It is also possible that the linkage could be a mixed-acyl anhydride and this linkage was also synthesized and studied by mass spectrometry (MS) and CID-MS/MS. Understanding these structures could provide new insights into the mechanisms of T2D and perhaps lead to enhanced prevention and treatment.

INTRODUCTION

Type 2 Diabetes

This work centers on T2D, which is a major problem affecting increasing numbers of people. According to the American Diabetes Association (ADA), T2D is described as a condition in which blood glucose levels are excessively high (hyperglycemia). This results either from cells not responding to the insulin being supplied or from the pancreas not producing enough insulin (ADA, http://www.diabetes.org/diabetes-basics/diagnosis). As the pathogenesis of T2D develops, the glucose ingested through the diet cannot get into the cells and the excessive blood glucose level is toxic (ADA, http://www.diabetes.org/diabetes-basics/diagnosis). Prolonged exposure of higher than normal plasma glucose levels will cause the glucose to undergo a reaction with proteins in the body to form advanced glycation end-products (AGE) (Ansari and Dash, 2013) (Goldin, *et al.,* 2006), that contribute to cardiovascular disease (Goldin, *et al.,* 2006) (Anguizola, *et al.,* 2013), liver damage, and blindness (Anguizola, *et al.,* 2013).

Metabolic Syndrome is a Precursor to Type 2 Diabetes

The word "Syndrome" is defined as a pattern of symptoms that characterize or indicate a particular health condition. In the specific example in this thesis, reference is made to metabolic syndrome (MetS). In order to be diagnosed as having MetS, one must have at least three symptoms listed in Table 1.1 occur at the same time

(AHA,http://www.heart.org/HEARTORG/Conditions/More/MetabolicSyndrome/About-Metabolic-Syndrome_UCM_301920_Article.jsp) (Kahn, 2005) (Table 1.1).

Table 1.1. Risk Factors for Metabolic Syndrome. List of risk factors that, if at least three occur together define metabolic syndrome, and can raise a person's risk of becoming Type 2 Diabetic. (American Heart Association)

Risk Factors for Metabolic Syndrome
Abdominal obesity
Triglyceride levels of 150 mg/dL or greater
HDL cholesterol less than 40 mg/dL in men or less than 50 mg/dL in women
Systolic blood pressure of 130 mmHg or greater
Diastolic blood pressure of 85 mmHg or greater
Fasting glucose of 100 mg/dL or greater
Insulin resistance or glucose intolerance

Prevalence and Demographics

The number of persons afflicted with T2D is predicted to be 366 million in 2030 while there were approximately 171 million afflicted with this disease in 2000 (Brunton, 2008). In the years of 2010 and 2012, 25.8 and 29.1 million persons in America were afflicted with T2D (ADA, American Diabetes Association, http://www.diabetes.org/diabetes-basics/statistics/). The Center for Disease Control (CDC) reported a rising trend of the number of new cases of U.S. adults diagnosed with T2D (CDC, as shown in Figure 1.1.

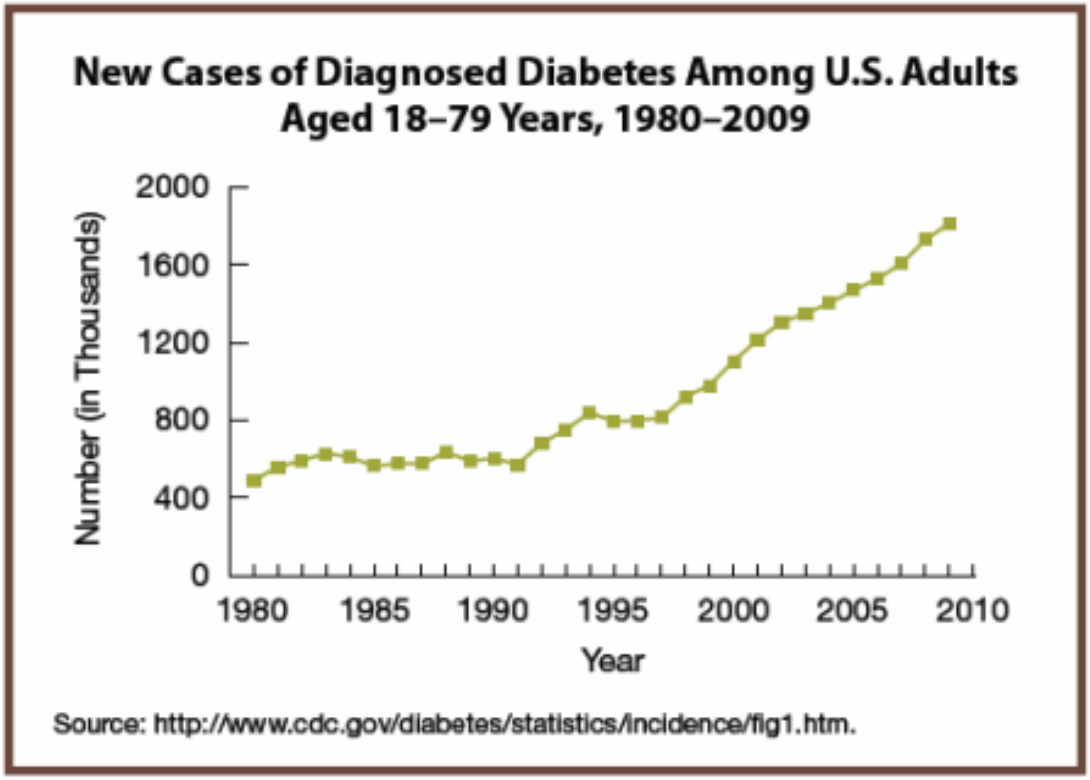

Figure 1.1. New cases of U.S. Adults diagnosed with T2D each year over a 29 year span. This shows that the number of new cases was relatively level early on but as the years progressed it has shown an increase each year.

Type 2 Diabetes and
Body Weight Association

It is a widely believed myth that if people are overweight they will eventually develop diabetes and people who are at a healthy weight do not develop diabetes (ADA, http://www.diabetes.org/diabetes-basics/myths/). Being overweight is actually a rather low risk factor for developing diabetes. Risk factors estimate the likelihood of one developing a specific condition but as the word "risk" implies is not definite that the specific condition will develop. Many overweight people never become diagnosed with

T2D and many people with a healthy weight develop T2D. (ADA, http://www.diabetes.org/diabetes-basics/myths/)

Impaired Glucose Tolerance

Impaired glucose tolerance (IGT) is considered to be a pre-diabetic state, where people are beginning to be insulin resistant. An oral glucose tolerance test (OGTT) may be performed to determine if a person has an impaired tolerance to glucose. It is not a commonly used test at this time, but is considered the gold standard for diagnosing IGT and T2D. However, the OGTT is routinely used to diagnose gestational diabetes. In order to undergo a proper OGTT, the patient should first fast overnight. Blood is first drawn to measure the baseline level of fasting glucose. They are then asked to drink 75 g of glucose dissolved in water. After a 2-hr time period, blood will again be drawn to determine the concentration of glucose. If blood glucose levels after the 2-hr time period are less than 200 mg/dL, but greater than or equal to 140 mg/dL, they are categorized as being IGT (Nathan *et al*., 2007) and are considered to be pre-diabetic. It is not until OGTT levels are greater than or equal to 200 mg/dL that they are highly glucose intolerant and are diagnosed to have T2D. When a person is considered to be IGT the underlying problem is that the cells are not responding to the insulin being supplied by the β-cells of the pancreas, which is described as insulin resistance (IR). To compensate for the increasing concentrations of glucose, the β-cells tend to secrete more insulin to the point where the β-cells can undergo dysfunction and stop secreting insulin altogether. (Weir and Bonner-Weir, 2004)

Compounds Relating to Insulin Resistance

Non-esterified Fatty Acids. The metabolism of ingested tri-acyl glycerols (TAG) is controlled by insulin (Sparks and Sparks, 1994). When a person ingests glucose, insulin levels rise, and lipolysis (mobilization of fatty acids from triglycerides) is suppressed (Burns, *et al*,. 1979). The body tries to reduce blood sugar levels after a glucose load is ingested. The body may be able to store some glucose as glycogen, but most of a large glucose load is converted directly to fat. There is need to utilize as much sugar as possible, rather than utilizing fat stored in adipose tissue upon a glucose load. Most body cells prefer to burn fat at all times, if there is sufficient oxygen available.

When a person goes into a fasting state, insulin levels are low and lipolysis occurs to generate plasma non-esterified fatty acids (NEFA) that may be used to obtain energy from respiration. High insulin drives conversion of glucose to fat, low insulin favors lipolysis. After ingestion, TAG are broken down into NEFA for absorption and then are re-esterified to TAG for transport (Sparks and Sparks, 1994) (Donnelly, *et al*., 2005) and storage in the liver and adipose tissue (Donnelly, *et al*., 2005). However, insulin resistance is associated with dysregulation of lipid metabolism and increased levels of NEFA (Raal, 2009). The adipocytes can also become resistant to insulin and are less able to trap NEFA and prevent lipolysis from occurring (Raal, 2009).

Biomarkers. There has been a great deal of research seeking biomarkers for specific diseases and the work most relevant to T2D will be outlined below. Gall, *et al*., (2010), reported α-hydroxybutyrate (α-HB) to be an early biomarker of IR. The study

included a cohort of 399 non-diabetic subjects, with a gradation of fasting glucose, and insulin resistance, in order to determine biochemical correlates (Gall, *et al.,* 2010). Low plasma glycine was the only metabolite found to predict the development of T2D seven years ahead (Wang-Sattler, *et al.,* 2012). Newgard and coworkers (2009, 2012) have reported elevation in branched-chain amino acids correlating with the development of IR. Participants in the Framingham Heart Study (FSH) were followed to determine biomarkers strongly associated with T2D. The study found that 2-aminoadipic acid (2-AAA) indicated an increased risk of future T2D, 12 years prior to the onset (Wang, *et al*., 2013a).

Insulin Secretion and β-cell Dysfunction

At the early stages of IR, the β-cells can compensate by releasing more insulin (Weir and Bonner-Weir, 2004). Impaired Fasting Glucose (IFG), is another type of pre-diabetes being an intermediary stage between normal glucose tolerance (NGT) and T2D (Heianza, *et al.* 2012). IGT and IFG can last for many years before the onset of T2D (Nathan, *et al.,* 2007). IFG is defined as having a higher than normal level of glucose while fasting. When one is diagnosed as having IGT or IFG, they are in an IR state (Nathan, *et al.,* 2007). Regardless of whether a person is IFG or IGT, these states can eventually lead to T2D (Nathan, *et al.,* 2007).

As IR progresses, the β-cells can undergo dysfunction (losing the ability to sufficiently secrete insulin) and hyperglycemia becomes higher (Weir and Bonner-Weir, 2004). As IR and β-cell dysfunction further increases in severity, hyperglycemia escalates, and leads to the development of T2D (Weir and Bonner-Weir, 2004).

Current Methods of Diagnosing Type 2 Diabetes

The pre-diabetic status, IGT, is currently best diagnosed by the OGTT test (Nathan, *et al*., 2007). In order to confirm a person to be of a pre-diabetic state of IGT, their levels of glucose after the 2-hr OGTT test must be greater than or equal to 140 mg/dL and less than 200 mg/dL (Nathan, *et al*., 2007), however, the value greater than 200 mg/dL is diagnostic for T2D. In order to test for IFG, one must undergo a blood sugar test after having fasted overnight. A blood sample is taken from the patient and the glucose level is determined. If the fasting glucose level is below 100 mg/dL, than the fasting glucose levels are considered normal (ADA, http://www.diabetes.org/diabetes-basics/diagnosis/). However, if the levels are higher than 100 mg/dL, but lower than 126 mg/dL, this is indicative of IFG (Nathan, *et al*., 2007) (ADA,). If it is 126 mg/dL or above, than the patient should undergo the OGTT to confirm T2D (Nathan, et al., 2007) (ADA, http://www.diabetes.org/diabetes-basics/diagnosis/).

Another method for detecting suspected T2D is determining the levels of glycated hemoglobin (HbA_{1c}), (Mayo Clinic, http://www.mayoclinic.org/tests-procedures/a1c-test/basics/definition/prc-20012585). When prolonged hyperglycemia has developed, glucose forms AGE products with all proteins (Goldin, *et al.,* 2006). These AGE products are typically measured of the glycated hemoglobin, since it is an abundant protein. This test reflects ones average glucose levels over the past 2-3 months (ADA, http://www.diabetes.org/living-with-diabetes/treatment-and-care/blood-glucose-control/a1c/). Two HbA_{1c} tests are performed on separate occasions, and if the value of glycated hemoglobin is over 6.5%, the results indicate T2D (Mayo Clinic,

http://www.mayoclinic.org/diseases-conditions/type-2-diabetes/basics/tests-diagnosis/con-20031902).

Human Serum Albumin

Primary Structure and Function

HSA is the most abundant protein found in the plasma and occurs at a concentration near 45 mg/mL (Ascenzi, *et al*., 2006). HSA contains 585 amino acids with 17 disulfides (Fujiwara and Amisaki, 2011), is synthesized in the liver (Quinlan, *et al*., 2005), and contains a primary structure of α-helical chains separated by random coils. The primary purpose of HSA is to transport fatty acids, hydrophobic compounds, and metal ions in the plasma (Sadler and Viles, 1995). Figure 1.2 shows that seven fatty acid (FA) binding sites on HSA have been identified, labeled FA1 – FA7. Each site has the ability to bind a fatty acid (Fasano, et al., 2005). Although there are seven FA sites, under normal physiological conditions, HSA carries on average two FA at a time (Chuang and Otagiri, 2002). However, HSA is responsible for binding other hydrophobic molecules at or near these sites (Fasano, *et al*., 2005).

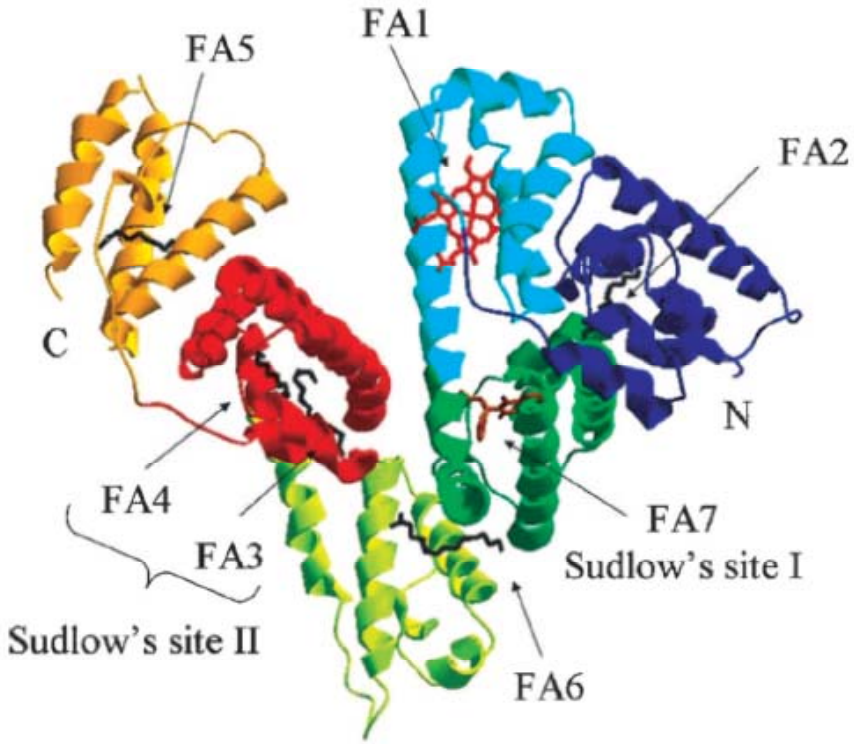

Figure 1.2. X-ray crystal structure of Human Serum Albumin (HSA). Each fatty acid binding site is labeled FA1-FA7, and is complexed with a fatty acid. The heme binding site is shown occupied in FA1. Sudlow's site II is in the location of FA3 and 4 and Sudlow's site I overlap with FA7. (Fasano, *et al*., 2005)

The alpha-helices of HSA fold together into three domains, I, II, and III (Sugio, *et al*., 1999). Each of these domains is homologous in structure and contains 10 helices. These 10 helices are further divided into six helical, anti-parallel, and four helical anti-parallel sub-domains known as A and B, that are connected by extended loops (Sugio, *et al*., 1999).

Compounds that Bind to
Human Serum Albumin

The two main binding sites are known as Sudlow's site I and II (Mandula, *et al*., 2006) (Sudlow, *et al*., 1975) (Sudlow, *et al*., 1976). Sudlow's site I overlaps fatty acid

binding site 7, FA7, located in sub-domain IIA. Sudlow's site II is also known as the Warfarin binding site. (Mandula, *et al*., 2006) (Dockal, *et al*., 2000). Warfarin is an anti-coagulant (Hirsh, *et al*., 2003) and is a commonly used drug. Site I also binds bulky heterocyclic anions such as salicylates, insulin-raising drugs (sulfonamides), and other drugs (Dockal, *et al*., 2000). Sudlow's site II, located in sub-domain 3A, overlap FA3 and FA4, and mainly binds aromatic carboxylates, including: thyroxin, ibuprofen, and the Benzodiazepines (Dockal, et al., 2000).When purified HSA was first crystallized, Kendall concluded that it was associated with free fatty acids (FFA) (Kendall, 1941). Later it was found that bound FFA help to stabilize the protein and protect it from denaturation (Spector, 1975). Each fatty acid binding site has positively charged amino acids inside of the binding pocket that bind to the negatively charge carboxylate group of the FA. The binding pocket is lined with hydrophobic residues to stabilize the alkyl chain of the FA (Choi, *et al*., 2002). As chain length increases, the affinity for binding increases, due to the hydrophobic interactions (Choi, *et al*., 2002). Most of the total binding energy of the FA with HSA comes from the hydrophobic interactions with the alkyl chain (Spector, 1975).

When red blood cells (RBC) get old, the hemoglobin is broken down into individual amino acids and the heme moiety is converted into biliverdin by heme oxygenase and then into bilirubin by biliverdin reductase (Stec, *et al.,* 2012). Bilirubin is transported to the liver by HSA to become conjugated and excreted in the bile (Stec, *et al.,* 2012). Figure 1.3 shows the crystal structure of HSA complexed with bilirubin. HSA plays a vital role in bilirubin excretion, and there are dire consequences if bilirubin

homeostasis is disturbed, since bilirubin is a toxic product of heme catabolism (Weisiger, *et al.,* 2001).

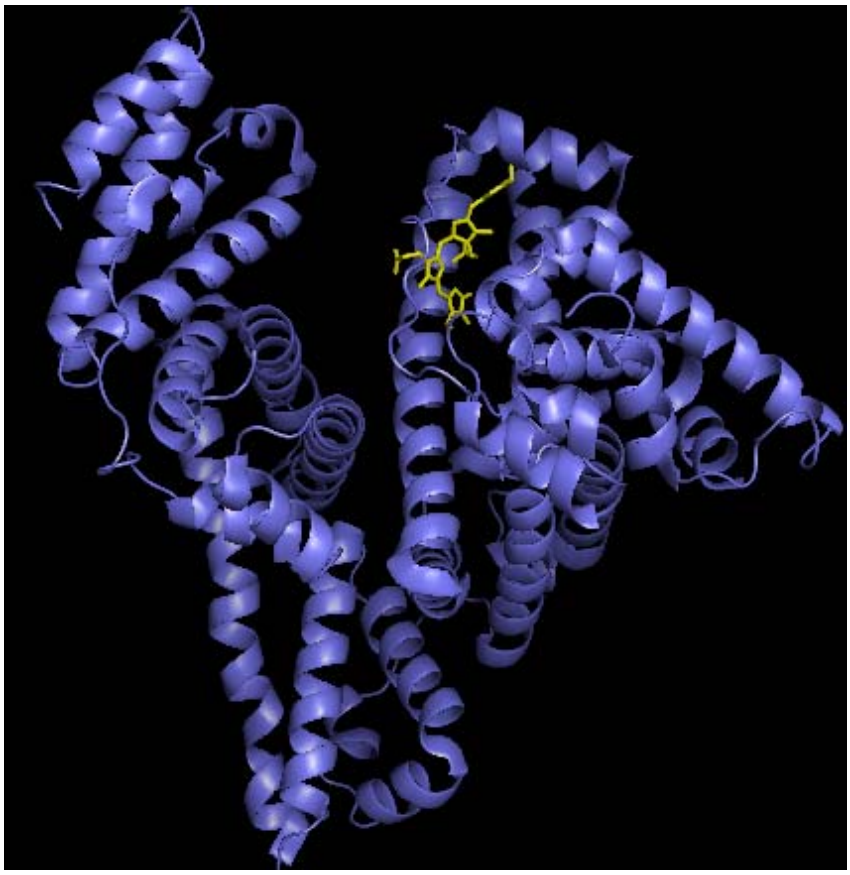

Figure 1.3: X-ray crystal structure of HSA with Bilirubin (yellow) complexed to the protein. This is the same binding site where Heme binds, which is located in FA1 in subdomain 1A. (2VUE, http://www.ebi.ac.uk/pdbe-srv/view/entry/2vue/summary.html)

Metal Binding in Human Serum Albumin

There are four main metal binding sites in HSA; the N-terminal copper and nickel-binding motif (ATCUN) which binds Cu(II) and Ni(II), the multiple-binding site (MBS)/Site A, which primarily binds Zn(II), but also binds other divalent metal ions, and

site B, which has been found to bind Cd(II) with a high affinity, and the reduced thiol, Cys34, which binds gold and platinum (Lu, et al., 2008).

The N-terminal site binds Cu(II) and Ni(II) ions with the residues Asp-Ala-His involving the side chains and the nitrogen's of the peptide bonds. MBS/Site A coordinates metal binding to Zn(II) by the carbonyl-oxygen of Asn99, the imidzaole nitrogens of His67 and His247, a carboxylate oxygen of Asp249, and water or a negatively charged ion such as Cl^-. Although the location of Site B is unknown, Cd(II) NMR studies have indicated that one nitrogen ligand is involved in binding. It has also been found that Sites A and B bind Cd(II) with about the same affinity. As the last metal binding site described, Cys34 is the only cysteine in a reduced state. HSA has a total of 35 cysteine residues, and 34 are involved in di-sulfide bridges that link the domains together and stabilize the tertiary structure of the protein. (Sugio, *et al*., 1999)

Dysregulation of Binding Capacity in Type 2 Diabetes

In the metabolic state of T2D, substantially elevated levels of circulating glucose and FFA's are present (Boden and Laakso, 2004). This thesis will describe how elevated levels of glucose (Tripathi, *et al*., 2014) and FFA contribute to the dysregulation of HSA's binding and ligand carrying capabilities (Anguizola, *et al.,* 2013).

Higher Concentration of Fatty Acids. As previously described, under normal physiological conditions, approximately two molecules of FA are carried per HSA molecule (Chuang and Otagiri, 2002). When IR increases and dyslipidemia is more apparent, more FFA's circulate in the blood and the ratio of FFA's to HSA increases

(DeFronzo, 2004). The increased ratio can have competitive effects on the binding of other compounds to HSA, such as the binding of; albumin-bound bilirubin (Thiessen, *et al*., 1972), warfarin, salicylates, bromsulfophthalein, sulfadiazine, and others (Rudman, et al., 1971).

Advanced Glycation End-products. HSA is normally glycated in the range of 0.6-3% (Anguizola, 2013). When the metabolic status has reached T2D, the average blood glucose level is greatly elevated and the amount of glycated HSA can increase two- to five-fold (Anguizola, 2013). This glycation is a non-enzymatic process that occurs when a reducing sugar reacts with a free amine on a protein The α and/or ε amine moieties first form reversible Schiff bases (Day, *et al*., 1978) and then react further to form a more stable Amadori product (Song and Schmidt, 2012). The Amadori products can form with any protein, and can also react with lipids, and amino groups in nucleic acids (Luevano-Contreras and Chapman-Novakofski, 2010). Figure 1.4 shows a schematic representation of the glycation process of an amino acid to form an AGE (Luevano-Contreras and Chapman-Novakofski, 2010). The Amadori products go through a series of chemical reactions, finally forming the Maillard product (Ansari and Dash, 2012), to form the non-reversible AGE(Luevano-Contreras and Chapman-Novakofski, 2010).

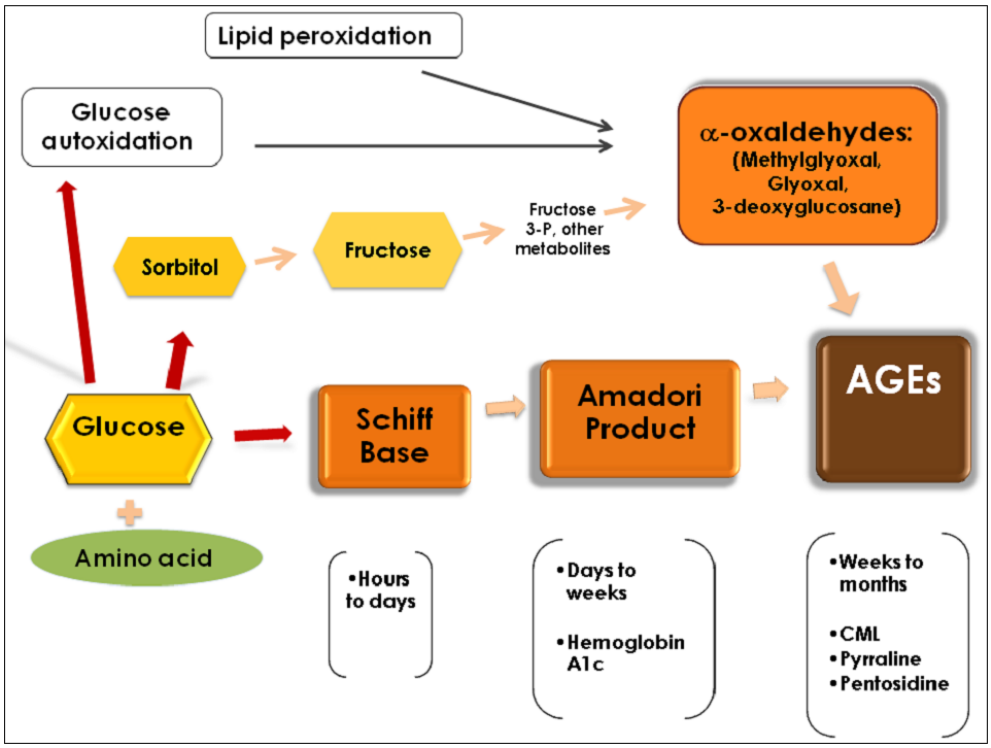

Figure 1.4: Amino acids of proteins can undergo glycation to form AGE. Upon binding of glucose to an amino acid on a protein, further reactions include the formation of a Schiff Base followed by the formation of the Amadori Product preceding the formation of AGE's (Luevano-Contreras and Chapman-Novakofski, 2010)

Glycine and its Many Biological Associations

Glycine, Glucose Disposal, and Insulin Secretion

Our lab recently found novel glycine-containing lipids that differ greatly in T2D, compared to HC (Bowden, 2011). Other prior studies have related glycine in processes related to T2D (Wang-Sattler, *et al.,* 2012) (Xie, *et al.*, 2013). For example, low plasma glycine was the only plasma metabolite measured (out of 108) that was found to predict the development of T2D seven years ahead (Wang-Sattler, *et al.,* 2012). Glycine, is a building block for the synthesis of proteins, glutathione, heme, methyl donors, and plays

a number of other roles in metabolism, including the synthesis of FA (Gannon, *et al*., 2002). Glycine has been classified as a non-essential amino acid, since it can be made in the human body. More quantitative considerations, however, indicate that under some conditions insufficient glycine can be produced for the needs of the body, so glycine has been reclassified as a conditionally essential amino acid (Wang, *et al*. 2013b). Examples of metabolic roles of glycine are in the biosynthesis of nucleic acids, bile acids, porphyrins, creatine phosphate, choline, and other amino acids (Gonzalez-ORTIZ, *et al*., 2000). Figure 1.5 shows a major path of glycine metabolism, which is the conversion into serine by serine hydroxyl methyl transferase (SHMT) and then the conversion into pyruvate and oxaloacetate (OAA) (Dasarathy, *et al*., 2009). Figure 1.5 shows two possible metabolic pathways of OAA; it can either be shuttled into the tricarboxylic acid (TCA) cycle or become a precursor for glucose in gluconeogenesis (Dasarathy, *et al*., 2009).

People with T2D benefit from low carbohydrate, high protein and high fat diets. Studies have been done to determine how dietary protein affects glucose levels. When human subjects, with and without T2D, ingested casein or gelatin protein (50-100 g), there was an increase in insulin concentration and this effect was larger in subjects with T2D (Berger and Vongaraya, 2010). Protein, ingested with glucose in the OGTT, reduces the integrated glucose response curve to the OGTT challenge in type 2 diabetic subjects (Nuttall, *et al*., 1984). Protein ingestion appears to be beneficial to patients with T2D, since protein ingestion tends to reduce the concentration of glucose in the blood and thus

presumably reduces deleterious effects of excess glucose and attendant complications (Anguizola, *et al.* 2013) (Goldin, *et al.* 2006).

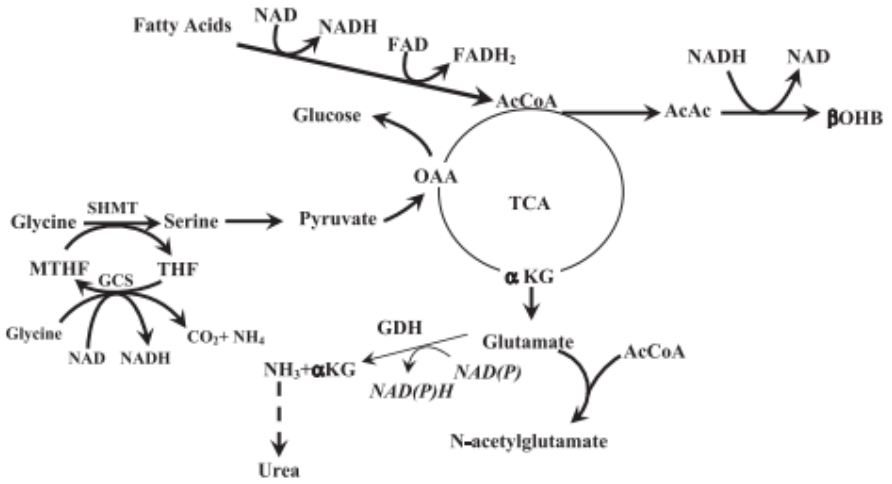

Figure 1.5: A major role of glycine is to provide a carbon for the methyl donor, 5,10-Methylenetetrahydrofolate (MTHF). This is required for many crucial methylation reactions, however, glycine can also be used to make glucose through the conversion to OAA. Glycine is converted into serine, through a 1-carbon donation, before it can be converted into OAA (Dasarathy *et al*., 2009).

When it was determined that ingestion of protein can stimulate the release of insulin from the β-cells, it was of interest to determine if the administration of individual or a mixture of amino acids could have the same effect. Studies have shown that the oral ingestion of certain amino acids (van Loon, *et al.* 2003) or intravenous administration caused a reduction in blood glucose and a rise in insulin (De Boer, 1994). Seven proteins were tested to assess their insulinotropic effects, and the most potent protein was gelatin. Gelatin is an atypical protein that contains approximately 30% glycine residues (Gannon, *et al*., 2002). This finding motivated research to determine if the administration of oral glycine increased insulin or reduced the glucose response independently of insulin (Gannon, *et al*., 2002). Gannon, *et al*., 2002, studied the effects of oral glycine on nine

healthy subjects using the OGTT. Five grams of oral glycine reduced the glucose area response resulting from ingestion of 75 grams of glucose (Gannon, *et al*, 2002). This clearly showed that glycine has a profound effect on the removal of plasma glucose from the blood; however, the glycine effect was not caused by an effect on the insulin response (Gannon, *et al*, 2002). They suggested that some unknown hormone or metabolic factor was controlled by glycine that in turn increased insulin sensitivity.

It has also been found under another experimental design, that incubating mouse β-cells with glycine increased the levels of cytoplasmic Ca^{2+} (Ahmed, *et al.,* 1999). The influx of Ca^{2+} into the beta cell, following membrane depolarization, is required for insulin release.

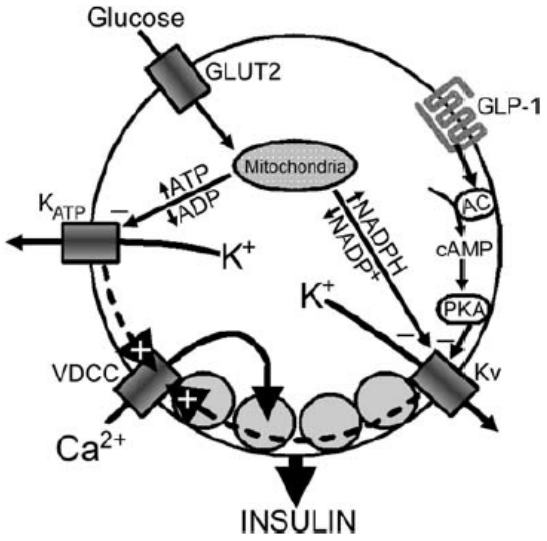

Figure 1.6: Glucose, upon entering into the β-cell, causes the rise in ATP and nicotinamide adenine dinucleotide phosphate (NADPH). This causes closure of the K_{ATP} channels and membrane depolarization, leading to Ca^{2+} influx, and secretion of insulin. (MacDonald and Wheeler, 2003)

As seen in Figure 1.6, glucose enters the β-cell via the Glucose transporter 2 (GLUT-2) transmembrane protein. Glucose becomes catabolized by glycolysis and the products enter into the TCA cycle to produce reducing equivalents. These reducing equivalents feed electrons into the electron transport chain to produce ATP. The rise in ATP causes closure of the ATP-sensitive potassium channel (K_{ATP}) and prevents K^+ from exiting the β-cell. The closure of the K_{ATP} channel causes depolarization of the plasma membrane and opening of the voltage activated Ca^{2+} channels, allowing influx of Ca^{2+}. The influx of Ca^{2+} causes insulin release by exocytosis. (Newsholme, *et al*., 2006) (MacDonald and Wheeler, 2003). Glycine, acting as an excitatory neurotransmitter, causes Ca^{2+} entry into neuronal cells through voltage gated Ca^{2+} ion channels (Reichling, *et al*., 1994)

Glycine is also involved in the increase in insulin concentration through the stimulation of glucagon-like peptide-1 (GLP-1) release. When a meal is ingested and the nutrients move through the gut lumen, nutrient sensing intestinal L-cells release glucagon-like peptide-1. GLP-1 has been found to enhance the glucose dependent release of insulin from the pancreas. Previous studies had found that the ingestion of several different amino acids triggered the release of GLP-1. This work determined that glycine potentiates the release of GLP-1 by binding to glycine receptors on L-cells. (Gameiro, *et al*., 2005).

Glycine and Insulin Resistance

Insulin resistance is a major problem associated with the pathology of T2D and when it is occurs along with decreased ability of β-cells to provide high levels of insulin, it can lead to the elevated blood sugar characteristic of T2D (Gall, *et al*., 2010). As previously described, people become more resistant to insulin, in the pathogenesis of T2D (ADA, http://www.diabetes.org/diabetes-basics/type-2/). Insulin resistance creates longer and higher levels of glucose present for long periods of time (Anguizola, *et al.* 2013) (Goldin, *et al.* 2006). Increasing IR requires ever higher levels of insulin that tends to cause severe strain on the β-cells (Weir and Bonner-Weir, 2004). The pancreas tries to keep up with the demand of the high levels of glucose present, by producing more insulin (Weir and Bonner-Weir, 2004). However, the β-cells can eventually stop secreting insulin, which in turn leads to β-cell dysfunction (Weir and Bonner-Weir, 2004). Several different amino acids have been found to improve insulin sensitivity in elderly subjects with T2D (Solerte, *et al*., 2004).

A mixture of amino acids containing leucine, lysine, isoleucine, valine, threonine, cysteine, histidine, phenylalanine, methionine, tyrosine, and tryptophan showed a significant decrease in insulin resistance and an increase in insulin sensitivity in both short-term (34 weeks) and long-term (60 weeks). (Solerte, *et al*., 2004) (Solerte, *et al*., 2008). In the Relationship between Insulin Sensitivity and Cardiovascular Disease (RISC) study, plasma glycine levels were found to be correlated with insulin sensitivity with an excellent p-value of 2.79E-11. (Gall, *et al*., 2010).

Glycine and Glutathione

One of the most prominent correlates with T2D is elevated levels of reactive oxygen species (ROS) (Wright, E. *et al.* 2006). Increased glucose levels result in the formation of increasing amounts of AGE (Anguizola, *et al.,* 2013). AGE can then cause the increase of the inflammatory cytokine, NFkB, which in turn increases other cytokines that are involved in the inflammatory process (Wright, E. *et al.* 2006). Various defense mechanisms are used to reduce ROS and combat inflammation (Sekhar, *et al.,* 2011). One of the most prominent defense systems in the body is the glutathione system which reduces the levels of ROS (Sekhar, *et al.,* 2011). Glutathione (GSH) is synthesized from cysteine, glutamate, and glycine by a two-step reaction (Galant, *et al*., 2011) (Figure 1.7).

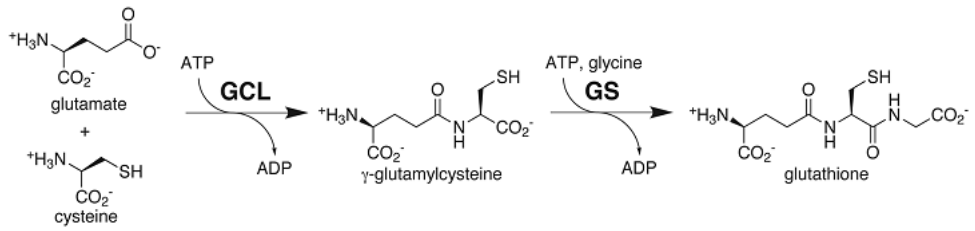

Figure 1.7. The process of synthesizing reduced glutathione is a two-step reaction. The first one, being an ATP-dependent reaction, utilizes glutamate-cysteine ligase (GCL) and the second reaction, also an ATP-dependent reaction, requires glutathione-synthase (GS) to form the final product. (Galant, *et al*., 2011)

A major problem associated with T2D is the reduction of cellular glutathione concentrations. Sekhar, *et al*., (2011) hypothesized that in uncontrolled T2D, GSH deficiency was due to low amounts being synthesized. Furthermore, they also hypothesized that supplementation of the precursors to glutathione, glycine and cysteine, would increase GSH levels. This was studied with diabetic and non-diabetic human

subjects. After 14 days, Sekhar, *et al*., (2011), found that administering the precursor amino acids to glutathione (glycine and cysteine) restored the GSH synthesis rate (Sekhar, *et al.,* 2011).

Glycine can aid in the synthesis of GSH by another mechanism as outlined in Figure 1.8 (Dasarathy, *et al*., 2009). Figure 1.8 shows that glycine can be converted to serine by a reaction catalyzed by SHMT (Dasarathy, *et al*., 2009). Serine can then go through a series of reactions which can lead to the formation of cysteine and GSH (Dasarathy, *et al*., 2009).

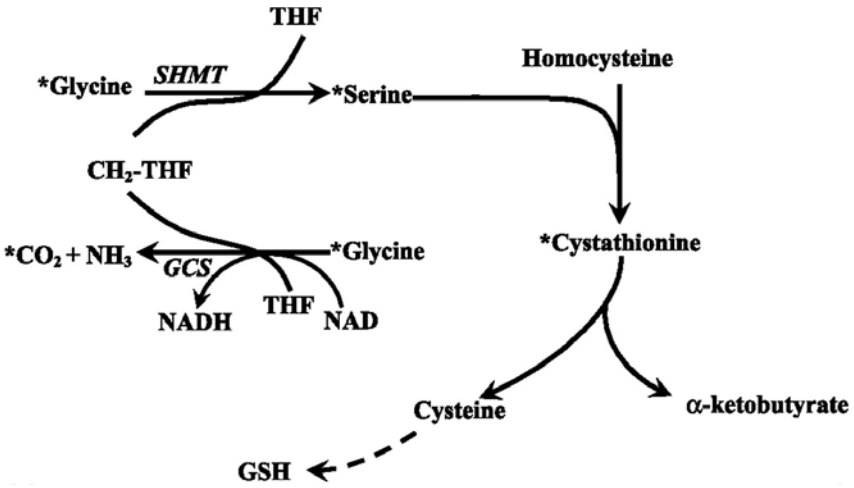

Figure 1.8: As shown in Figure 1.5, glycine can be directly converted to serine via SHMT. Serine can eventually be used to synthesize GSH. In this figure, serine synthesized from glycine gets converted to cystathionine, and then to cysteine, which is a precursor to GSH. (Dasarathy, *et al*., 2009)

Glycine as a Biomarker

Low levels of plasma glycine have been identified as a biomarker for the future onset of T2D (Wang-Sattler, *et al*., 2012). In a large cohort study, KORA (Cooperative

Health Research in the Region of Augsburg), three metabolites were found to have significantly altered levels in people who developed IGT seven years in the future with excellent P-values ranging from 2.4E-4 to 2.1E-13. These three metabolites are glycine, lysophosphatidyl choline 18:2 (LPC 18:2), and acetylcarnitine. Glycine and LPC were independently confirmed as correlated with T2D in a second large, European Prospective Investigation into Cancer and Nutrition (EPIC)-Postdam cohort. Glycine and LPC were both determined to be predictors of IGT and T2D 7 years before onset. (Wang-Sattler, *et al*., 2012)

Glycine Metabolism

Glycine Conjugation in Xenobiotic Disposal

Wöhler found in the urine of his dog, who he fed benzoic acid with his food, needle-shaped prisms. These were first thought to be benzoic acid crystals, but were later identified as a crystalline glycine adduct of benzoic acid, hippuric acid (Keller, 1842). This was the first discovery of glycine-conjugation (Waluk, *et al*., 2010) in biology. Glycine can conjugate with other xenobiotics at the N-acyl end (Liska, 1998). Normally benzoic acid is toxic to the body, but conjugation with glycine to produce hippuric acid renders it a water-soluble, non-toxic substance, and is then able to be excreted in the urine (Liska, 1998). Conjugation is an important process in the detoxification of many xenobiotic compounds (Glatt, 2000). When coupled with endogenous compounds, water solubility is increased by glycine conjugation, so they are more easily excreted and are less able to be reabsorbed back into the body (Glatt, 2000). This process is involved in “Phase II metabolism” and occurs in the liver (Glatt, 2000).

Many xenobiotic compounds first undergo “Phase I metabolism”, where they may be either reduced, oxidized, or hydrolyzed to become more polar and then can be subjected to “Phase II metabolism” (Jancova, et al. 2010) for increased elimination.

Glycine Conjugation in Signaling. Although glycine-conjugation is known for detoxification of toxic compounds, it also participates in cell signaling through a family of lipid signaling molecules. The products of glycine N-conjugation with medium and long chain fatty acids can participate in neuronal signaling (Waluk, *et al*., 2010). N-fatty acyl glycine compounds have been found to be involved in membrane depolarization, Ca^{2+} influx, and eventually exocytosis of insulin-containing vesicles (Ikeda, *et al*., 2005). The first fatty-acyl glycine compound identified was N-arachidonoyl glycine (Waluk, *et al*., 2010). Other fatty glycyl and fatty acyl amides have been identified as well, such as a family of arachidonoyl amides containing a subfamily of compounds conjugated with glycine, ethanolamine, GABA, as well as others (Rimmerman, *et al*., 2008). N-palmitoyl glycine was found to induce Ca^{2+} influx in native adult dorsal root ganglion (Rimmerman, *et al*., 2008) and N-arachidonoyl glycine was found to be an insulin secretagogue, increasing the intracellular concentration of Ca^{2+}, by stimulation of the voltage-dependent Ca^{2+} channels of mouse pancreatic islet cells (Ikeda, *et al*., 2005).

A question has come up in our research: are the novel glycine-containing lipids we have found associated with T2D (linked via the carboxyl-terminal of glycine) produced by the body or do they come from the gut-microflora? Dr. Jared Bowden found similar glycine-containing lipids in mouse/rat plasma (Bowden, 2011). Rodents have distinct gut-microflora, but this gut-microflora might still produce these compounds of

interest. The human gut-microflora is composed of at least 10^{14} bacteria from approximately 1,000 different species, the size of the nuclear genome of the microflora exceeds the size of the human genome by two orders of magnitude (Neish, 2009), and possesses a few hundred more times as many genes as in humans (Wikoff, *et al.,* 2009). Metabolites produced by the gut-microflora have been found to be conjugated by glycine for Phase II detoxification previously described. Wikoff *et al*., (2009), showed that germ-free mice had lower levels of certain conjugated glycine compounds in the serum than conventional mice (Wikoff, *et al*., 2009). This question has not been resolved, but presumably can be resolved once the structures of the glycine-lipids are established.

Glycine and Iron Metabolism

Dysregulation of iron-metabolism has been found to be a problem in pre-diabetics and diabetics (Sharifi, *et al*., 2008) (Fernàndez-Real, *et al*., 2002). An elevation is consistent with the relation between iron, oxidative stress, and insulin levels, illustrated in Figure 1.9. Ferritin is an intracellular protein that stores iron (as Fe^{3+}) and releases it as needed. When ferritin releases iron, the iron is converted into Fe^{2+}, a more soluble form of iron that can diffuse out of the cell into the extracellular layer. When Fe^{2+} is in the extracellular layer, it is considered free iron. Figure 1.9 shows Fe^{2+} can contribute to oxidative stress. As diagrammed in Figure 1.9, increases in oxidative stress can inhibit insulin from transversing from the extra-cellular to the intra-cellular layer (Fernàndez-Real, *et al*., 2002).

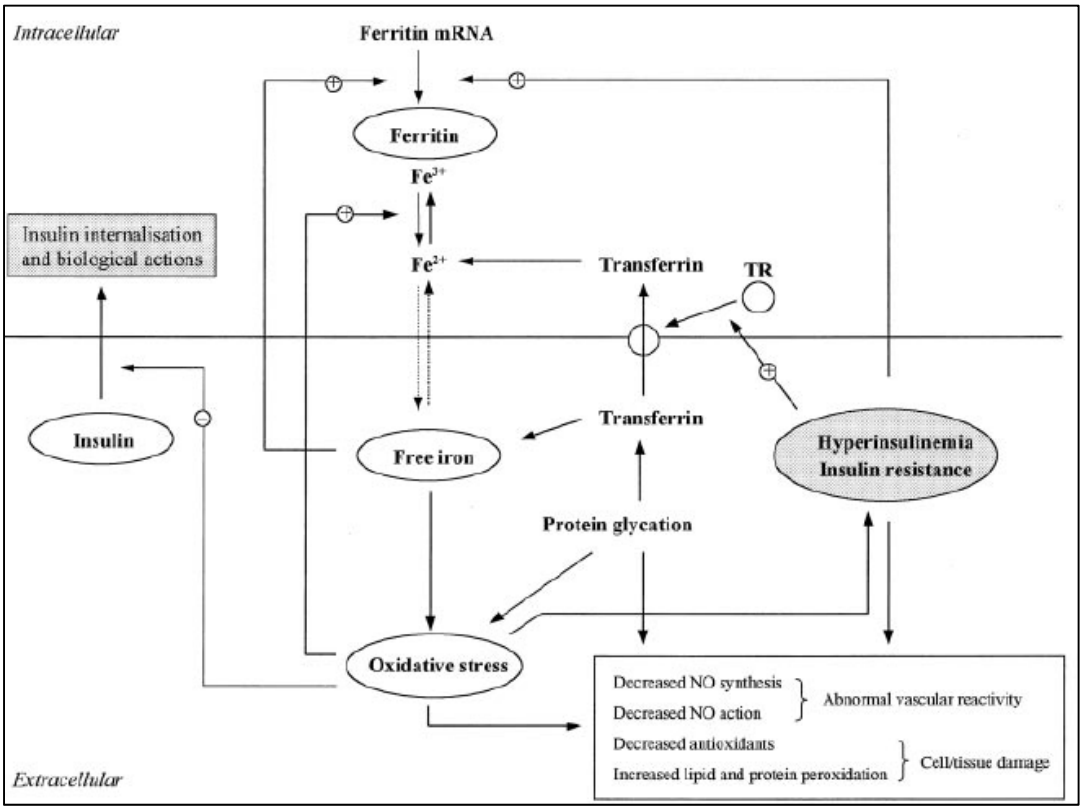

Figure 1.9: Free iron has various roles as outlined. Oxidative stress (OS) is shown to directly prevent insulin from entering the cell, which is problematic in persons with insulin resistance. It can allow ferritin to release its bound Fe^{3+} to become Fe^{2+} and partition into the extracellular layer, raising the free iron and thereby leading to more oxidative stress. It causes a further decrease in other antioxidants, as well as contributing to hyperinsulinemia and insulin resistance. (Fernàndez-Real, *et al*., 2002)

Wang-Sattler *et al*. 2012 found that lower levels of plasma glycine predicted the development of IGT and dT2D seven years. Glycine has been shown to be involved in iron-metabolism. Delta-aminolevulinate synthase 1 (ALAS-1) condenses succinyl-CoA with glycine to produce 5-aminolevulinic acid (ALA) in the rate-limiting step of the production of heme (Figure 1.10). This pathway also shows how insulin is related to ALAS-1 and in turn, how it is associated with glycine. This work proposes how increasing levels of insulin inhibit ALAS-1 expression. However, as IR progresses and

less insulin gets into cells, the expression of ALAS-1 goes up. This could explain why individuals with low levels of plasma glycine have a much greater risk of developing IGT and T2D.

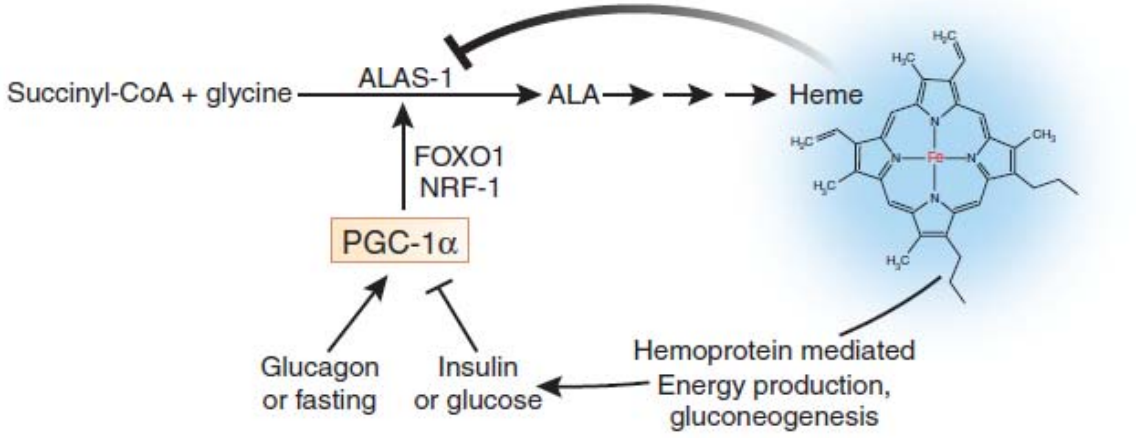

Figure 1.10. Glycine is involved in the rate limiting step in the synthesis of heme. ALAS-1 catalyzes the formation of ALA, which is the first and rate-limiting step. Several additional steps yields the final formation of heme. Heme is also involved in other processes; where increasing levels can prevent insulin production. (Phillips and Kushner, 2005)

Higher levels of glycine would be involved in the production of more heme. This could tie up the free-iron into heme, hence reducing the levels of free, pro-oxidant Fe^{2+}.

Biosynthesis and Degradation of Glycine

Serine and Serine Hydroxymethyltransferase. Glycine is centrally involved with generating 1-carbon units carried on folate that are crucial for many biological methylation reactions (Perry, *et al*., 2007). SHMT is involved in the conversion of serine to glycine and glycine

to serine (Perry, *et al*., 2007). SHMT is a pyridoxal-phosphate dependent isozyme, and exists in the mitochondrion and cytoplasm (Perry, *et al*., 2007). SHMT possesses a pyridoxal-phosphate cofactor (Perry, *et al*., 2007). When dietary Vitamin-B6 is ingested, hydrolysis occurs and forms pyridoxal phosphate (PLP) (Okada, *et al*., 1996). PLP is then incorporated into SHMT (Lamers *et al*., 2008) (Perry, *et al*., 2007).

Glycine Cleavage System. Glycine is involved in many steps of biosynthesis, for example; in purine, protein, and glutathione metabolism (Lamers, *et al*., 2008). Glycine is catabolized by the glycine cleavage system (GCS) (Lamers, *et al*., 2008).

$$\text{Glycine} + \text{THF} + \text{NAD}^+ \rightleftharpoons \text{5,10-methylene-THF} + \\ + \text{CO}_2 + \text{NH}_3 + \text{NADH}$$

Figure 1.11: The catabolism of glycine by by the GCS. Glycine is broken down and produces CO_2, NH_3, and a 1-carbon methylene, that transforms THF into 5,10-methylene-THF. (Kikuchi, 1973)

Figures 1.5 and 1.8 each show the involvement of SHMT in the synthesis of serine. Figure 1.11 shows the reaction of the donation of a methylene group from MTHF to glycine. Tetrahydrofolate (THF1) can then re-obtain the methylene group, as glycine is broken down into CO_2, NH_3, and reduced nicotinamide adenine dinucleotide (NADH) to produce MTHF (Kikuchi, 1973). The methylene group donated to THF1 is known as a 1-carbon unit and is involved in the folate cycle (Lamers, *et al*. 2008) (Perry, *et al*., 2007) and a large number of essential methylation reactions in biology.

Prior Work in the Dratz Laboratory at MSU

Extraction, Derivation, and Analysis of Lipids from Human Serum Albumin

Dr. Scott Laffoon found 10 proteins in plasma that changed with strong p-values ($p<0.05$) in the plasma of newly diagnosed, untreated F-T2D compared to F-HC (Laffoon, 2010). Of those 10 plasma proteins, 9 of them are found to be carried by HSA, however the HSA was removed from the plasma before proteomic analysis of the less abundant proteins (Laffoon, 2010). It was proposed that the HSA binding properties were changed in T2D. Dr. Jared Bowden studied a number of properties of HSA comparing healthy vs. T2D (Bowden, 2011). The HSA was purified from plasma, frozen, lyophilized, and solubilized in a 0.88% KCl solution. The bound metabolites and lipids were extracted for analysis, using a modified 2:1 DCM:MeOH Folch extraction (Folch, *et al*. 1957) (Figure 1.12), substituting dicholoromethane (DCM) for chloroform (vanKuijk, *et al*., 1986). The hydrophilic compounds partition into the water:MeOH layer, while; fatty acids, lipids, and other hydrophobic compounds partition into the DCM:MeOH layer. It turned out that the most interesting compounds were contained in the DCM:MeOH layer. These could be semi-purified by washing of the DCM:MeOH layer to yield a MeOH depleted DCM layer (DCM2). (Bowden, 2011)

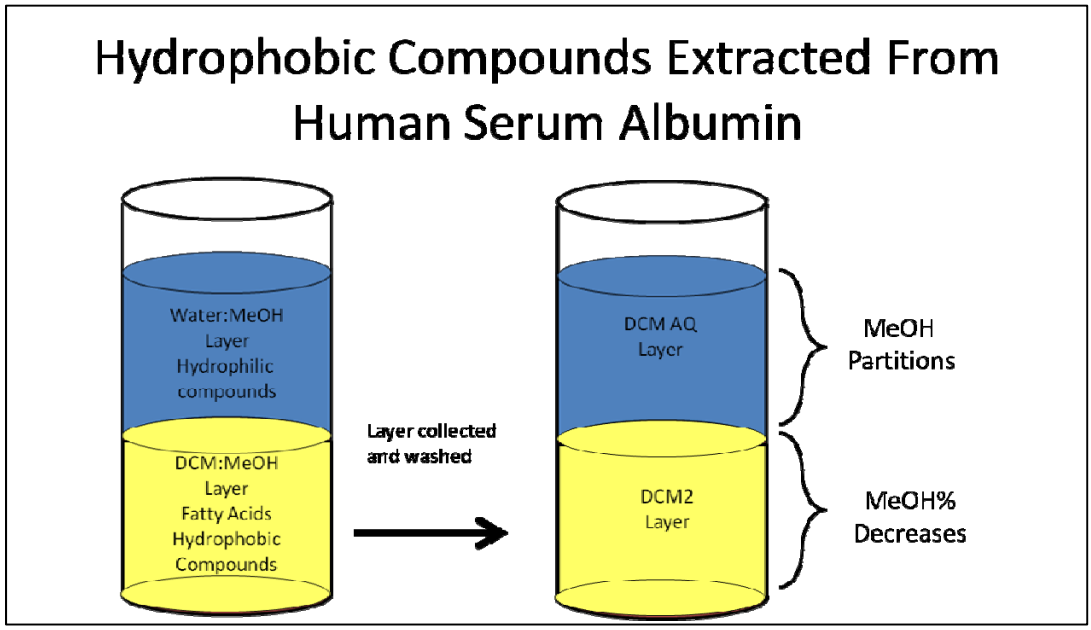

Figure 1.12: Extraction of the compounds carried by HSA. The hydrophobic compounds partition into the DCM:MeOH layer, while the hydrophilic compounds partition into water:MeOH layer. The DCM:MeOH layer is washed with water to create a DCM:AQ layer and a more MeOH depleted DCM layer (DCM2). (Bowden, 2011)

The DCM2 layer was harvested and a portion was used for derivatization with PFB-Br, to form PFB-esters of the various types of lipids present (Figure 1.13). For example, PFB-Br can trans-esterify triglycerides, diglycerides, monoglycerides, cholesterol-esters, and phospholipids (van Kuijk, *et al.,* 1985). The rationale to using PFB-Br to derivatize the samples was that it increases the sensitivity of detection by negative ion chemical ionization (NICI) gas chromatography mass spectrometry (GCMS) (Pawlosky, *et al.,1992*).

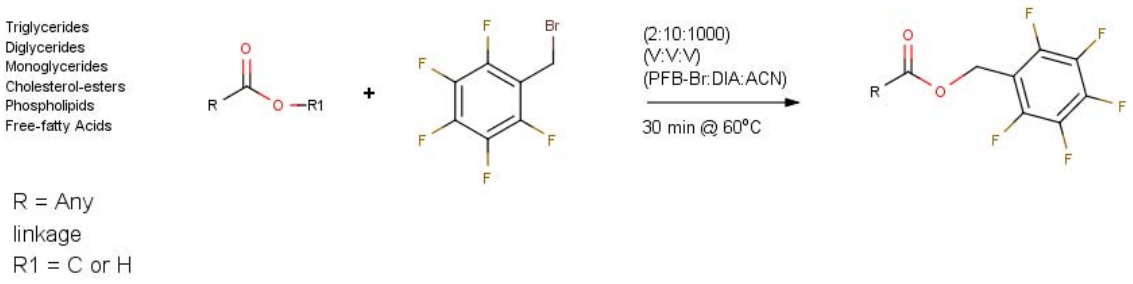

Figure 1.13: Schematic representation of the derivatization of lipids with pentafluorobenzyl bromide (PFB-Br). Lipids are reacted with PFB-Br at a ratio of (2:10:1000), (V:V:V), (PFB-Br:DIA:ACN). This reaction is incubated at 60°C for 30 min and the products can be analyzed by MS. (DIA=Diisopropylamine, ACN=Acetonitrile).

Since we do not know the structure of R1 we do not yet know what happens to R1 in this reaction. Figure 1.14 shows that most peaks in the GC chromatogram were attributed to fatty acids by their molecular weights, since the PFB falls off in NICI to yield the negative ion of the PFB esters (vanKuijk, *et al*,. 1985, Bowden, 2011) and the corresponding number of carbons are labeled (the C_{15} was spiked into the sample for use as an internal standard). However, there were two peaks present, labeled as 254 mass-to-charge (m/z) and 434 m/z, that did not correspond to the molecular weights of any known fatty acid .

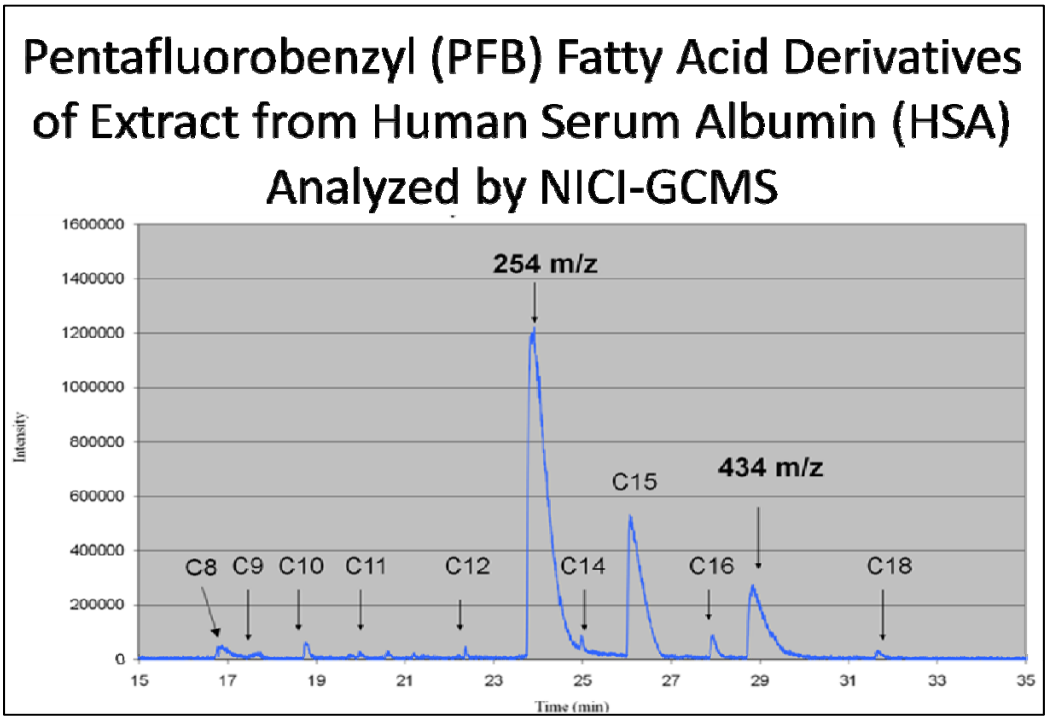

Figure 1.14: Analysis of the products of the PFB-Br reaction from the DCM2 layer, by NICI-GCMS, reveals many fatty acids present. The 254 m/z and 434 m/z peaks do not correspond to the molecular weights of any known fatty acid. (Bowden, 2011)

The PFB derivatized material was analyzed using positive ionization-electrospray ionization-quadropole-time-of-flight-mass-spectrometry ESI-Qtof-MS. The 254 and 434 m/z compounds (which appear as 256 and 436 in the positive ion ESI), were identified as being a mono- and di- PFB-glycine. Authentic PFB-glycine was prepared and analyzed by Electron-ionization-gas-chromatography-mass-spectrometry) (EI-GCMS) and ESI-Qtof for fragmentation and the fragmentation confirmed to be that of mono- and di- PFB-glycine. Tri-PFB glycine also was present in but this broke down in the NICI-GC-MS. It was determined that the ratio of the 254 m/z and 454 m/z had both increased in the T2D samples by 2-fold compared to HC ($p< 0.005$), strongly suggesting involvement of glycine-containing lipid compounds in T2D. (Figure 1.15) (Bowden, 2011)

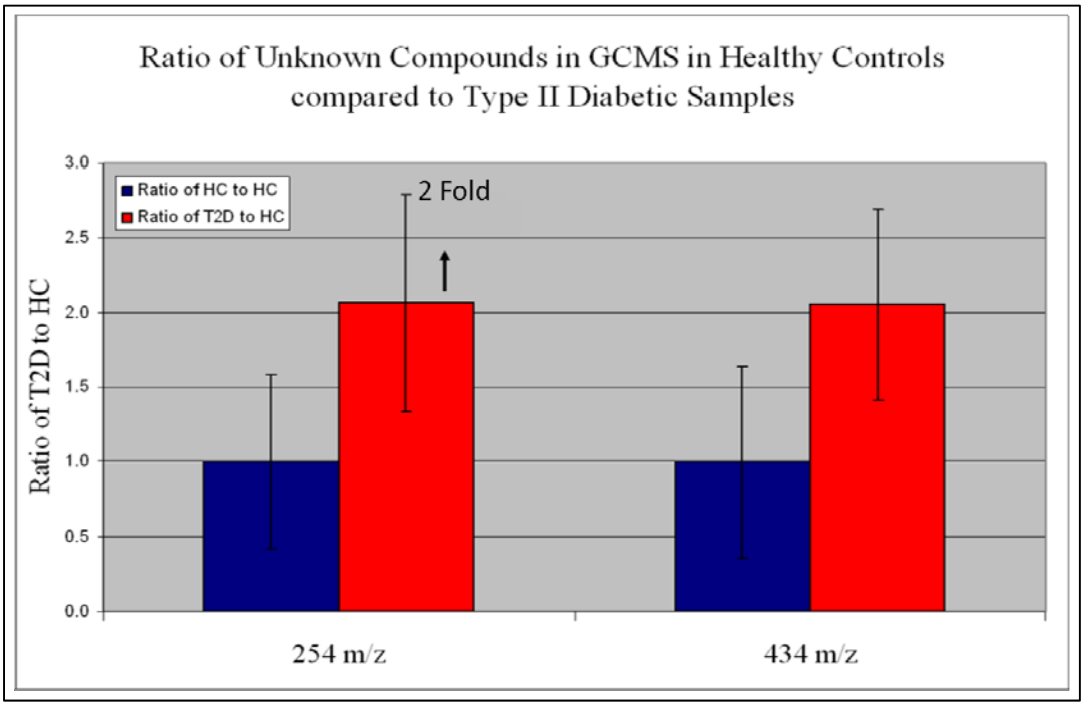

Figure 1.15: The peaks found in NICI-GCMS corresponding to 254 m/z and 434 m/z are found in both T2D and Healthy Control. The levels of these compounds were used to normalize the ratios of the compounds in T2D/HC, and both peaks were found to be 2-fold higher in T2D compared to HC. (Bowden, 2011)

The derivatized compounds corresponding to the 254 m/z and 434 m/z were analyzed by GC-EI-MS in electron impact (EI) ionization mode. The fragmentation pattern in Figure 1.16 show peaks that match the fragment masses of derivatized PFB-glycine of the di- and tri- PFB compounds.

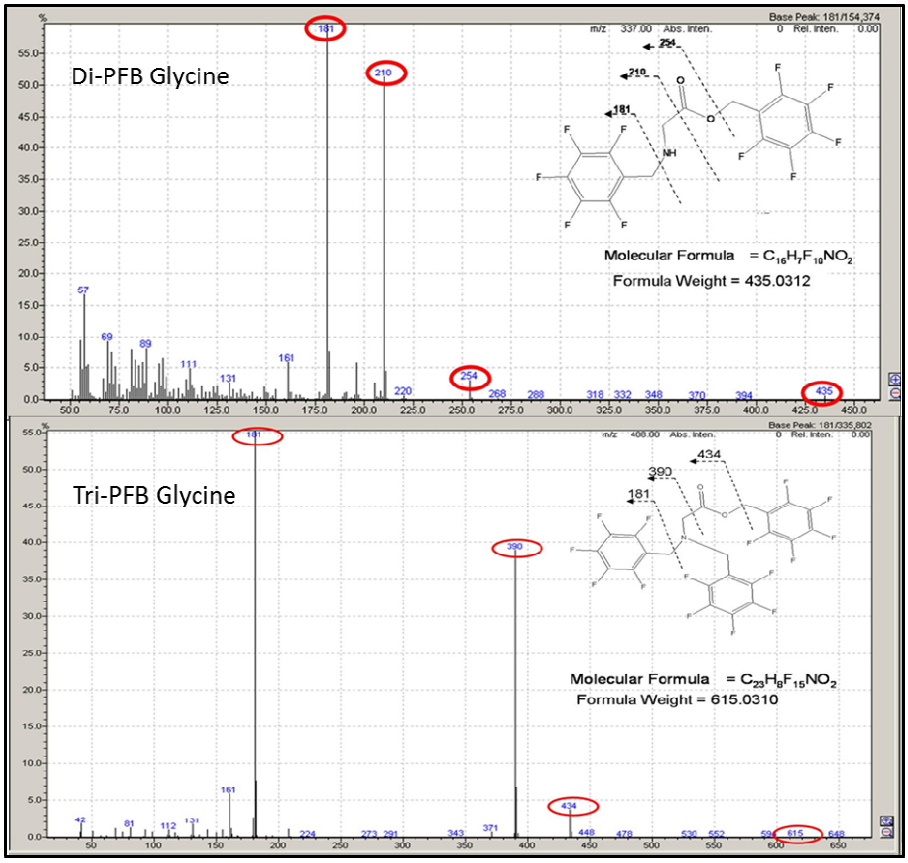

Figure 1.16: EI-GCMS of the 254 m/z and 434 m/z peaks. The top MS spectrum shows the fragmentation pattern in which the fragments of di-PFB glycine match the peaks that appear and are circled in red. The bottom MS spectrum shows that of tri-PFB glycine. (Bowden, 2011)

In order to confirm that the 254 m/z and 454 m/z peaks were of mono- and di-PFB glycine, authentic free glycine was derivatized with PFB-Br and analyzed by EI GCMS as well (Figure 1.17). The GC chromatogram show the peaks that correspond to 254 m/z and 454 m/z have the same retention time (RT) as the PFB derivatized glycine from HSA, respectively, as well as the same fragmentation pattern using EI.

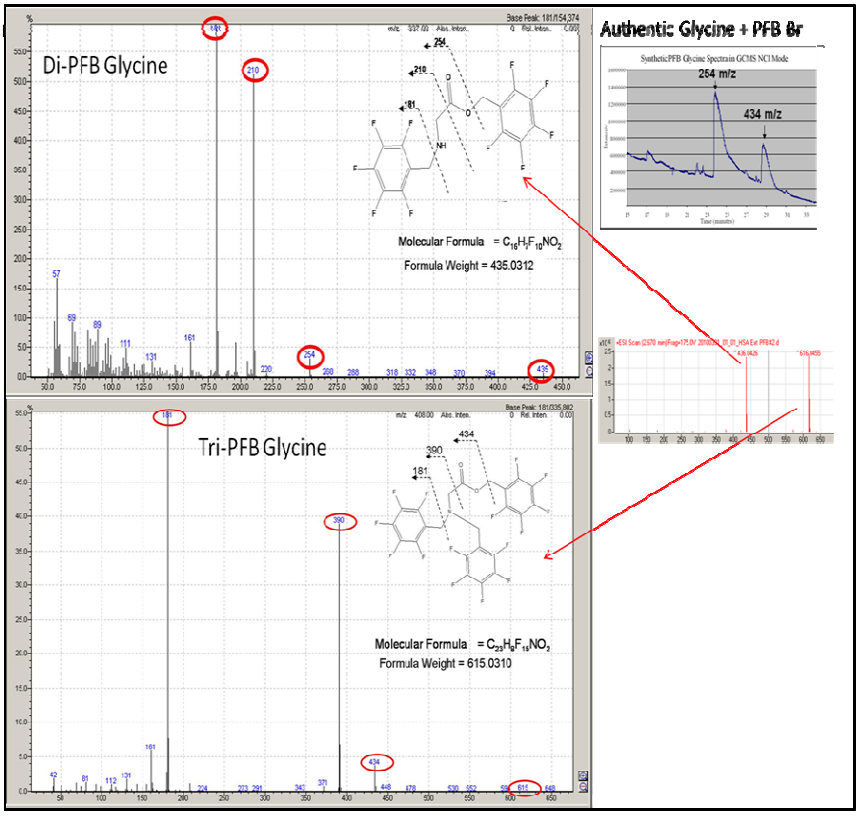

Figure 1.17: EI-GCMS of authentic glycine derivatized with PFB-Br. The MS of the di-PFB-glycine and tri-PFB glycine are shown. Each shows the fragmentation peaks that are indicative of PFB-glycine. The inset shows the GC chromatogram in NICI mode and the lower inset shows the parent accurate masses measured in positive ion ESI-MS mode on the Agilent 6538 Qtof. (Bowden, 2011)

It was important to determine the possibility that the derivatized glycine might have originated from free glycine in plasma bound to HSA. Free ^{13}C-glycine was spiked into the plasma before the 2:1 DCM:MeOH modified Folch extraction to determine which layer it partitioned into. It was found that all of the ^{13}C-glycine had partitioned into the hydrophilic water:MeOH layer and no detectable amounts had partitioned into the hydrophobic layers. This information, indicated that a hydrophobic moiety must be attached to glycine which allowed the glycine to be carried on HSA and to be carried into the hydrophobic layers upon the modified Folch extraction and the DCM2 extraction.

Linkage Studies of the Unknown Glycine-containing Lipids

It was necessary to determine the end of glycine that was attached to the hydrophobic moiety. Dr. Bowden found that glycine linked at the carboxyl end via an ester linkage, liberated PFB-glycine upon deriviatization but glycine linked via an amide linkage did not (Table 1.2) (Bowden, 2011). An eventual goal of the present studies is to determine the chemical identities of the hydrophobic compounds linked to glycine, and the first step is to narrow down the possible chemical linkage(s) of glycine that may be present in these compounds.

It was inferred that the compounds of interest were glycine-containing lipids, linked to a hydrophobic moiety via the carboxyl-end. Stable conjugated amino acid lipids linked at the carboxyl end were not reported at the time of completion of Bowden's work, however amino-acyl adenylates are well known in biology, containing carboxy-phospho anhydride esters (Nakajima, *et al.,* 1984) (Kluger, *et al*., 1996). Amino-acyl t-RNA synthetase enzymes use ATP to activate amino acids to form amino-acyl AMP (containing carboxy-phospho anhydride esters) and free inorganic pyrophosphate (PP_i). However, the amino-acyl adenylates do not exist long as they are readily used ribosomes to generate growing proteins, and acyl-phospho anhydrides are not very stable compounds either (Nakajima, et al. 1984) (Kluger, et al., 1996).

Compound	Formula	Glycine cleaves during Derivitization	Structure
Glycocholic Acid (Bile Salt)	$C_{26}H_{43}NO_6$	No	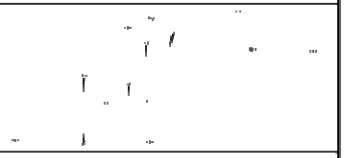
Reduced Glutathione	$C_{10}H_{17}N_3O_6S$	No	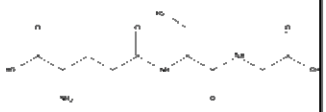
Oxidized Glutathione	$C_{10}H_{17}N_3O_9S$	No	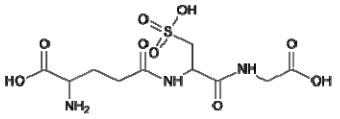
Oleolyglycine	$C_{20}H_{37}NO_3$	No	
Glycine Benzyl Ester	$C_9H_{12}NO_2$	Yes	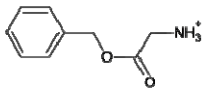
O-octadecyl glycine	$C_{20}H_{41}NO_2$	Yes	

Table 1.2: Compounds were either purchased or synthesized. Each structure contains a glycine moiety bound either at the N-terminus or C-terminus. These glycine-containing compounds were derivatized using the PFB-Br reaction outlined in Figure 1.13. The purpose was to determine which chemical linkages that allows PFB-Br cleavage, producing PFB-glycine. Structures that have a glycine moiety linked at the amino end were not cleaved during PFB-derivatization, but carboxy esters were cleaved by PFB-Br. (Bowden, 2011)

Discovery of a Family of Glycine-containing Lipids

To further understand the involvement of these glycine-containing lipids in T2D, RP-HPLC was used to separate the compounds from the DCM2 extract from purified

HSA in three metabolic states; F-T2D, F-HC, and NF-HC. Blood was obtained from each metabolic status and was centrifuged to separate the plasma from the RBC. Agilent HSA Affinity Spin Cartridges were used to purify HSA from other plasma proteins. The lipids were extracted using the modified Folch extraction previously described. The lipids of the DCM2 layer were fractionated using RP-HPLC. The fractions were dried and resolubalized in 200 µL of a (70:30) MeOH:water solution. Two microliters of each were removed and reacted with 50 µL of the PFB-Br solution at 60^{o}C for 30 min. Each derivatized fraction was prepared for analysis on ESI-Qtof-MS in positive ionization mode. Figure 1.18 shows each fraction number of the T2D samples of F-HC NF-HC, and F-T2D, monitoring fractions at 436 m/z, that correspond to protonated di-PFB glycine. F-T2D and F-HC show one peak with different RT values, indicating at least one glycine-containing lipid is present in each metabolic state. However, since these peaks elute from the LC at different RT values, they are not the same compounds. The RP fraction 4 and 5 of F-T2D is not present at fraction 4 and 5 in F-HC, which indicates this glycine-containing lipid of this chemical structure is specific to T2D. N-HC, however, shows at least 5 distinct compounds present, including peaks in the region corresponding to F-HC and F-T2D.

The ESI-Qtof-MS/MS of the intact lipids in each fraction (before derivatization with PFB-Br) could not be matched to any known compound in the LipidMaps (35,000 compounds) or the METLIN metabolite (60,000 compounds) data bases.

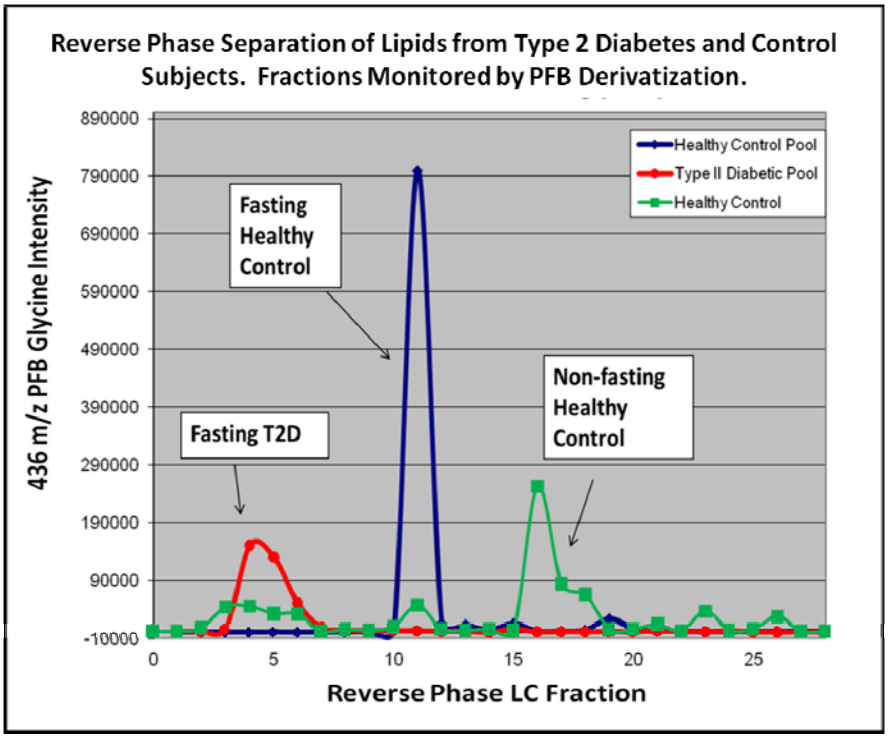

Figure 1.18: After RP separation, each fraction was derivatized with PFB-Br and further analyzed by ESI-MS. The content of the 436 m/z of PFB-glycine and each metabolic state were overlaid from each biological sample. The F-T2D is labeled as the red tracing, where the glycine-containing lipid is found in the 4^{th} – 6^{th} fraction. The F-HC is labeled as the blue tracing where the glycine-containing lipid is found in the 11^{th} fraction. The NF-HC is labeled as the green tracing, and has at least glycine-containing lipids, which are found in fractions 3-6, 11, 16-18, 23, and 26.

Thus, the next goal was structure elucidation of these glycine-containing lipids by NMR. NMR spectroscopy can provide more structural information than MS and tandem-mass spectrometry (MS/MS), however, NMR is less sensitive than MS. Thus, it is necessary to have much more material for NMR in order to have sufficient signal-to-noise and have the ability to determine functional groups and chemical linkages present and locations in the compounds of interest. This background leads to the beginning of the experimental aspects of this thesis.

METHODS

Analysis of Lipids Carried by Human Serum Albumin

Immuno-affinity Purification

Approximately 150 milliliters of blood was obtained from NF-HC volunteers in purple top vacutainers, containing EDTA as an anticoagulant. The RBCs were separated from the plasma by centrifugation at 1000*g for 10 min. The plasma was removed and stored in Eppendorf tubes in 1 mL aliquots at -80^{o}C until use. When plasma samples were ready for use, they were removed from -80^{o}C and allowed to come to room temperature. The plasma was diluted 1:4 with Agilent Buffer A (PN# 5185-5987) and 50 µL was loaded onto each of 12 - 0.45 mL Agilent HSA Affinity Removal Spin Cartridges (PN# 5188-5334) that had been pre-equilibrated with 4 mL of Buffer A. The columns were centrifuged at 100*g for 1.5 min, followed by washing of the columns two times with 400 µL of Buffer A at 100*g for 1.5 min. The HSA was eluted from each column using 2 mL of Agilent Buffer B solution using a lure-lock syringe. The HSA/Buffer B eluent was pooled from each of the 12 columns, frozen at -80^{o}C in 25 mL aliquots, and lyophilized overnight.

Extraction of Lipids

Upon completion of the lyophilization, the total dried HSA material was resolubalized in 1 L of a 0.88% KCl. Two-hundred milliliters was transferred at a time to a separatory funnel and extracted using the modified Folch extraction (Folch, 1957) of 200 mL of the 2:1 DCM:MeOH (v/v), that was used to separate the hydrophobic and

hydrophilic compounds from HSA. The hydrophobic lipids partitioned into the DCM:MeOH layer, while the hydrophilic compounds partition into the MeOH:water layer. The DCM:MeOH layer was removed and washed with 200 mL of water (to produce the DCM2 layer), and depleting the DCM:MeOH layer of MeOH. The DCM of the DCM2 layer was then evaporated under dry nitrogen.

The dried hydrophobic extract (364.6 mg) was brought up in an solvent mixture composed of ACN:MeOH until the material dissolved and water was added for a total composition of 4 % organic and 96 % aqueous (0.5 mL of ACN, 1.0 mL of MeOH, and 36 mL of water). The sample was separated on an Agilent 1100 series HPLC using a Phenomenex Jupiter 4u Proteo 90A Reverse Phase Column, using the following gradient conditions: 4% ACN/96% water for 10 min, 10% ACN/90% water for 7 min, 100% ACN for 3.1 min, and 4% ACN/96% water for 14.9 min at a rate of 2.00 mL/min. Thirty 2 mL fractions were collected, dried down, and stored at -20^{o}C. A total of 30 fractionation runs were continually combined with the same fraction numbers that were previously dried down by pouring the eluent into each dried down tube and drying the new set down.

Derivitatization of the Hydrophobic Extract

When all runs were combined into one set of fractions from the 30 HSA purifications runs, there were resolubalized in 200 µL of a (70:30) MeOH:water solution. A separate solution of authentic glycine was prepared in 2 mL of Milli-Q water. Two microliters of each were removed and put into a separate Eppendorf tube. To each 2 µL of sample, 50 µL of the PFB-Br derivatizing solution was added. The 2:10:1000 (V:V:V) PFB-Br:DIA:ACN stock solution of PFB derivatizing reagent was prepared fresh,

moments before. The remainder of the 198 µL of MeOH:water solubilized fractions were dried down by speed-vac overnight and stored at -20^{o}C. The reaction was incubated for 30 minutes at 60 ^{o}C. After completion of the reaction, 150 µL of Milli-Q water was added to each tube and each sample analyzed by ESI-LC-QTof-MS using an Agilent 6538 LC-Qtof-MS. The intensity of the 436 m/z, corresponding to di-PFB glycine, was monitored. The intensity at 436 m/z of from each fraction was plotted against each RT in Excel, as shown in Figure 3.1.

Analysis of the Glycine-containing
Lipid(s) by MS, MS/MS, and NMR

After the fractions harboring the glycine containing lipids were located, the dried down fractions were solubilized in 0.5 ml of MeOH/water and analyzed by MS and MS/MS using direct injection on the Agilent 6538 Qtof-MS. All major peaks in the MS spectrum were selected and fragmented using CID-MS/MS at 10, 20, 30, 40, and 50 eV.

The RP-HPLC fractions that harbored the glycine-containing lipid(s) were brought up in 600 µL of deuterium oxide (D_2O) for analysis by ^{1}H-NMR at 500 MHz on a Bruker NMR Spectrometer. The residue that was not soluble in D_2O was taken up in 600 µL of deuterated methanol (CD_3OD) for analysis by NMR on a Bruker 600 MHz Spectrometer equipped with a cryoprobe. Sensitivity comparisons between the two instruments were established by measuring the same sample of 5 mM glycine dissolved in CD_3OD on both machines.

Synthesis of Amino-acyl Phospho Anhydride Standards

An amino-acyl phospho anhydride was suspected and appears to be quite fragile, as described in the results and discussion. Searches for commercial sources of synthetic analogue compounds with the same hypothesized linkages were pursued. Such compounds were either not commercially available or had very long shipping times. Therefore, the synthesis of amino-acyl phospho anhydride compounds were initiated to be used as stability standards in the glycine-lipid extraction and analysis process. The first synthesis pursued required dimethyl phosphate, which had to be prepared from the trimethyl form.

Dimethyl Phosphate Sodium Salt

A modified version of the following protocol was used (Zervas and Dilaris, 1955) to convert trimethyl phosphate to dimethyl phosphate sodium salt (Figure 2.1).

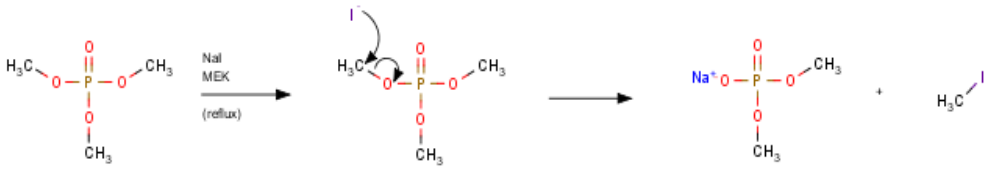

Figure 2.1: Synthesis of dimethyl phosphate from trimethyl phosphate. Trimethyl phosphate was refluxed with sodium iodide (NaI) in methylethylketone (MEK). The negatively charged oxygen of the phosphate group forms a salt with a sodium ion from the NaI. The I^- removes the methyl and forms methyl iodide (CH_3I. The resulting product, dimethylphosphate sodium salt, was obtained (Zervas and Dilaris, 1955).

Trimethyl phosphate (Sigma) (3.3 mL, 28.5 mmol) was added to a 100 mL round bottom flask (RBF) containing NaI (4.7 g, 31.4 mmol) (Alfa Aesar, 99+% dry weight)

and refluxed in 40 mL of MEK for 1 hr. The solution was filtered through a Whatman filter paper (55mm) and the white precipitate was washed with acetone (previously dried over potassium carbonate (K_2CO_3)). The acetone was evaporated under a high vacuum (Zervas and Dilaris, 1955). A mass of 2.82 g was obtained with a 66.7% yield.

N-Fmoc-glycyl
Monomethylphosphate Sodium Salt

The goal using the following protocol was to generate 9-Fluorenylmethoxycarbonyl (N-Fmoc) amino-acyl monomethylphosphate sodium salt, using three N-Fmoc amino acid analogues (glycyl-, leucyl-, and phenylalanyl-). The purpose of the synthesis of these compounds was to link N-Fmoc amino-acids to methyl phosphate to form carboxy-phosphoanhydride esters to be used as internal stability standards.

N-Fmoc glycine (0.5 g, 1.68 mmol) (Advanced Chem Tech) was put into a long 24/40 RBF and a flow of nitrogen was initiated for 15 min. To it, 10 mL of thionyl chloride ($SOCl_2$) (Alfa Aesar, 99+%) was added through a septum and heated to reflux for 2 hr. After reflux, the solution was allowed to cool and the $SOCl_2$ was removed by vacuum distillation (Figure 2.2). The dimethyl phosphate sodium salt (0.273 g, 1.85 mmol) was added to an oven dried 2-neck round bottom flask, and purged with dry nitrogen for approximately 15 minutes. Twenty milliters of dry tetrahydrofuran (THF2), from a Benzophenone/Sodium still, was added to the dimethyl phosphate sodium salt, while stirring. The freshly distilled N-Fmoc glycyl chloride was dissolved in 20 mL of dry THF2. The N-Fmoc glycyl solution was added to the stirring dimethyl phosphate

sodium salt through a septum. A reflux condenser was attached to the 2-neck flask and allowed to reflux overnight. The protocol was modified from the reflux time of 10 hr to a reflux time of overnight. (Kluger and Cameron, 2002) (Figure 2.2)

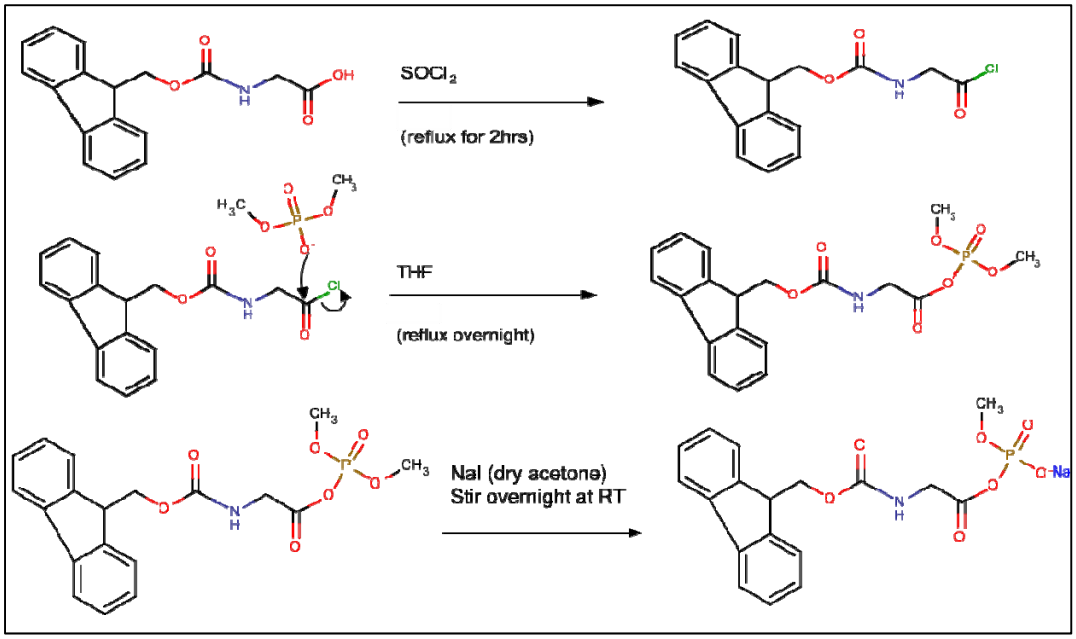

Figure 2.2: N-Fmoc glycine was converted to N-Fmoc glycyl chloride by refuxing in $SOCl_2$ for 2 hrs. The dimethyl phosphate was refluxed with N-Fmoc glycyl chloride in dry THF2 overnight to synthesize N-Fmoc glycyl dimethyl phosphate (Kluger and Cameron, 2002). The last reaction was performed to remove a methyl group using NaI (Kluger, *et al.,* 1990) in acetone dried over K_2CO_3, while stirring overnight.

The mixture was filtered to remove most of the precipitate, and the desired product was present in the filtrate. The THF2 was evaporated and was further removed by high vacuum overnight. A mass of 0.710 g was obtained, that corresponded to a 104 % yield. The ^{1}H-NMR of N-Fmoc glycyl dimethylphosphate was obtained using a Bruker 300 MHz NMR in deuterated chloroform ($CDCl_3$) and shown in Figure 3.11. A phosphorus-NMR (^{31}P NMR) was not obtained.

After the synthesis of F-moc glycyl dimethyl phosphate, one of the two methyl groups was removed, using a modified protocol (Kluger, *et al*., 1990). N-Fmoc glycyl dimethylphosphate (0.4 g, 0.988 mmol) in 4 mL of dry acetone was mixed with NaI (0.6 g, 4.00 mmol) in 2.5 mL of dry acetone and then allowed to stir overnight to react at room temperature. The N-Fmoc glycyl monomethylphosphate sodium salt precipitate was filtered, washed with dry acetone, and the acetone was evaporated to yield the dry product (Kluger, *et al*., 1990). The successful synthesis was confirmed by MS/MS. The highest yield obtained was 28%, however, we had learned from discussion with organic chemists that the N-Fmoc group can be cleaved by free amines. This would pose a problem in the extraction process in plasma, since there are many compounds containing free amines. Human plasma contains many compounds possessing free amines, which can cleave the N-Fmoc moiety. A new synthetic approach was then taken since we were advised by organic chemists that the N-Fmoc group was likely to be rather labile in plasma.

Bis(tetraelthylammonium) Ethylphosphate

Since the susceptibility to cleavage by amine-containing compounds is an issue when using the N-Fmoc protecting group, we looked for a new approach. The scheme outlined in Figure 2.3 was a new synthetic approach taken.

Figure 2.3: Synthesis of Bis(tetraelthylammonium) ethylphosphate. A 40 % Tetraethyl ammonium solution was reacted with dichloro-ethyl phosphate to yield the desired product. (Kluger, *et al*., 1996)

Water was added to a 100 mL RBF and cooled in an ice bath. While stirring, 5.9 mL of ethyl dichlorophosphate (Sigma) was slowly added to the water over 10 min. The solution was stirred for 1 hr and the water was removed by vacuum. A 40 % solution of tetraethylammonium hydroxide (2 eq, 37.0 mL) was added to the residue and the solution was titrated to pH 7.00 with hydrochloric acid (HCl). The solution was frozen and lyophilized to remove most of the water, leaving a light orange paste. A ^{31}P NMR in D_2O was obtained for the desired product, however, this was not referenced to the typically used phosphorus standard using 85% H_3PO_4.

N-boc Glycl Ethylphosphate
Tetraethylammonium Salt

Figure 2.4: N-boc glycine was activated with DCC in dry DCM. Upon activation, Bis(tetraethylammonium) ethylphosphate was reacted with the activated N-boc glycine in order to form N-boc glycyl ethylphosphate tetraethylammonium salt (Kluger, *et al*., 1996)

N-(tert-butoxycarbonyl)-L-glycine (N-boc glycine) (210 mg, 1.2 mmol) was added to an RBF under nitrogen for 10 minutes. To it, 20 mL of dry DCM from a calcium hydride (CaH_2) still was added and the solution was stirred. Dicyclohexylcarbodiimide (DCC) (205 mg, 1.2 mmol) (Acros Organics, 99%) was added and the solution was stirred for at least 5 minutes. Tetraethylammonium ethylphosphate (0.391 g, 1.0 mmol) was dissolved in 5 mL of DCM and injected into the stirring solution through a septum. The solution was allowed to stir for approximately 1 hr, while the progress was monitored by taking aliquots and analyzing them by ^{31}P NMR. A phosphorus peak was apparent in the ^{31}PNMR spectrum in $CDCl_3$ at -7.3803 ppm, corresponding to the compound in an acyl-phosphate linkage. (Kluger *et. al*., 1996), reports ^{31}P NMR to be around -7 ppm in $CDCl_3$ and the starting material to have a chemical shift at 1.68 in D_2O, however, they did not show results for the glycyl analogue. Once the ^{31}P NMR showed the formation of product, the mixture was filtered to remove the dicyclohexyl urea (DCU). The filtrate was washed twice with a 50 mM sodium phenyl phosphate solution buffered to pH 5 to keep the rate of hydrolysis at a minimum (Di Sabato and Jencks, 1961).

The aqueous phase was frozen and lyophilized overnight. The dried material was dissolved in acetone and filtered to remove the acetone insoluble sodium phenyl phosphate. The acetone solution was applied to a Sep-pak Silica 35 cc cartridge; containing 10 g sorbent (Waters, WAT043355) column that had been pre-equlibrate in dry acetone. The literature methods did not specify an elution solvent, therefore, it was necessary to determine what solvent system would elute the desired product but minimize

the possible contribution to hydrolysis. Solvent systems; 100% MeOH, 75:25 Acetone:MeOH, and 50:50 Acetone:MeOH were used as mobile phases via thin-layer chromatography (TLC). The solvent system 75:25 Acetone:MeOH was used as it showed product migration but had the same retardation factor (R_f) values as the 50:50 Acetone:MeOH, therefore, we chose the 75:25 Acetone:MeOH. The lowest percentage of MeOH was chosen, since MeOH can contribute to hydrolysis. N-Boc glycyl ethylphosphate tetraethylammonium salt was eluted with a 75:25 Acetone:Methanol solution. The eluent was evaporated and the compound was further dried under high vacuum resulting in a 52 % yield.

The product was analyzed by ^{1}H NMR , ^{31}P NMR, and MS. The accurate mass obtained using ESI-MS confirmed the presence of the desired compound as shown in the results. The tetraethyl ammonium salt turned out to be very MS unfriendly (which had not been noted in the literature) and produces a very large persistent signal that was very difficult to remove from the mass spectrometer. Therefore, even though we successfully synthesized a desired carboxy-phosphanhydride compound, we decided to utilize a protecting group on the amino end of glycine that we could easily detect by absorbance and fluorescence, without the need to monitor by MS.

Dansyl Protected Amino-acyl Compounds

We decided to use a fluorescent protecting group, and chose 5-(dimethylamino)naphthalene-1-sulfonyl chloride (Dansyl-Cl), as a widely used protecting group for the amino end of glycyl-, leucyl-, and phenylalanyl-ethylphosphate tetraethylammonium salts. Figure 2.5 shows the planned reaction scheme to produce the

Danyl-glycyl-ethylphosphatetetraethylammonium salt. First Dansyl-Cl is reacted with glycine to form Dansyl-glycine (DNS-gly). This was first done on a small scale in order to determine the RT of DNS-gly on RP-HPLC. Unfortunately the reaction did not indicate a successful synthesis then it was planned to be scaled up in order to make sure enough DNS-gly was on hand to move onto the next reaction in which DNS-gly was reacted with Bis(tetraethylammonium) ethylphosphate in the same DCC coupling reaction as with the N-boc amino-acyl ethylphosphate tetraethylammonium salts. However, the inability to obtain a successful synthesis drove us to obtaining DNS-gly commercially.

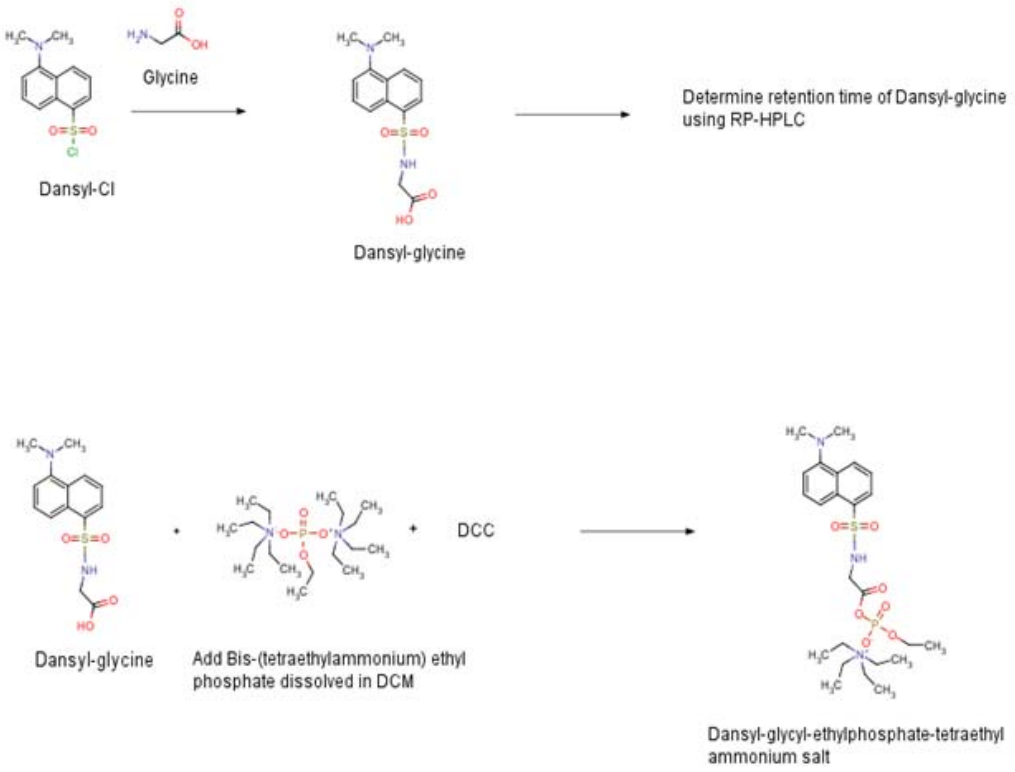

Figure 2.5: The fluorescent derivatizing agent, Dansyl-Cl is reacted with glycine to yield DNS-gly, to determine RT on HPLC. DNS-gly can be used in a DCC coupling reaction to yield DNS-gly ethylphosphate tetraethylammonium salt.

Dansyl-glycyl Ethylphosphate

Tetraethylammonium Salt. (The following was taken from a PhD thesis by Tzvetkova, 2008). DNS-gly (Sigma-Aldrich) (99.3 mg, 1.3 eq) was added to a RBF under nitrogen. Two milliliters of dry DCM was added to the DNS-gly and stirred. Dicyclohexylcarbodiimide (DCC) (51.5 mg, 1.0 eq) was then added to the DNS-gly/DCM solution. This reaction was allowed to run for 5 minutes for the DCC to activate the DNS-gly. Ethyl phosphate tetraethylammonium salt (95.9 mg, 1.0 eq) (mixed separately with 3 mL of DCM) was injected into the reaction through a septum. This reaction was allowed to run for 1 hr, and at that time a ^{31}P NMR was taken to monitor the progress of the reaction. The solution was then filtered and compounds were extracted into the water layer. (Tzvetkova, 2008) The water layer was frozen in -80^{o}C and lyophilized overnight and the DCM layer was evaporated under nitrogen. The dried layers were stored in -80^{o}C until use.

Dansyl-glycyl C16:0 Anhydride. DNS-gly was removed from -20^{o}C and allowed to come to room temperature before opening. DNS-gly (14.6 mg, 1.2 eq) was added to a 25 mL RBF and purged under nitrogen for about 15 min. One milliliter of dry DCM was added and the mixture was stirred. DCC (8.7 mg, 1.0 eq) was added and the mixture was stirred for 5 min. Palmitic acid (C16:0) was solubilized in 250 µL of a 0.1 % Butylated hydroxyltoluene (BHT)/DCM solution and was added to the RBF. The entire reaction was stirred for 2 hr. After 30 min, it was noted that some of the DCM had evaporated; therefore 750 µL of DCM was then added. After the 2 hour reaction, the mixture was filtered through a Buchner funnel to remove the DCU and washed 2 times with

approximately 2 mL each time of DCM. The clear yellow DCM eluent (~ 5 mL) was split in half and both were dried under nitrogen. One was prepped for MS and the other was stored in -20^{o}C. The lack of being able to positively identify the compound in the MS, lead us to fractionate using RP-HPLC. The Phenomenex Jupiter 4u Proteo 90A Reverse Phase Column previously used to fractionate the sample that was fully dissolved in ACN and filtered through a 0.45 µm syringe filter (VWR International). One hundred microliters was injected onto the RP HPLC column, with the following gradient conditions: 85% ACN/15% water to 95% ACN/5% water for 35 min, 95% ACN/5% water from 35.01 min to 85%ACN/15% water until 45 min. The peak profiles were monitored at diode array detector (DAD) signals of 250 nm, 280 nm, 330 nm, and 335 nm and fractions were collected at a flow rate of 1.00 mL/min. The fractions were dried down and stored in -20^{o}C. HPLC runs of DNS-gly, DCC, and a mixture of DNS-gly with DCC, were done in order to determine if it could lead to the determination of the fraction(s) of interest that may harbor the anhydride.

It was thought that perhaps the anhydride may have been stuck to the column. So a different solvent system was used (A = ACN and B = 1:1 MeOH:Isopropanol (IPA)) with the following gradient conditions: 95% ACN/5% 1:1 MeOH:IPA for 35 min, to 0% ACN/100% 1:1 MeOH:IPA for 15 min, 50.01 min at 95%ACN/5% 1:1 MeOH:IPA up until 45 min. However, no peaks of interest were found when monitoring at the 330 and 335 nm diode array detectors (DAD). Another run was initiated with an injection of 10 µL of a 1 mg/mL anhydride/ACN sample. This was ran using the latter gradient conditions with using the IPA/MeOH as solvent B and fractions were collected at a 1.00

mL/min flow rate and the HPLC tracing is seen in Figure AB. Fractions were dried down and stored in -80^{o}C.

The peaks that were seen in the 330 and 335 nm DAD signals, regardless of being present or not in the 230 and 280 DAD signals, were brought up in 200 μL of ACN and serial dilutions were performed. Each fraction of interest from both elutions were analyzed by +ESI MS.

RESULTS

Analysis of Lipids from Human Serum Albumin Hydrophobic Extract

Detected Pentafluorobenzyl-Glycine

Two microliters of each RP-HPLC fraction from purified NF-HC HSA hydrophobic extract was derivatized with PFB-Br and analyzed by ESI-LC-Qtof-MS to identify which fractions harbored the glycine-containing lipid(s). The intensity of the 436.03 m/z signal was plotted vs. the corresponding fraction number. Figure 3.1 identifies fractions 7 and 8 to contain the glycine-containing lipid(s).

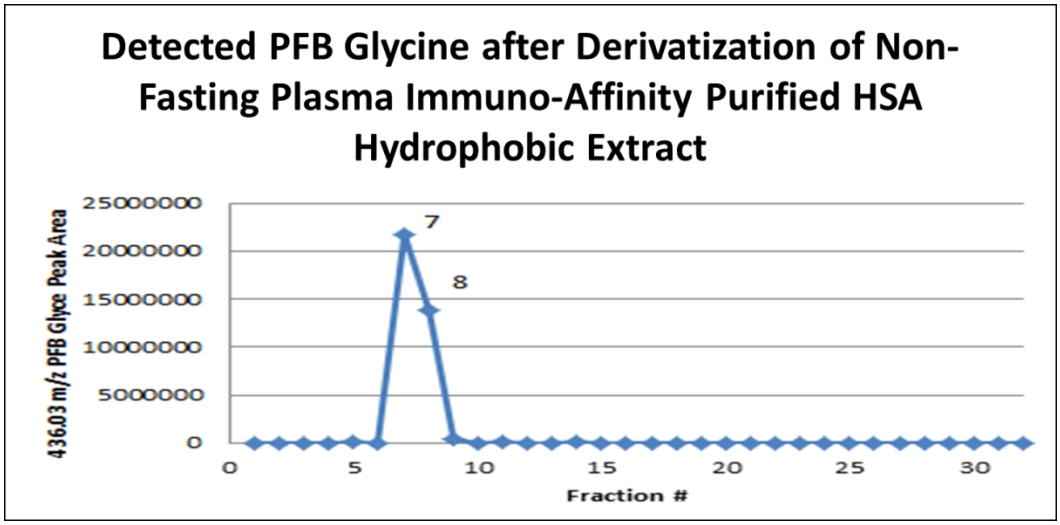

Figure 3.1: Two microliters of each RP-HPLC fraction of the HSA hydrophobic extract was derivatized with PFB-Br. Using LC-ESI-QTof-MS in PI mode, the 436.03 m/z signal, corresponding to the di-PFB glycine, from each sample was manually plotted vs. its corresponding fraction from the RP HPLC fraction. The greatest signal is seen in fractions 7 and 8.

Analysis of the Derivatized
Glycine-containing Lipid

MS of Reverse Phase Fraction 7 and 8. Fractions 7 and 8 were combined and a few microliters were directly injected into the ESI-Qtof-MS (Figure 3.2) and analyzed in positive ionization mode. All major peaks present in the MS were fragmented by CID-MS/MS to determine if a glycine fragment could be detected.

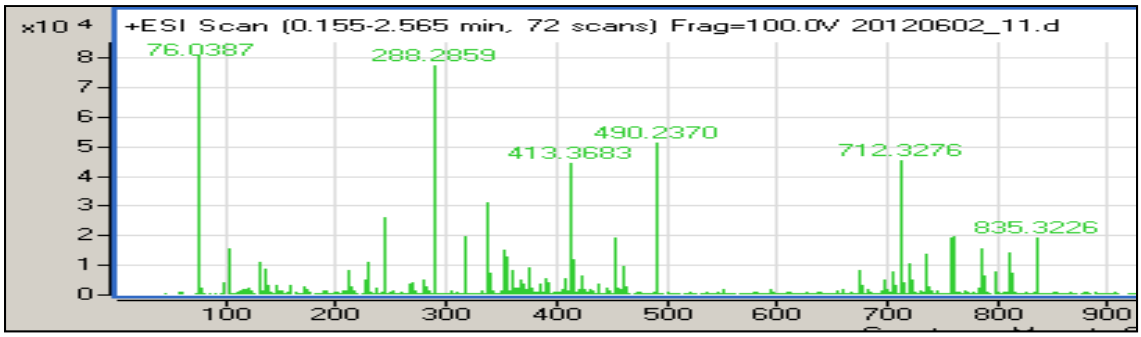

Figure 3.2: Direct Injection of the combined fraction 7 and 8 and analysis by ESI-QTof-MS. Each major peak was fragmented by CID-MSMS in positive ionization mode to determine if it yielded a glycine fragment.

The MS (Figure 3.2) shows a 76.0387 m/z fragment, which had been identified to be that of protonated free glycine [Gly+H^+]. As mentioned in the introduction ^{13}C-glycine, when spiked into the 2:1 DCM:MeOH extraction, does not partition into the DCM layer. From this we were assured that it is not free glycine from plasma but perhaps could be that of either fragmentation in the ionization source or of a break-down product of hydrolysis from the glycine-containing lipid or both.

CID-MS/MS of
712.3276 m/z of Fraction 7 and 8. The only peak to liberate a glycine fragment was that of 712.3276 m/z, when fragmented at 10 electron volts (eV). This peak was then

selected for CID-MS/MS at 20, 30, 40, and 50eV (Figure 3.3). When 10eV was applied, a neutral loss (NL) of 75.0309 was observed. This was determined to be that of a fragment of free glycine. As more fragmentation energy is applied, NL's of 56.06 begin to appear. With a mass accuracy of 14 ppm of the 56.0618 NL fragment, it was determined that this mass corresponds to a butene fragment of an unsaturated hydrocarbon. The Metlin Database allowed identification of m/z and NL fragments labeled in the 50eV spectrum. The NL fragments of 56.06 were NL fragments mostly from lipids. Fragments corresponding to 147.1145 m/z and 189.1616 m/z appeared in the 50eV spectrum and were identified as being polyunsaturated fragments corresponding to the formulas of $C_{11}H_{15}$ and $C_{14}H_{21}$, respectively. One of the most intriguing fragments found in the 50eV MS/MS spectrum is that of a NL of 97.9766. Using the Mass Hunter software, it was determined that this corresponds to phosphoric acid which had a mass accuracy of 3 ppm.

^{1}H-NMR of the D_2O

Soluble Portion of Fraction 7 and 8. The combined fraction 7 and 8 was brought up in D_2O and the water soluble portion was analyzed by ^{1}H-NMR (Figure 3.4) on a Bruker 500 MHz NMR Spectrometer and the insoluble portion was allowed to settle to the bottom of the tube. In addition to the HOD peak, a singlet appearing at 3.405 ppm was attributed to that of the methylene protons of glycine. Glycine is highly soluble in water with a solubility limit of 3 M, while lipids are not water soluble**.** This peak present at the shift where glycine appears in D_2O and the appearance of a peak in the MS (Figure 3.2) corresponding to 76.0387 m/z, indicates that its appearance is due to hydrolysis of the hydrophobic glycine-containing compound originally isolated from purified HSA.

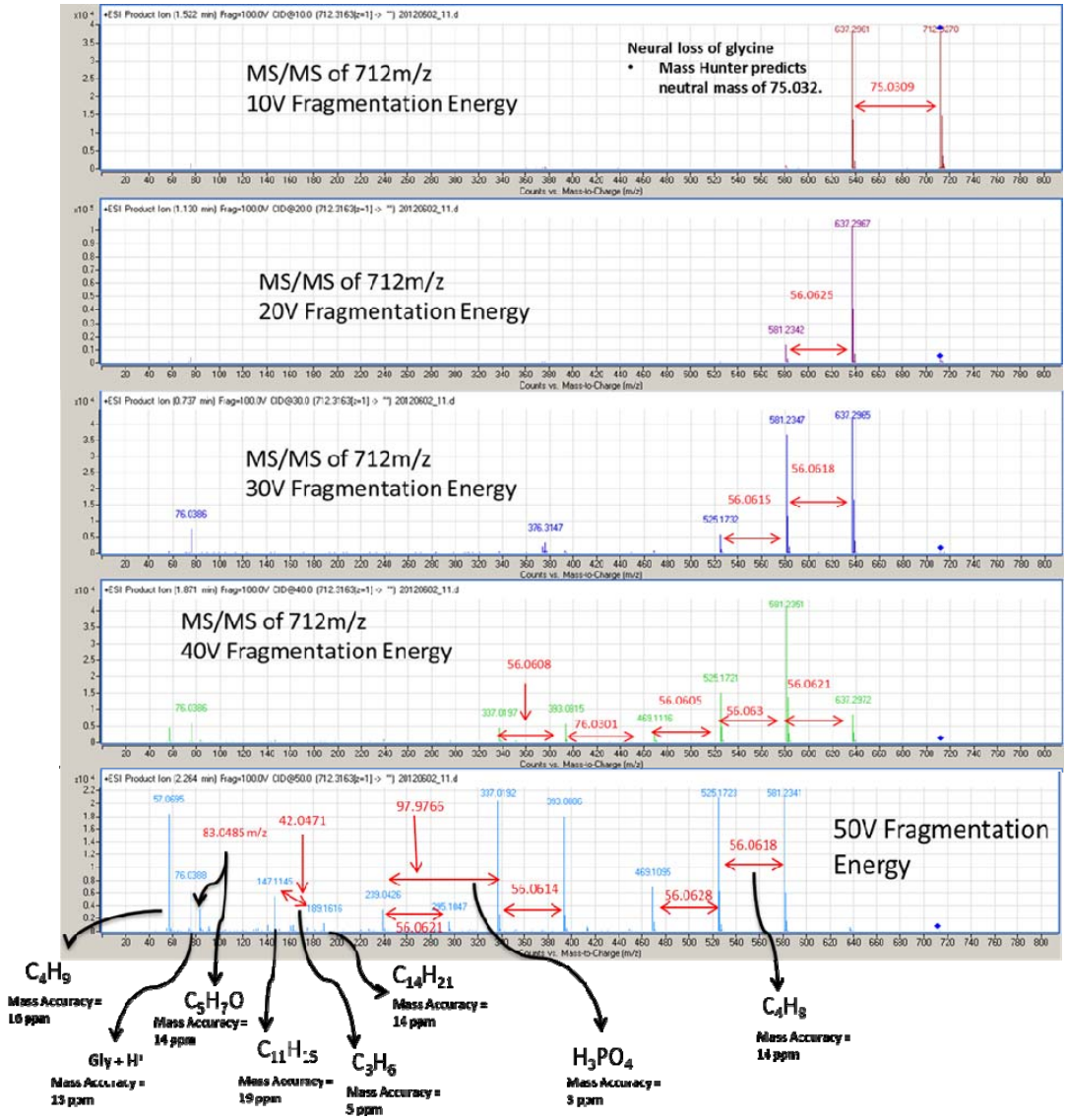

Figure 3.3: CID-MSMS of fraction 7 and 8 using direct injection. 10eV MS/MS yields a NL of 75. Further eV energies caused more fragmentation. Fragmentation indicated lipid attachment, since 56.06 NL fragments correspond to an aliphatic fragment. The 97.9766 was highly indicative of a phosphate group being present.

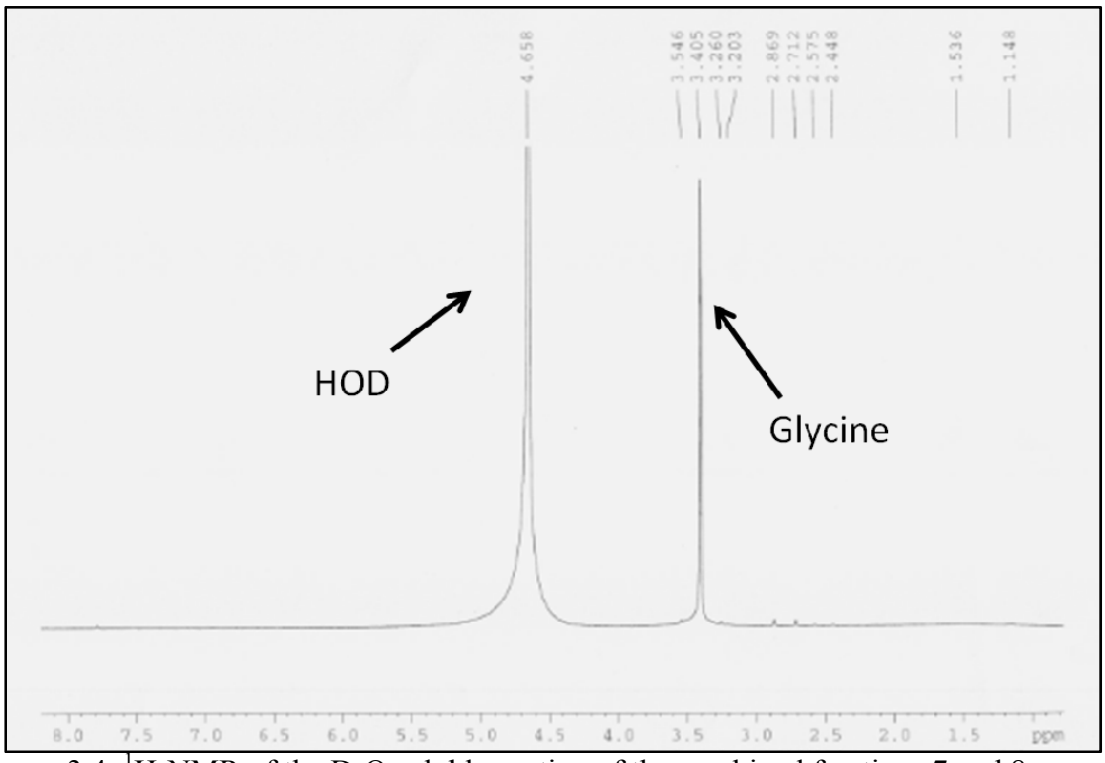

Figure 3.4: ^{1}H-NMR of the D_2O soluble portion of the combined fractions 7 and 8. Analysis was done using a Bruker 500 MHz NMR Spectrometer.

^{1}H-NMR of the D_2O Insoluble

Portion of Fraction 7 and 8 in CD_3OD. The water insoluble portion of combined fractions 7 and 8 was dried and brought up in CD_3OD. Some material was soluble in CD_3OD and some was insoluble. The CD_3OD soluble material was analyzed by 1D ^{1}H-NMR (Figure 3.5), as well as a 2D ^{1}H-^{1}H COSY (Figure 3.6).

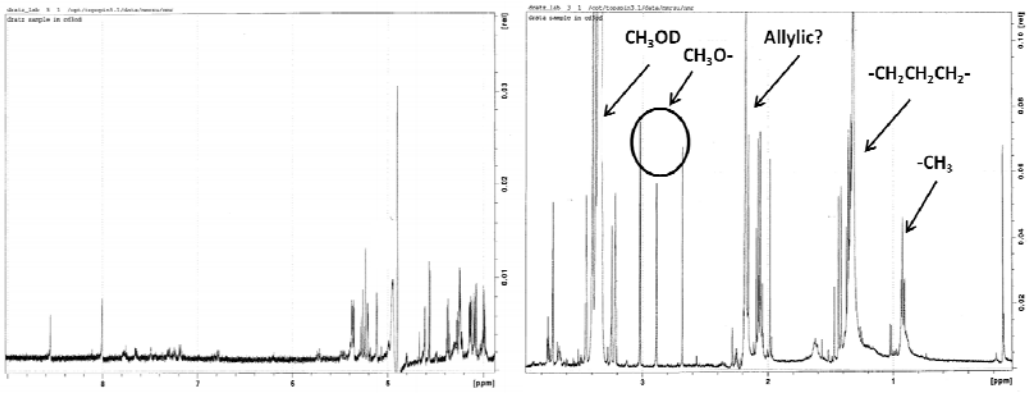

Figure 3.5: The insoluble D_2O portion of fraction 7 and 8 was solubilized in CD_3OD. Some of the material went into solution and some did not. The very large peak just over 3.3 ppm is from the CHD_2OD of CD_3OD.

Many peaks are present that fall into the aliphatic region, as expected since most of the compounds in the HSA hydrophobic extract are lipids. When D_2O insoluble portion was mixed with CD_3OD, some dissolved and some did not.

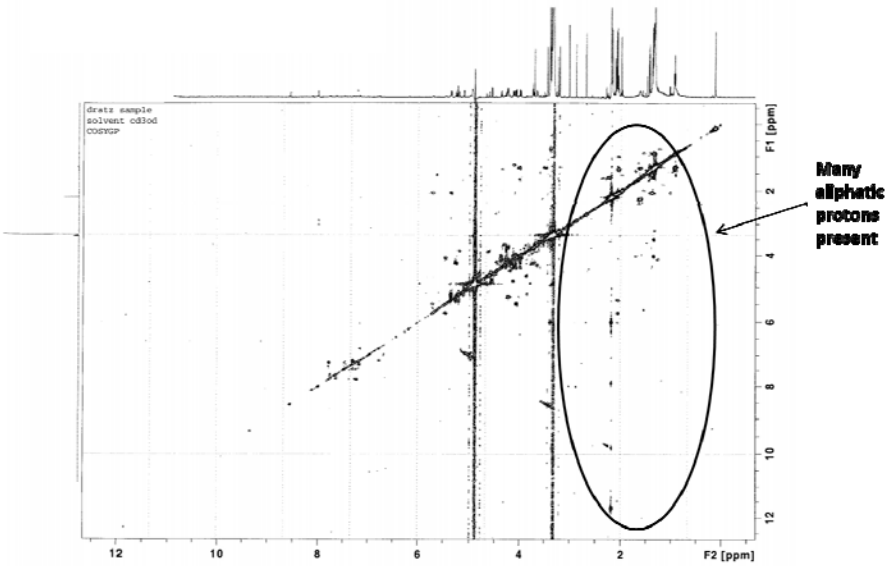

Figure 3.6: 2D ^1H-^1H COSY of the CD_3OD soluble portion of fractions 7 and 8. Since these fractions are impure, the elucidation of the possible structure of the glycine-containing lipid was not feasible. The vertical streaking comes from the very intense CHD_2OD and HOD.

Determination of the Relative
Degree of Hydrolysis of the
Glycine-containing Lipid

In order to determine more information about the relative stabilities of anhydride linkages, further analyses were done. In referring back to Figures 3.4 and 3.5, we had decided to further analyze these spectra by comparing the relative signal of a singlet present in the CD_3OD spectrum that was suspected to be that of the methylene protons of glycine, which may have still been linked to the lipid moiety. The 3.4 ppm region of Figure 3.5 was expanded as shown in Figure 3.7A, revealing two singlets present in the region expected for the glycine methylene protons. Previously we had overlooked this since both glycine and CHD_2OD come in at around similar chemical shift values and the intensity of the CHD_2OD is very large. Referring to Figure 3.7A, it was determined that the singlet at 3.395 ppm was that of free-glycine, since the distance between that peak and far most right peak of CHD_2OD was found to be close in value to the difference of the distance between authentic glycine and the solvent peak as shown in Figure 3.7B) (5 mM glycine, CD_3OD) . The agreement was found to be 0.002 ppm. Therefore, we hypothesized that singlet peak at 3.372 ppm, corresponds to the lipid-bound glycine. The D_2O insoluble portion (Figure 3.5) had residual soluble glycine left over when dissolved in CD_3OD, so it was expected that there would be a peak corresponding to free-glycine in the CD_3OD spectrum. It was suspected that the peak in between the 3.395 peak and the $CHCD_2OD$ peak (3.372 ppm) was that of the glycine still attached to the lipid moiety.

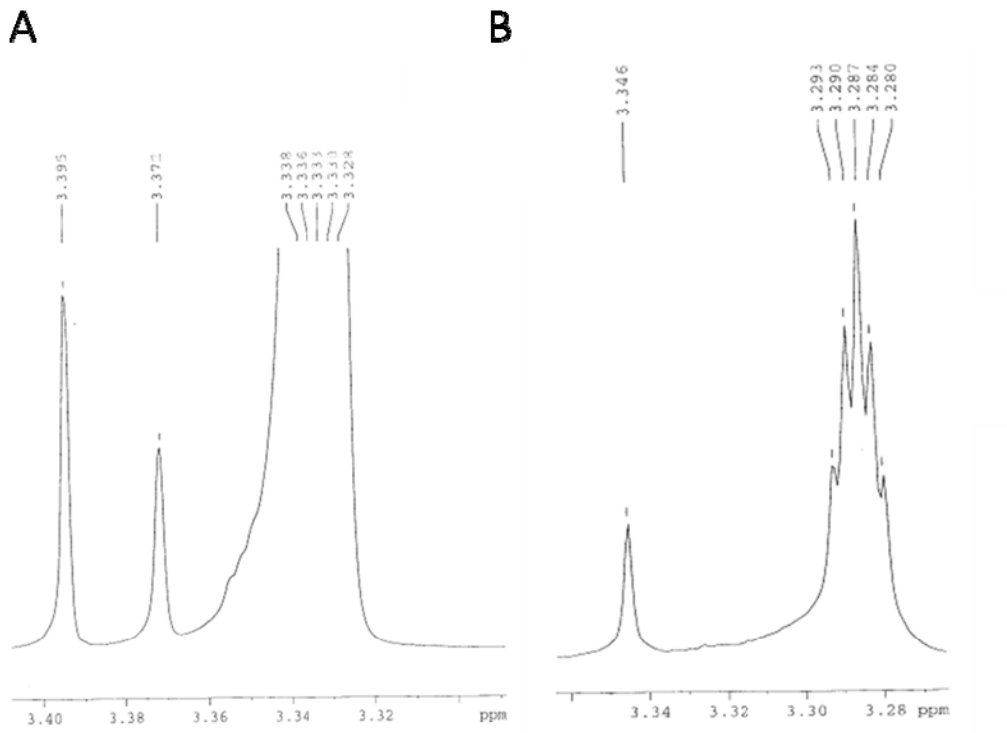

Figure 3.7: ^{1}H NMR spectra comparison of the zoomed-in 3.3 ppm region of the D_2O insoluble portion of fraction 7 and 8 (A); and the same region of authentic glycine in a 5mM glycine sample (B). Both were run in CD_3OD. A was run on a Bruker 600 MHz Spectrometer equipped with a cryoprobe and B on the Bruker 500 MHz NMR.

The D_2O soluble portion of fraction 7 and 8 was analyzed on the Bruker 500 MHz NMR and the CD_3OD soluble portion of fraction 7 and 8 was analyzed on the Bruker 600 MHz NMR Spectrometer equipped with a cryoprobe. Dr. Scott Busse, did a comparison with a 5 mM glycine sample prepared in CD_3OD (Figure 3.7B) to determine the relative difference in sensitivity of the 500 MHz and 600 MHz NMR spectrometers at MSU. The samples to be compared were analyzed on two different instruments, with different receiver gain values, different locking solvents, and different number of scans. We needed to find a correction value to directly compare the intensity of the glycine peak of the D_2O soluble portion of fraction 7 and 8 to the intensity of the suspected glycine peak

(attached to the lipid moiety). This could give an indication of how unstable the glycine-containing compound was under our extraction and preparation conditions that this thesis focuses on. It was determined that the relative differences in intensities of the two peaks of interest were 25 after correction for the different instruments and analysis settings, meaning that the D_2O glycine peak had 25 times more intensity than that of the singlet of interest (thought to originate from glycine in the lipid of interest) in the CD_3OD soluble portion (Figure 3.7A) of fraction 7 and 8. Thus, we appeared to recover only about 4-5% of the compounds of interest in our initial large scale preparation. This pointed out the need for known reference compounds for stability tests at each step of the extraction and sample work up, to seek conditions where the stability can be improved.

^{1}H-NMR of the CD_3OD

Insoluble Fraction in $CDCl_3$. The CD_3OD insoluble portion was brought up in CD_3OD and analyzed by ^{1}H-NMR. Figure 3.8 shows the ^{1}H-NMR spectrum. Most peaks come from the aliphatic region and since lipids are hydrophobic, and some of these presumably are from the hydrophobic breakdown product of the glycine-lipids of interest. However, since the sample is not pure, it is quite difficult to piece together a possible structure of the compound of interest

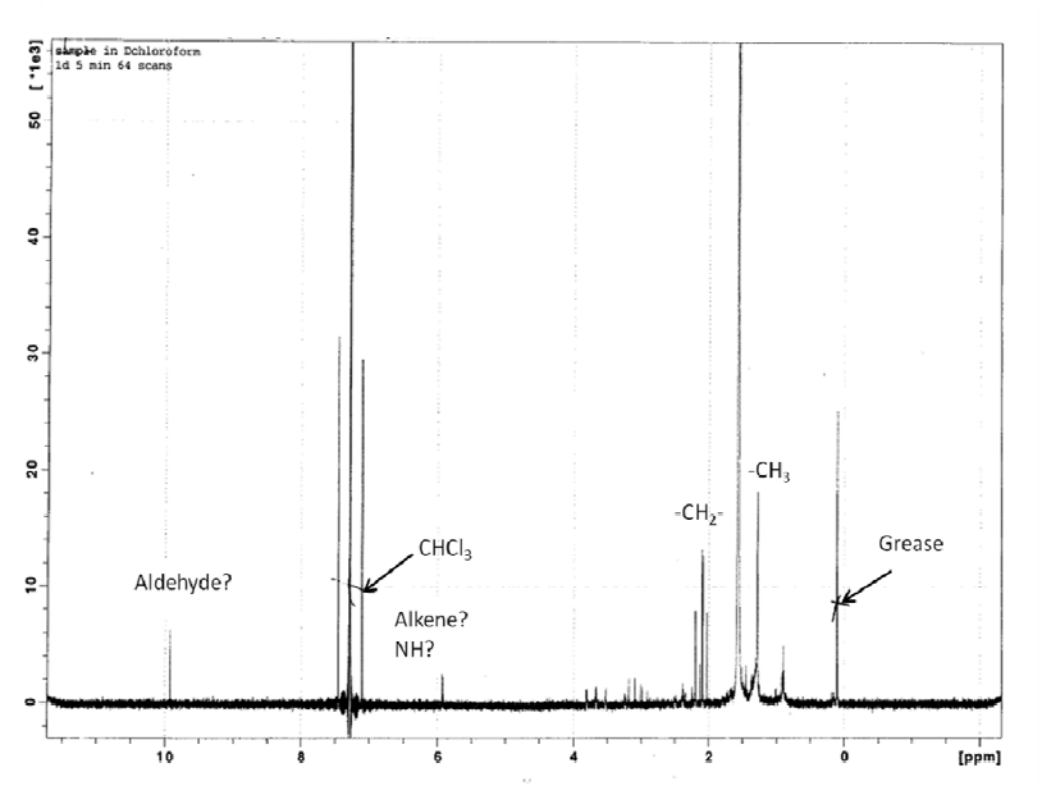

Figure 3.8: ^{1}H-NMR of the CD_3OD insoluble portion analyzed in $CDCl_3$. Spectrum was obtained using a Bruker 600 MHz Spectrometer equipped with a cryoprobe.

Hypothesis of Acyl-phospho Anhydrides

Understanding the Fragility of Acyl-phopsho Andydrides

Based on the fragility of the glycine-containing lipid and the presence of a NL of 97.9766, we hypothesized that glycine is attached to a phosphate moiety via a mixed acyl-phospho anhydride linkage. Current understanding of the literature shows that amino acids frequently linked at the acyl end to a phosphate moiety in an amino-acyl adenylate. This is very important process in biological function because these activated amino acids are used for every amino acid incorporated in protein synthesis.

Figure 3.9 shows the general structure of an amino-acyl adenylate and to the right shows the hypothesized backbone structure of the glycine-containing lipid that corresponds to the mass to charge of 712.3276 m/z. Since the height ratio of the 76.0387 m/z to the 712.3276 m/z peak is roughly 2:1, with there being a very large singlet peak in Figure 3.4 of the 1D ^{1}H-NMR, and the neutral loss of the glycine moiety fragmenting at a very low CID energy also is consistent with a very fragile linkage. As mentioned in the introduction, glycine esters had not been previously found in biology. The glycine-containing compounds that are well known in biology are the N-Acyl glycine compounds.

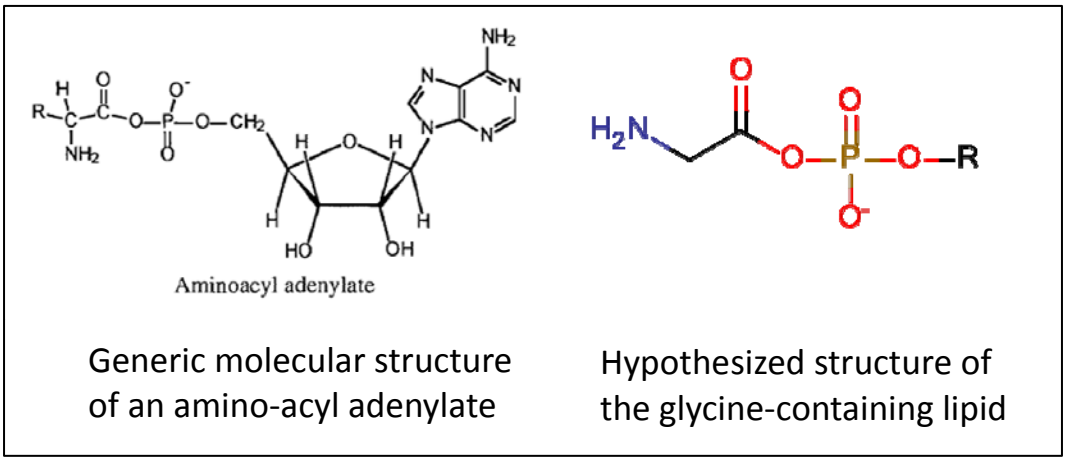

Figure 3.9: Amino-acyl adenylate compounds are the activated intermediates in the synthesis of all peptide bonds in proteins. They are short lived as they are used up. (Structure on the left: Kluger, et al., 1996) The structure on the right is hypothesized to be backbone of the acyl phospho anhydride moiety in our compound of interest.

Since the glycine-containing lipids, our lab had discovered, have not previously been found in biology, their apparent fragility under mild conditions could explain their lack of previous discovery. It is well known in organic chemistry that derivatives of carboxylic acids have different degrees of stability. The acid chloride compounds being

the most unstable and the free carboxylate's being the most stable. Anhydrides and acyl phosphate compounds are considered more reactive than esters. Our goal was to develop the best method in stabilizing compounds with these linkages when exposed to the water layer during extraction and exposure to the water present in the elution fractions after HPLC.

Extensive search of the primary literature dating back to the 1950's and 1960's in order to determine more about the hydrolysis of acyl-phospho anhydrides. An extensive study on the rate of hydrolysis of acetyl phenyl phosphate with various buffers at different concentrations and pH values was found (Di Sabato and Jencks, 1961). All buffers tested catalyzed the hydrolysis of acetyl phenyl phosphate except for phenyl phosphate. Other buffers increased the rate of hydrolysis in proportion to the buffer concentration, above the rate found extrapolated to zero buffer concentration, as shown in Figure 3.10 (Di Sabato and Jencks, 1961).

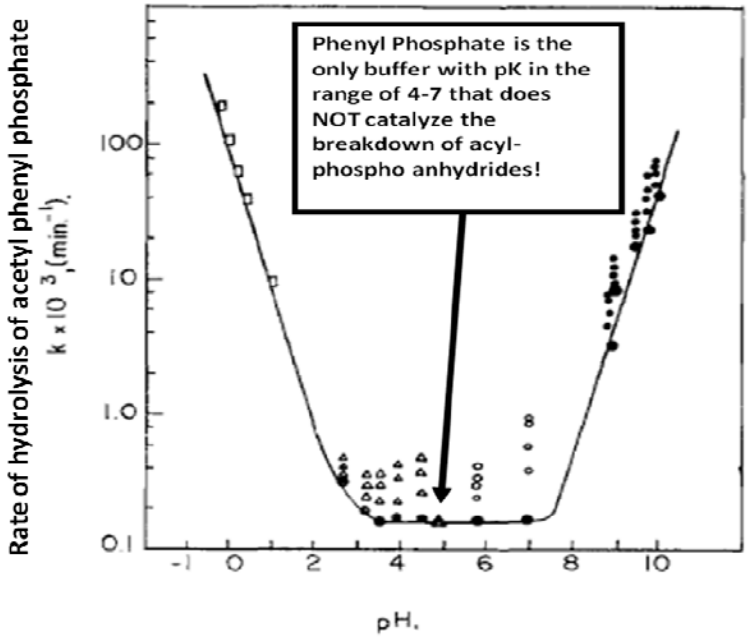

Figure 3.10: The rate of hydrolysis of acetyl phenyl phosphate was measured at various pH values based on the type of buffer that was used and different concentrations. ▲ , corresponds to two different concentrations of sodium phenyl phosphate (0.05 M and 0.2M). Sodium phenyl phosphate is the only buffer to not increase the rate of hydrolysis above that of extrapolated zero buffer concentration.

Analysis of Synthesized N-protected Amino-acyl Phosphospho Anhydride Compounds

Dimethyl Phosphate Analysis by ^{31}P NMR

A protocol from (Zervas and Dilaris, 1955) was used to convert tri-methyl phosphate to dimethyl phosphate sodium salt in a one-pot reaction. ^{31}P-NMR of phosphorus coupled to proton shows a successful synthesis (Figure 3.11) as the phosphorus signal is split by the six neighboring protons to give a septet.

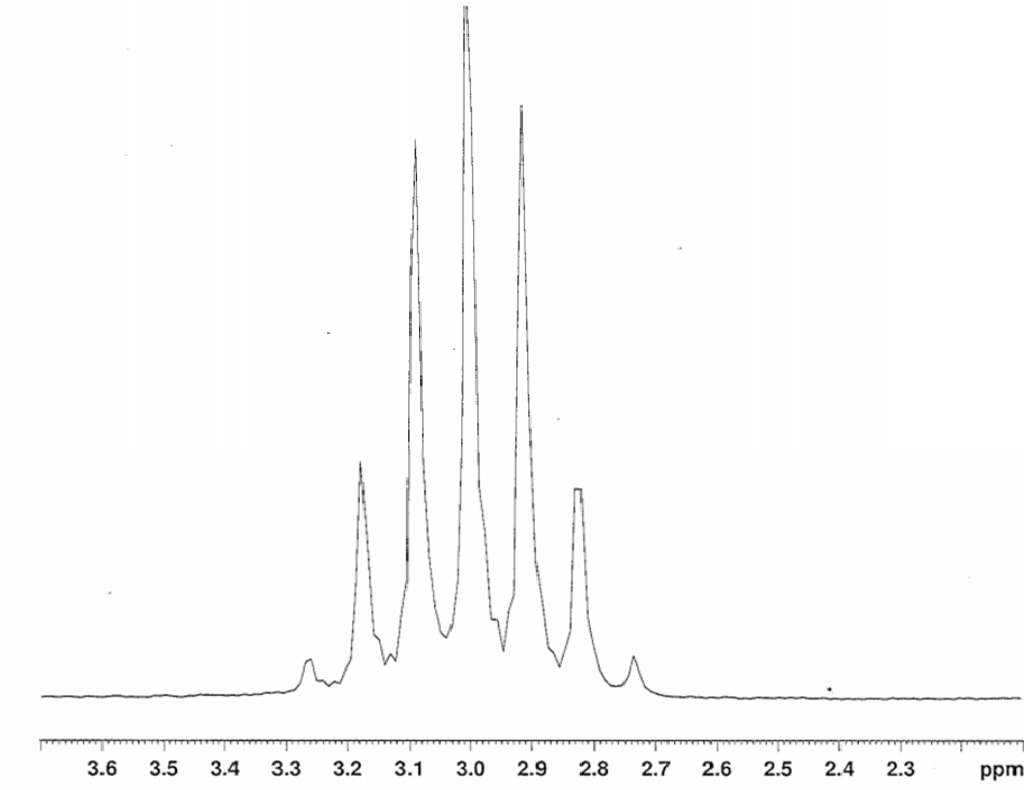

Figure 3.11: ^{31}P NMR proton coupled spectrum of dimethyl phosphate sodium salt. The septet affirms the successful synthesis as phosphorus can couple to proton as has a splitting value of n + 1. Since dimethyl phosphate has six protons present that equates to a septet.

N-Fmoc Glycyl Dimethyl Phosphate

^{1}H NMR in $CDCl_3$. Figure 2.2 first shows the synthesis of N-Fmoc glycyl dimethyl phosphate. N-Fmoc glycine was first converted to N-Fmoc glycyl chloride using $SOCl_2$. The N-Fmoc glycyl chloride was then reacted with dimethyl phosphate to generate N-Fmoc glycyl dimethyl phosphate. NaI was used to remove one of the two

methyl groups to generate the desired product. Figure 3.12 shows the successful assignment of each proton to the appropriate chemical shift of N-Fmoc glycyl dimethyl phosphate. It is worth noting that there are two doublets between 3.7 and 4.0 ppm. Both were found to be from the methyl protons of dimethyl phosphate, since they both had the same J-coupling to phosphorus. It was concluded that the smaller doublet is that of residual dimethyl phosphate starting material. The ^{1}H-NMR shows successful synthesis, however, a ^{31}P NMR was not obtained.

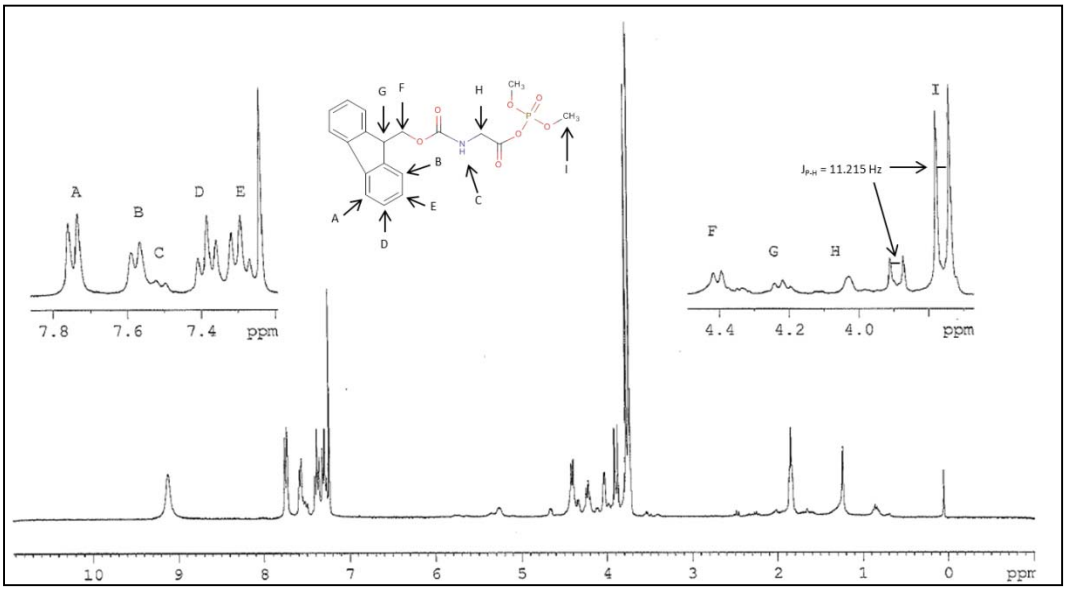

Figure 3.12: ^{1}H-NMR spectrum of synthesized N-Fmoc glycyl dimethyl phosphate. Each proton in the compound was able to be assigned a chemical shift in the spectrum. This spectrum was measured in $CDCl_3$ on a Bruker 300 MHz Spectrometer.

N-Fmoc Glycyl Monomethyl
Phosphate Sodium Salt

Negative Ion CID-MS/MS Upon synthesis and purification of the N-Fmoc glycyl monomethyl phosphate sodium salt, a MS was obtained. Direct injection using CID-

MS/MS in negative ion ESI-mode (Figure 3.13) shows successful synthesis. A desired parent mass of 390.0789 m/z was detected. This parent mass fragmented to yield a NL of [N-Fmoc glycine – OH], which gave rise to a mass fragment of 110.9858 m/z that corresponds to methylphosphate. Methyl phosphate quickly decomposes to yield a NL of methanol forming phosphite, with an m/z of 78.9595.

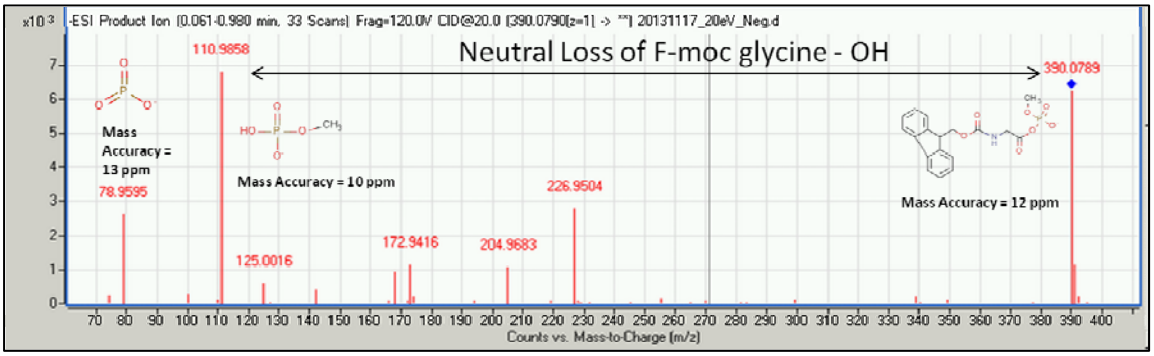

Figure 3.13: ESI-NI-MS/MS of N-Fmoc glycyl monomethyl phosphate sodium salt using direct injection. CID energy of 20eV was used to fragment, using an Agilent 6538 ESI-QTof-MS spectrometer.

While the ^{1}H-NMR of the N-Fmoc glycyl dimethylphosphate and NI-ESI of the N-Bmoc glycyl monomethylphosphate sodium salt show successful synthesis, it was determined that the N-Fmoc group can be cleaved by free-amines. Plasma is known to harbor many compounds which contain free amines. Since our yield was rather low and they can be susceptible to cleavage by free amines, it was decided to seek a new synthetic approach.

Analysis of N-boc Glycyl
Ethylphosphate Tetraethylammonium Salt

^{1}H-NMR in $CDCl_3$. A 40% Tetraethylammonium hydroxide solution was reacted with ethyl diclorophosphate to generate Bis(tetraethylammonium) ethyl phosphate. The product was then used in a DCC-coupling reaction with N-boc glycine to generate N-boc glycyl ethyl phosphate tetraethylammonium salt. The appearance of each respective peak and the appropriate splitting patterns in the ^{1}H-NMR spectrum indicated that the product was made, as the other amino-acyl ethyl phosphate tetraethylammonium salts chemical shifts were reported by Kluger, *et al*., 1996. The ^{1}H-NMR is shown in Figure 3.14.

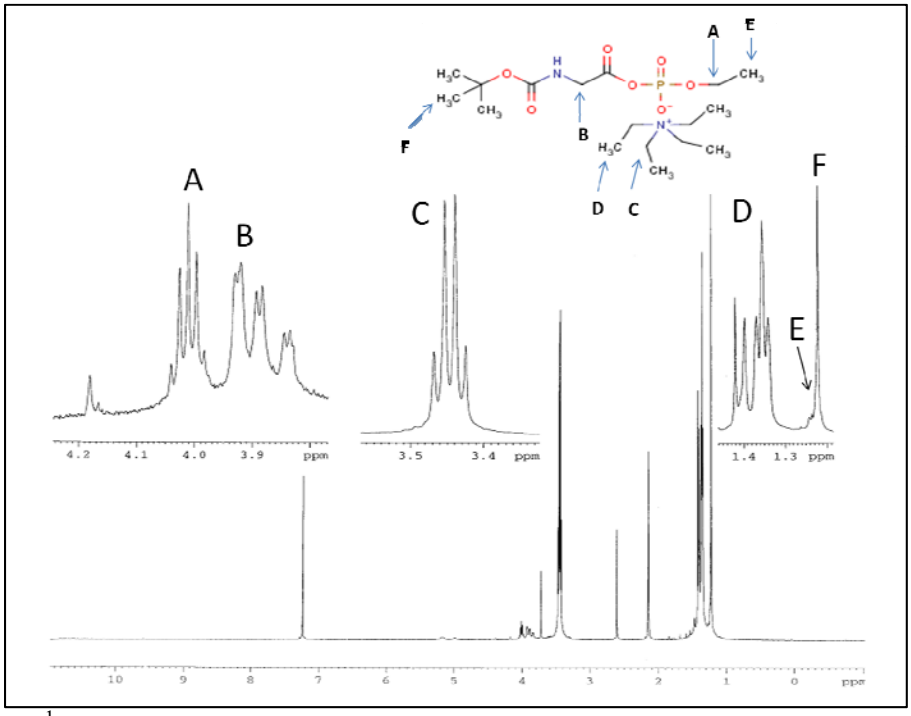

Figure 3.14: ^{1}H-NMR of N-boc glycyl ethyl phosphate tetraethylammonium salt. All peaks were accounted for. It is assumed that the methyl group "E" is under "F" since both F and E are both singlets and most likely overlap in chemical shift.

^{31}P-NMR in $CDCl_3$. The appearance of a phosphorus peak at -7.49 ppm in Figure 3.15, indicated the formation of product. The phosphorus chemical shift for the N-boc compound was stated as made by (Kluger, *et al.*, 1996), the phosphorus shifts of other N-boc amino-acyl ethylphosphate tetraethylammonium salts were at about -7 ppm. This indicated that the compound was made. (However, the shift was not properly referenced to 85% H_3PO_4).

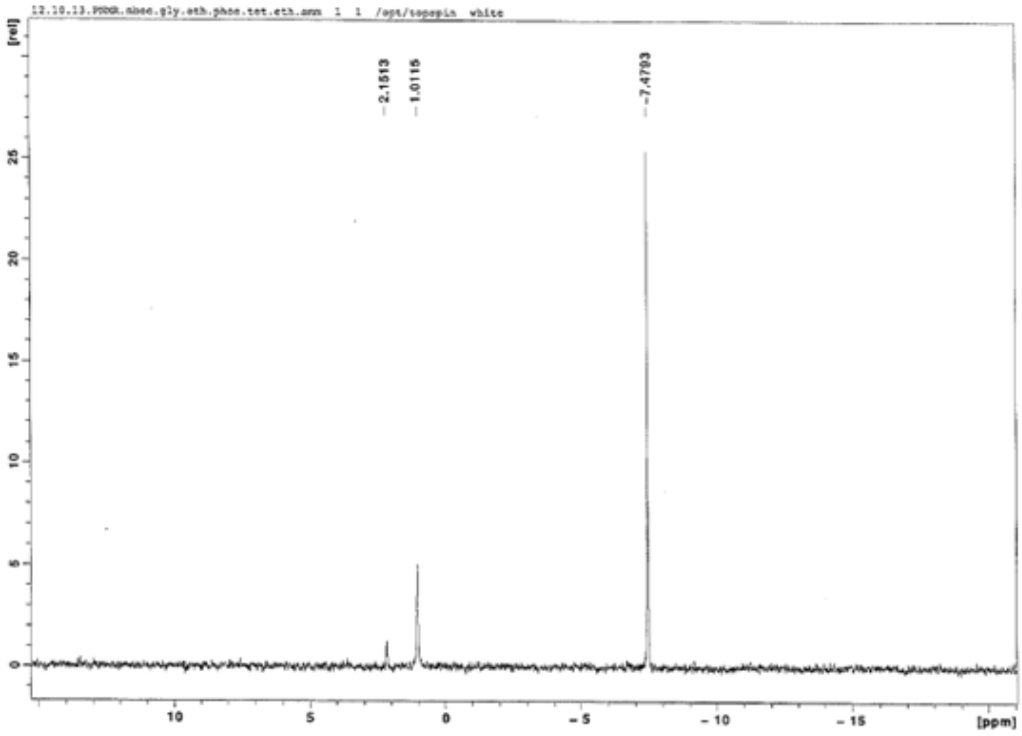

Figure 3.15: ^{31}P NMR of N-boc glycyl ethylphosphate tetraethylammonium salt. The shift at -7.47 ppm corresponds to the ethyl phosphate in the anhydride linkage, while the 1.01 ppm shift most likely corresponds to ethyl phosphate starting material.

CID-MS/MS in Negative Ion Mode. Upon successful synthesis of N-boc glycyl ethyl phosphate tetraethylammonium salt, as determined by the results of the ^{31}P-NMR

and ^{1}H-NMR, the synthesis was repeated substituting N-boc glycine for N-boc leucine and N-boc phenylalanine.

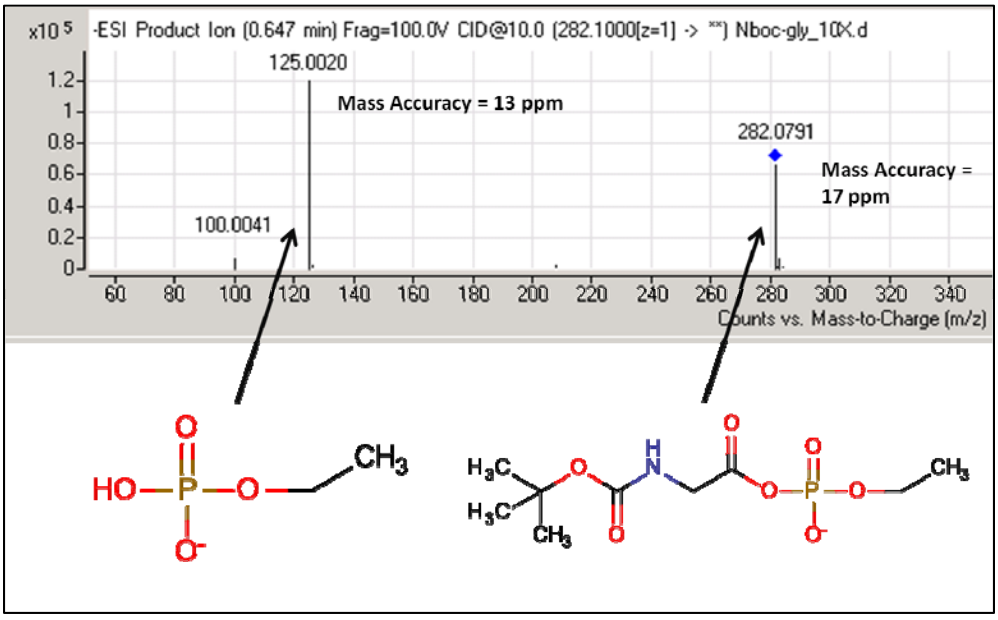

Figure 3.16: ESI-CID-MS/MS of N-boc glycyl ethyl phosphate in Negative Ionization mode. CID electron-voltage was 10eV. The m/z at 282.0791 was determined to be the parent mass of N-boc glycyl ethyl phosphate, while the 125.0020 is that of the ethyl phosphate.

Figure 3.16 shows the CID-MS/MS of N-boc glycyl ethyl phosphate in NI mode. The 282.0791 m/z corresponds to the compound minus the tetraethylammonium salt. Similar fragmentation was seen in Figure 3.13 in that cleavage was seen at the C-O bond of the anhydride linkage of F-moc glycyl dimethyl phosphate, to yield a NL of N-boc glycine minus OH. A fragment is seen that corresponds to 125.0020 m/z, which has been identified as ethyl phosphate.

However, upon analysis by CID-MS/MS using ESI in positive ionization mode, it was determined that the tetraethyl ammonium saturates the detector in the MS. This posed a problem in using these compounds and analyzing them by MS. Hence a different

approach in making N-protected amino-acyl phospho anhydrides was yet again sought after.

Analysis of Fluorescent Protected Amino-acyl Anhydrides

Dansyl-glycyl Ethylphosphate Tetraethylammonium Salt

As mentioned in the previous section, the tetraethyl ammonium salt saturates the detector of the MS and is not a suitable compound to study using MS. Therefore, we sought to use a protecting group that is fluorescent and follow it using HPLC to detect the relative amounts of hydrolyzed product. Dansyl-Cl is a reagent used for the N-terminal derivatization of amino acids, of which is fluorescent and UV active and can be used for detection using HPLC (Harris, 1988).

Dansyl-Cl was first reacted with glycine to produce DNS-gly for the purpose of the determination of the RT on RP-HPLC. Different amine quenchers were used in order to find one that would be efficient at quenching the reaction and form a product that would elute at a significantly different RT than DNS-gly would. The quenchers used were NH_3, pyridine, n-butyl amine, and glycine. Unfortunately, we were unable to detect successful synthesis.

It was then decided to purchase DNS-gly for these reactions. A protocol was obtained that used DNS-gly with a DCC-coupling reaction of ethylphosphate tetraethyl ammonium salt (Tzvetkova, 2008). Upon allowing for the 1 hr reaction time as outlined in the procedure, the reaction was analyzed by ^{31}PNMR. The ^{31} PNMR did not show a

shift that indicated successful synthesis, but did have a peak that was indicative of unreacted starting material.

DNS-glycyl C16:0 Anhydride

A separate synthetic approach was taken to perhaps determine the unknown-glycine containing lipid maybe a mixed carboxyl anhydride. Since we believed that this unknown glycine-containing lipid is an anhydride instead of an ester (due to increased instability of the compound), and also that there have been water-depth penetration studies of water into the micelles of phospholipids that have shown that the ester-linkages of the phospholipids are constantly exposed to water, so as a strong indicator that esters are much more stable than anhydrides (Simon and McIntosh, 1986).

It was hypothesized that perhaps this compound could be a part of a mixed carboxyl anhydride with glycine. In order to test if glycine maybe be attached to the unknown glycine-containing lipid via a mixed anhydride, we decided to synthesize a mixed carboxyl anhydride using DNS-gly and C16:0. The DCC-coupling protocol used for the synthesis of DNS-gly with ethyl phosphate tetraethylammonium salt (Tzvetkova, 2008), was used to synthesize DNS-gly C16:0 anhydride. DNS-gly was reacted with C16:0 in order to generate the DNS-gly C16:0 anhydride. Also, we determined that fatty acids can be used to make fatty-acid anhydrides using the same DCC-coupling reaction (Selinger and Lapidot, 1966) this lead us to believe that DCC could couple these to compounds together as an anhydride.

HPLC of Reaction Product Using
Solvent A: Water and Solvent B: ACN. The product obtained was needed to be fractionated on RP HPLC (Figure 3.17) in order to further purify for MS analysis. We were unable to identify based on the elution profile observing at 330/335 nm. We hadrun DNS-gly, DCC, and a 1:1 mixture of the two separately, on RP to rule out fractions that it most likely would not be in. The results did not indicate presence of the anhydride, so this indicated that it may still have been retained on the column.

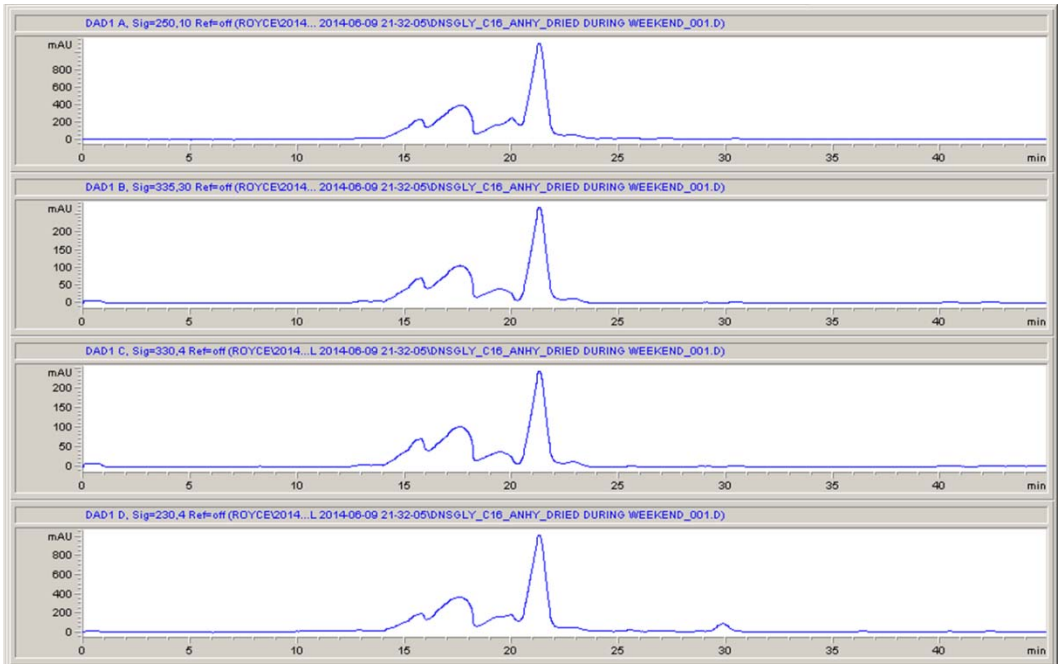

Figure 3.17: Four DAD signals were employed to determine if the DNS-gly-C16:0 product was made. A gradient outlined in the text was usedusing Solvent A: water and Solvent B: ACN. A Phenomenex Jupiter 4u Proteo 90A Reverse Phase Column was used.

HPLC of Reaction Product Using
Solvent A: ACN and Solvent B: IPA/MeOH. Hence, a different mobile phase using a different gradient was used to determine if any previously retained material could be eluted, (Solvent A: ACN, Solvent B: IPA/MeOH). After running the new gradient

conditions, it did not appear to be retained on the column. It was then decided to inject 10 µL onto the column, using the latter gradient conditions (Figure 3.18) previously stated, and collect fractions to be analyzed by MS.

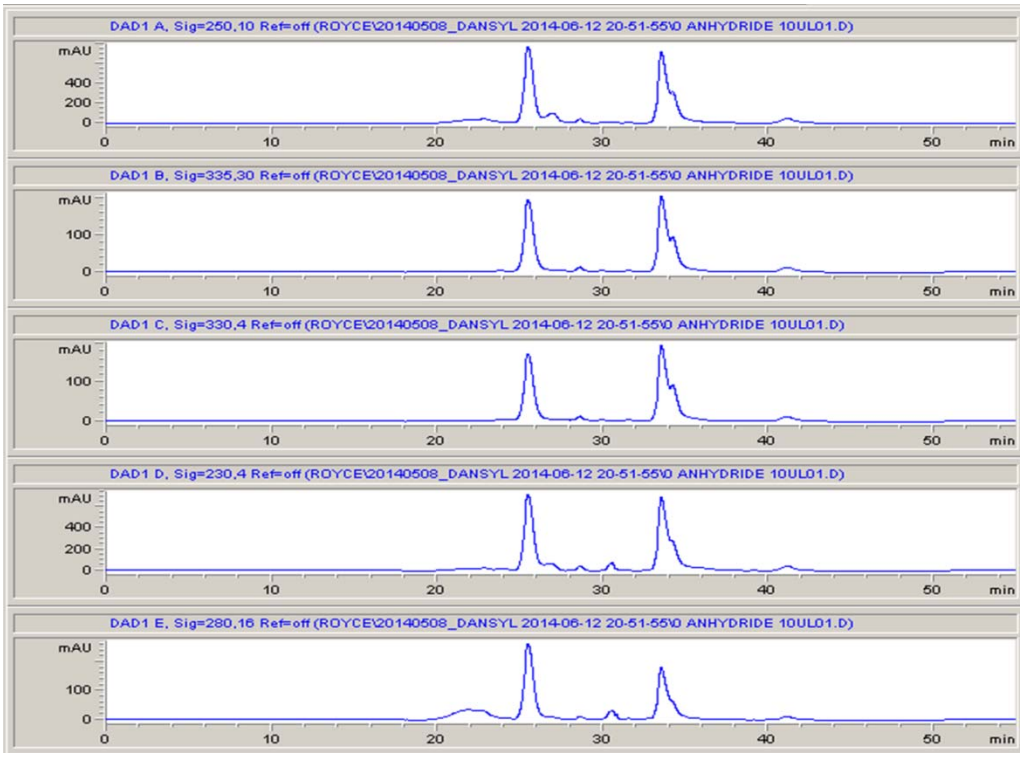

Figure 3.18: Sample was injected onto the Phenomenex Jupiter 4u Proteo 90A Reverse Phase Column and ran under new gradient conditions as well as a new mobile phase using Solvent A: ACN and Solvent B: IPA/MeOH)

CID-MS/MS in Positive Ion Mode. The major peaks present in Figures 3.16 and 3.17 and peaks that appeared in 330 and 335 nm (but not 230 and 280 nm), were analyzed by MS to determine if any harbored the DNS-gly C16:0 anhydride possessing a an exact mass of 546.3127 Fraction 34 (Figure 3.18) was determined to harbor the DNS-gly C16:0 anhydride by MS/MS (Figure 3.19).

In Figure 3.19, the results of the MS/MS indicate that DNS-gly C16:0 anhydride was successfully made. This is indicated by the presence of a 547.3151 m/z peak. Although it is not shown in detail, there are typical isotope peaks present that would occur when a compound contains sulfur. This was determined to have of accurate mass of 9 ppm. The compound was fragmented using CID MSMS which yielded a 309.0890 m/z product ion. This corresponds to the protonated DNS-gly and was found to have an accurate mass of 4 ppm. It indicates that fragmentation had occurred at the C-O bond of C16:0. The bottom spectrum is an inset of the top spectrum and shows a peak at 239.2363 m/z which may correspond to C16:0 minus OH, with this fragment retaining the charge. It still shows fragmentation happening at the same bond but the charge is being retained on the other side of the molecule. The mass accuracy was found to be 5 ppm.

Time Stability of N-boc Phenylalanyl Ethylphosphate Tetraethylammonium Salt

Upon purification of the N-boc phenylalanyl ethyl phosphate tetraethylammonium salt using a Sep-pak Silica 35 cc vacuum cartridge; 10 g sorbent cartridge (Waters, WAT043355) column, ^{31}P NMR was carried out in order to determine if the compound had eluted from the column and possibly stayed intact as well. Figure 3.20A shows the shift that corresponds to the phosphorus in the anhydride linkage. In comparison to Figure 3.20B, this shows that as the dried down material was stored in -20^{o}C for ~5 months, it is apparent that hydrolysis had taken place. Although it is known that the rate of hydrolysis is slowed down at very low temperatures, it is not stopped. In comparison of the two spectra, storage in -20^{o}C is not an ideal storage temperature for compounds

with these types of linkages. This shows, that if the unknown-glycine containing lipid is of an anhydride linkage that eventually over time it breaks down. We will store samples in the future at -196^{o}C and take steps to ensure that the stored samples are kept very dry. Much of the time during purification of the unknown glycine-containing lipid, the fractions were in their elution buffers while being dried down, and the length of these steps will be minimized by using freeze drying more extensively after more rapid organic solvent removal.

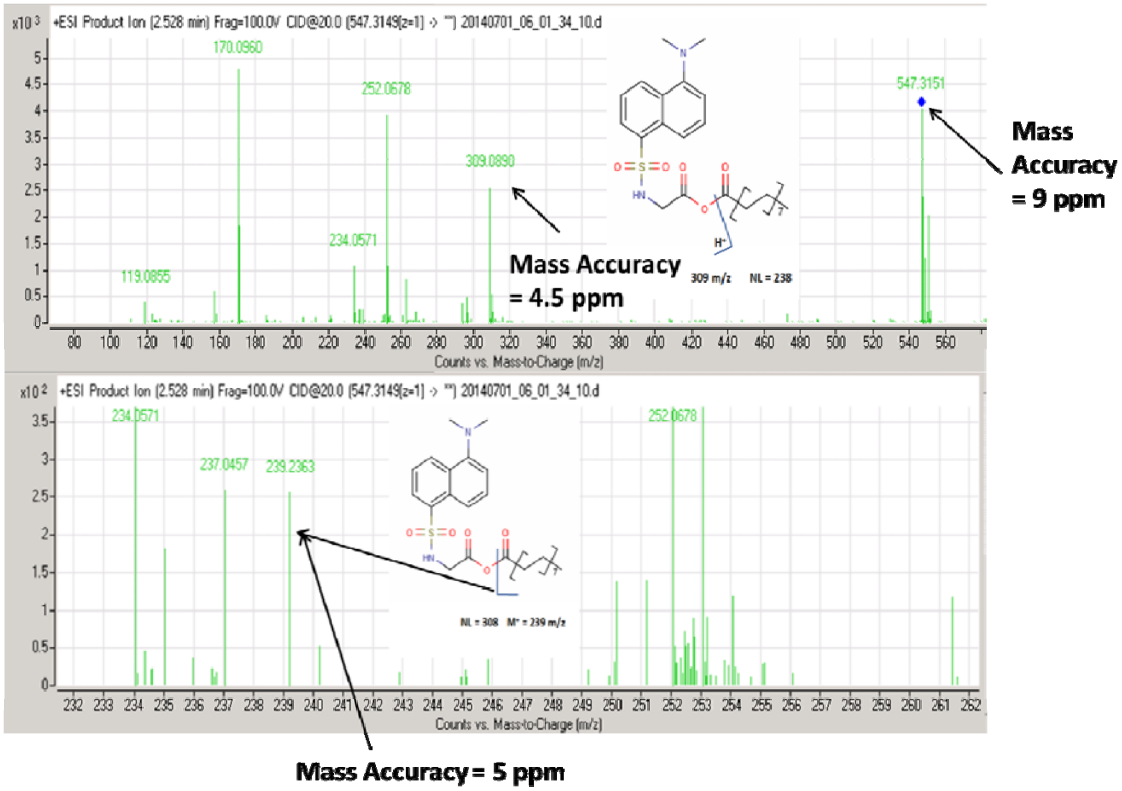

Figure 3.19: Direct injection of DNSGly-C16:0 anhydride. The peak at 547.3151 m/z was identified as that of DNS-gly-C16:0. Sulfur isotope peaks are seen as further indication that the parent mass contains a sulfur atom, as a dansyl group does. The top spectrum shows the MS/MS of 547.3151 at a CID @ 20eV. The top spectrum shows a peak at 309.0890 m/z, corresponding to protonated DNS-gly. The bottom spectrum is an inset that shows a fragment corresponding to C16:0 minus OH.

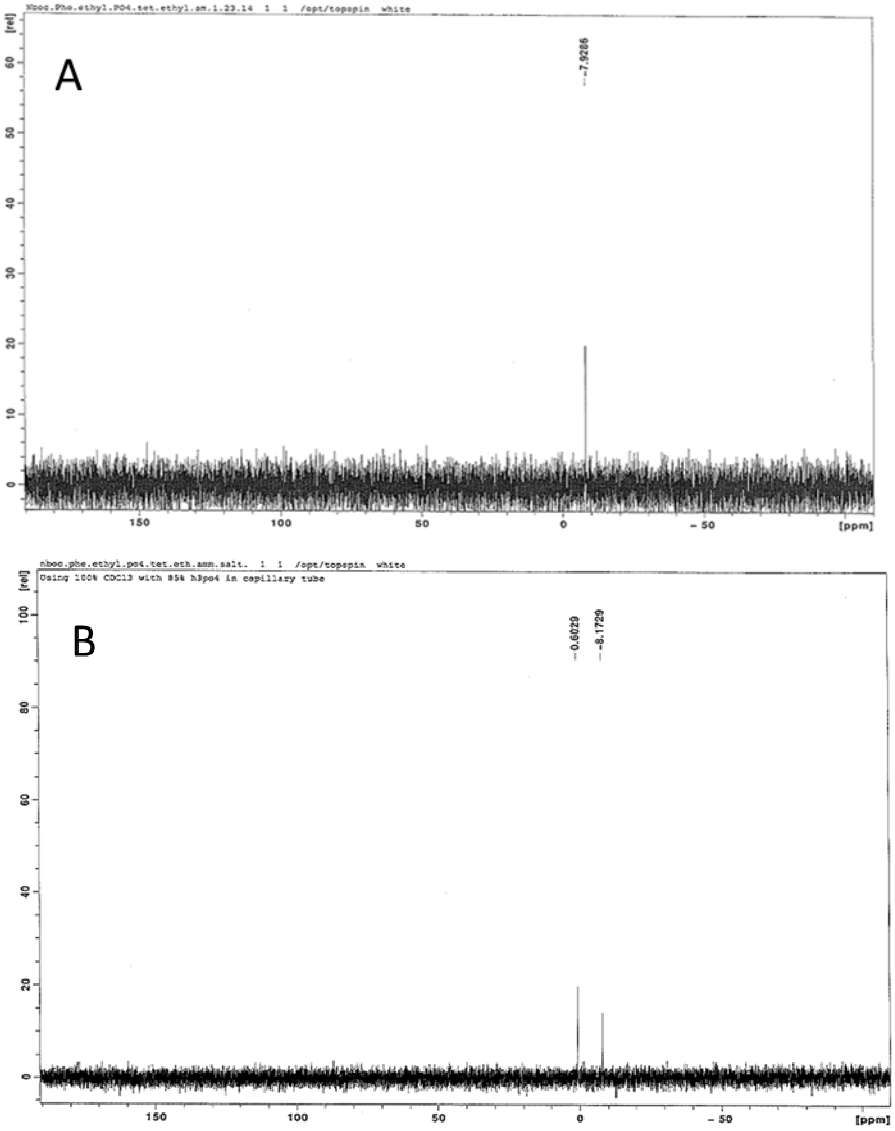

Figure 3.20: Comparison of the ^{31}P-NMR shifts of purified N-boc phenylalanyl ethylphosphate tetraethylammonium salt analyzed at two time points. Spectrum A was run in $CDCl_3$, and, was externally calibrated to 85% H_3PO_4 in D_2O. The spectrum still shows one phosphorus peak at -7.9 ppm, where the literature showed the chemical shift to be -6.8 ppm, indicative that the product was made and relatively pure from any starting material. Spectrum B was run in $CDCl_3$ at ~ 5 months later after being stored dried at -20^{o}C. Spectrum B was externally calibrated against 85% phorphoric acid in a capillary tube locking to $CDCl_3$.

DISCUSSION

Dr. Jared Bowden previously found that there are a family of glycine containing compounds that were changed in relative concentration of in T2D by 2-fold (Figure 1.15) **and the different compounds, separated by RP-HPLC changed by at least 50 fold between F-T2D and F-HC (Figure 1.18**). At this point in time similar glycine-containing lipid compounds have not been previously reported. Dr. Jared Bowden's dissertation showed that the novel compounds of interest were carried on HSA exclusively and that this general class of glycine-containing lipids occurred in both humans and mouse plasma. Dr. Bowden studied HSA to uncover how the cargo carrying capacities differ in T2D vs. HC. As he indicated in his thesis the literature clearly shows that binding of different compounds at one of its many sites can alter HSA's binding capacities at other sites via allosteric regulation (Bowden, 2011). Fatty acid analysis is typically done using derivatization techniques to make volatile products that can be detected using GCMS, and using PFB-Br as the derivatization reagent, can detect derivatized products down to the femto-molar level (Pawlosky, *et al., 1992*).

Dr. Bowden showed that authentic glycine, upon PFB-Br derivatization, has the same retention time and same fragmentation pattern as was derived from the unknown glycine-containing lipid compounds (Bowden, 2011), There is a considerable body of information in the literature that low plasma glycine levels predict the development of IGT and T2D seven years in the future (Wang-Sattler, *et al*., 2012), that 5 grams of oral glycine administered along with 75 grams of glucose in the OGTT greatly increases insulin sensitivity without effecting insulin levels (Gannon, *et al*., 2002), that proteins

high in glycine improves IR (Gannon, *et al*., 2002), and that glycine is a "conditionally essential" amino acid that cannot be produced in sufficient amounts under some physiological conditions (Wang, *et al*., 2013). This evidence together with Bowden's finding of a large change in the chemical species of these glycine-containing compounds in F-T2D and F-HC subjects, and the observation that both compounds interchange rapidly in the transition from fed to fasting (Figure 1.18) implies that the metabolism of these glycine-lipids are important in the mechanism of T2D and IR.

When glycine is derivatized by PFB-Br there are three places that it can attach: the oxygen as part of the carboxylate and two places on the amino group. We had seen in the fragmentation data that (specifically in Figures 1.16 and 1.17) m/z species were detected for mono, di and tri-PFB glycine. We chose to monitor at 436 m/z, in positive ion ESI-MS since it was found that the sensitivity is the highest when glycine is derivatized with two PFB molecules.

Other very important pieces of information were the studies showing that: A) The novel glycine-containing lipids partition into the DCM:MeOH layer upon extraction whereas authentic glycine partitions into the H_2O: MeOH layer, as shown by spiking plasma with authentic ^{13}C-glycine; B) Determination that PFB-Br cleaves the glycine-containing lipid(that is attached at the carboxyl end) to liberate PFB-glycine but not if it were bound as an amide to the amino end; C) Determination that the glycine-containing lipids possess different RT values on RP-HPLC; D) Assessment that amino-Schiff bases of glycine are not cleaved by PFB-Br, and E) that sulfur did not appear to be present in the MS, due to the lack of characteristic sulfur isotope ratios in the MS (tentatively

excluding thio-ester linkages). All of these previously stated foundational studies were important because they give insight in that these glycine-containing compounds/lipids were attached to a hydrophobic moiety, since the hydrophobicity of the lipid moiety pulls glycine into the DCM:MeOH layer. Furthermore, that the glycine-lipids are very different in F-T2D and F-HC since these different species have different RT values on RP-HPLC, indicating different interactions with the column and the solvent mobile phase. Furthermore, there is relatively rapid metabolism of these compounds and many other species present in NF-HC (Figure 1.18).

All the findings A-E above are very informative, but finding B is the primary statement that drove the investigations in this current thesis. Since Dr. Bowden had shown that (Refer to Table 1.2) PFB-Br cleaves esters but not amides, nor does it cleave a glycine-Schiff base, and the lipid attachment must be at the carboxyl end (Bowden, 2011). Furthermore, the MS and MS/MS data could not be matched to any of the lipid-soluble compounds in the Lipid Maps database (containing 35,000 lipids) or the METLIN metabolite database (containing about 60,000 metabolites).

At the start of the work for this thesis, it was clear that we needed to scale-up the amount of plasma processed to analyze for HSA cargo content, because our goal was to eventually determine the structure of these compound(s), so we need to use NMR in order to determine the atomic connectivity in the compounds of interest. NMR is far less sensitive than MS that we needed to process a great deal more plasma to obtain the HSA-bound lipid fraction. This work started by adopting the same extraction and analysis

methods as had been used in Jared Bowden's PhD work (Bowden, 2011), in order to study and analyze these compounds.

We started with NF-HC plasma, since it was easily available and appeared to contain both the glycine-lipid compounds characteristic of F-T2D and F-HC, as well as perhaps four additional glycine-lipids with different RP retention times (Figure 1.18). We pooled 150 mL of NF-HC plasma from several volunteer donors. When each fraction was obtained from the RP fractions of the NF-HC HSA hydrophobic extract and analyzed for glycine-containing lipids, using PFB-Br and the 436 m/z signal, there was a very large peak in Fractions 7 and 8. The preparative HPLC column used here had less resolution than the column used for the separation in Figure 1.18 and it is also likely that pooling the plasma from several (six) NF-HC donors had led to consensus compounds, whereas the other compounds in Figure 1.18 for NF-HC may be quite diet-dependent. Figure 3.1 shows, based on the signal of 436 m/z, which fractions harbored this lipid. Since it was likely that fractions 7 and 8 contained similar compounds, they were pooled together. Since it was our goal to learn more information about these compound(s), it was important to determine their masses and fragmentation pattern using MS/MS.

When Bowden carried out MS and MS/MS on the glycine-containing lipid compounds he observed neutral loss cleavage of the glycine moiety, at low CID energies on many of the MS features. This would suggest that evidence for glycine NL is a good strategy, when analyzing glycine containing lipids in our larger scaled-up preparations.

The 712.3276 m/z MS in positive ion mode was the m/z of most interest because it was the major m/z peaks that liberated glycine NL, when fragmented using CID-

MS/MS. However, it was interesting to also see a 76.0387 in the MS with no CID, that corresponds to the glycine-H^+ ion. We concluded that this MS feature was likely to be the product of hydrolysis of the compounds of interest, but it was possible that it was a fragment from the glycine-containing lipid since sometimes upon ESI ionization fragile compounds can decompose during ESI.

Each CID-MS/MS at increasing fragmentation energies reveals more information about the structure of this glycine-containing lipid. At the lowest CID energy, it is observed that a NL of glycine is the first to fragment, suggesting that this is the most fragile linkage in the compound. When the CID energy is increased in 10eV increments, more NL fragments were apparent. These mainly came from 56.06 fragments. In search on the Metlin Database, the fragment was identified as likely to be a butene fragment, usually associated with hydrophobic hydrocarbon chain containing compounds. When the CID energy was increased to 50eV there was a great deal of fragmentation taking place. More evidence of a hydrophobic chain being present were fragments that corresponded to a 189 and 147 m/z, identified as likely to be $C_{14}H_{21}$ and a $C_{11}H_{15}$, respectively. These fragments have high degrees of unsaturation (due to the low proton to carbon ratios), this indicates that the compound contains poly-unsaturation. However, the fragment of most interesting in this CID spectrum was the NL of 97.9766. This fragment was indicated as phosphoric acid (H_3PO_4), as having a mass accuracy of 3 ppm. It would have been desirable to obtain negative ion MS of these compounds, but that mode of the instrument was not working at the time these measurements were carried out.

When the material from fractions 7 and 8 was dried down and was put into D_2O, some of it did dissolve, but some did not dissolve (since the compounds of primary interest are hydrophobic). When analyzed by 1D ^{1}H-NMR, the D_2O soluble material revealed a rather larger singlet at the chemical shift where the methylene protons of glycine would appear in D_2O. The large peak in D_2O and the appearance of the 76 m/z in the MS spectrum, strongly indicated partial hydrolysis of the hydrophobic target compounds had taken place during the extraction and work up of the fractions for analysis. The comparison of the NMR intensities of the D_2O and following CD_3OD soluble material led to the conclusion that perhaps 95% of the glycine-lipid initially present in the hydrophobic extract had broken down by the time we reached the MS analysis. These pieces of information and the presence of the neutral loss of 98 in the 50eV CID in the surviving compound, matching phosphate very closely, led us to the hypothesis that glycine may be linked to the phosphate group, via a mixed anhydride linkage at the carboxyl end of glycine.

Although it was a possibility that these glycine-compounds could contain an ester linkage, water depth penetration studies have been done with phospholipids and determined that water does exist at the depths of the ester linkages in the head group (reference), which show long-term stability. This leads us to pursue the hypothesis that these compounds are mixed carboxy-phospho anhydrides. In order to better understand the fragility of acyl-phospho anhydrides and how to best stabilize them during the extraction and processing where it is in contact with water, the literature was searched back to the 1950s. It was found that at low and high pH levels the rate of hydrolysis of

acyl-phospho anhydrides increases rapidly but striking that virtually all pH buffers themselves strongly catalyze the hydrolysis rate. Sodium phenyl phosphate buffer was found to be the only buffer tested that did not increase the rate of hydrolysis of the acyl-phospho anhydride bonds as shown in Figure 3.10 (Di Sabato and Jencks, 1961). DiSabato and Jencks (1961) also found that trace transition metals also catalyzed the hydrolysis of the acyl-phospho anhydrides and that chelators such as EDTA may be useful for increasing the stability of the compounds of interest.

Our goal was to synthesize compounds that contain the same carboxy-phospho anhydride linkage we hypothesized would be in the glycine-lipid compounds and to follow them through the extraction processes, to determine at what stages they tend to fall apart, and how the conditions could be modified to increase their stability. Since the free amino group of glycine in the hypothesized anhydride linkage could participate in amino lysis with itself, we needed an N-protecting group on glycine.

An approach was chosen using N-Fmoc amino acids and dimethyl phosphate to synthesize N-Fmoc amino-acyl monomethyl phosphate anhydride compounds. The NMR and MS/MS showed successful synthesis. However, later realization led us to choose a different N-protecting group, since free amines in plasma can cleave the N-Fmoc group.

Another approach was chosen that used N-boc amino acids coupled with DCC to ethyl phosphate tetraethylammonium salt. ^{1}H-NMR and MS confirmed successful synthesis, but the tetraethylammonium counter ion turned out to be very MS unfriendly, saturating the detector, and leaving a very persistent residue in the MS. This was not an option that we could easily continue to use in further experiments.

So, yet another approach was taken. We thought to use the same DCC-coupling reaction as with the N-boc compounds but with a protecting group that we could following in HPLC that is fluorescent and UV active. Dansyl, which is commonly used in the analysis of amino acids by N-terminal labeling, can be used as a protecting group in the same DCC reaction. Thus we could still use the same approach to analyze the stability of the carboxy-phospho anhydrides during extraction, sample preparation and purification, but could use absorbance and/or fluorescence on HPLC instead of MS to follow the stability of the compounds of interest during the different steps of the procedure. The goal was to make Dansyl-glycyl, -leucyl, and –phenylalanyl to add during different steps of the extraction and sample processing procedure to determine where hydrolysis occurs and how changes in procedure may mitigate the loss/hydrolysis of the target glycine-lipid compounds.

The use of Dansyl-Cl with amino acids has been utilized for many years and there are a number of protocols that utilize this method. However, our initial synthesis was not a success so it was decided to obtain N-Dansyl glycine commercially. N-Dansyl glycine was reacted with Bis(tetraethylammonium) ethyl phosphate, however, the ^{31}PNMR did not indicate that the synthesis was a success, since the chemical shift indicated that starting material was the only compound present. This was surprising since the synthesis using the N-Boc protecting group showed the two peak ^{31}P-NMR indicating that the anhydride had been made, and synthesis of the N-dansyl glycine phospho anhydride should be pursued further in the future.

Another synthetic approach was used to determine if perhaps the compounds of interest could possibly be a mixed carboxy-carboxy anhydride. Since mixed acyl anhydrides and mixed acyl phosphate anhydrides are both quite unstable, it was decided to get more information on both species. N-Dansyl-glyine C16:0 anhydride was synthesized and MS revealed the compound was made successfully. The parent protonated mass had the typical sulfur isotope peak ratios present, and Dansyl possesses a sulfur atom. The MS/MS [in positive mode] revealed that cleavage primarily happened at the C-O bond of the palmitate group. This shows an important result that the free-glycine can be cleaved from the glycine-carboxy mixed anhydride. Recent analysis of the literature revealed a journal article by Murphy, R.C. and Axelsen, P.H., published in 2010, revealed an interesting fragmentation pathway in positive-ESI, resulting in a triple bonded oxygen that is positively charged. Figure 4.1 shows the fragmentation pathway substituting with the synthesized DNS-gly C16:0 Anhydride.

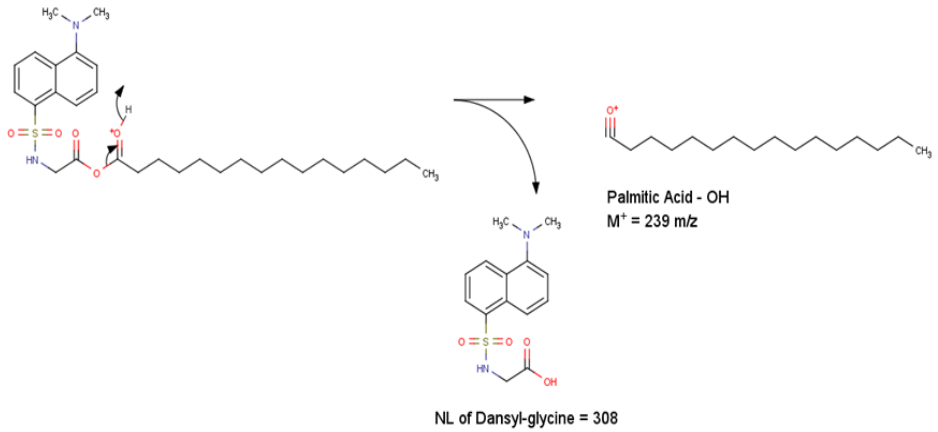

Figure 4.1: Possible fragmentation pathway of the DNS-gly C16:0 Anhydride. The pathway outlined in the referenced paper was substituted for the reactants used in this synthesis. Fragmentation yields C16:0 minus OH at 239 m/z and a NL of DNS-gly of 308. Both are seen in Figure 3.19. (Murphy and Axelsen, 2010)

A positive mass fragment in the bottom spectrum of Figure 3.19, corresponding to 239.2363 m/z, was found to have a good mass accuracy of 5 ppm. This highly suggests that this fragmentation pathway is occurring with this compound. The top spectrum of Figure 3.19 indicates that this compound can fragment to liberate a protonated glycine (in this case protonated DNS-gly) and the bottom inset shows that when fragmentation occurs, a NL of glycine (DNS-gly in this case) can occur. This relates back to the CID-MS/MS in Figure 3.3, where a NL of glycine is seen as well as protonated glycine. This is indicative of two ways that glycine can be fragmented from the same compound. This highly suggests that the unknown glycine-containing lipid of interest could be a mixed-acyl anhydride.

We have just recently discovered a journal article that reports the discovery of acyl-phospho anhydride phospholipids, containing phosphatidyl-aspartate and phosatidyl-glutamate as the head group. These were found in both rat and porcine brain. These appear to be the first identified amino-acyl phospho anhydride linkages in phospholipids. This shows that amino-acyl phospho anhydrides do exist in biology and may have important roles. (Omori, *et al.,* 2011)

CONCLUSION AND FUTURE WORK

In conclusion, the body of work described shows that novel glycine-containing lipids are strongly associated with T2D and much more needs to be explored to understand the structure and metabolism of these novel compounds. The lack of previous discovery is likely to be explained by the very fragile chemical linkage in the compounds of interest. We showed that conventional and rather mild extraction and sample preparation methods led to greater than 95% loss/hydrolysis of the compounds of interest. More work is needed to be done to stabilize the target compounds under extraction and sample work-up conditions in order to confirm that these compounds are of a mixed phospho-anhydride or mixed-acyl anhydride linkage and to determine which of the different hydrophobic compounds are present under different physiological states, as reflected in the different RP-HPLC retention times (Figure 1.18).

It would be of great benefit to obtain negative ionization mode MS and MS/MS of the unknown glycine-containing lipids, to see how the fragmentation occurs, as well as new insights into what possible functional groups could be present in the lipids. An attempt was madeobtain negative ionization-MS spectra when the 712 m/z was obtained in positive ionization mode, however, this was after the NMR spectra were were obtained. After the NMR spectra were obtained the rest of the intact compound perhaps had fully hydrolyzed. Negative ionization-MS and MS/MS will not only help lead to a better elucidation of the structure but should also help lead this research to understanding how this compound is involved in metabolism and what metabolic pathways are associated with it.

The protocol for making the N-dansyl-gly phospho anhydride compounds and with other amino acids needs to be fine-tuned in order to determine how to obtain successful synthesis of the compound. The most likely cause of unsuccessful synthesis could be water present in minute amounts that (in small amounts of starting material) would inhibit the reaction from taking place. Although the PhD thesis that this protocol was taken from stated that the reaction was completed at 1 hour and the mixing time for this reaction was about 1 hour, a longer mixing time may give more of an improvement. Synthesis of N-dansyl-leucine and N-dansyl-phenylalanine would be made following the same protocol as with the N-dansyl-glycine method once it is successful.

Once these compounds are made they can then be used as internal standards, (regardless if these are made as mixed acyl-phospho or mixed acyl anhydrides), that can be spiked into the plasma, the 2:1 DCM:MeOH extraction, and the various sample work up steps and the stability followed through each step. Adding in a known amount of fluorescent cis-Parinaric fatty acid internal standard, might be useful to determine the relative amounts of starting and ending amounts of the standard N-danyl-amino acids as well as the amounts of starting and ending amounts of glycine containing lipid. Pentadecanoic acid (C15:0) is commonly used as a standard for GCMS, however, cis-Parinaric acid is a fluorescent fatty acid that is commercially available and may be useful for recovery analysis during the workup procedures.

In order to be able to further elucidate the structure of this compound using NMR and MS, a much larger amount of material needs to be obtained. Thus, it will be important to scale up the plasma recovery and purify the material. However, it is very

important to treat the extract with special care, since the glycine containing lipids (as studied in this thesis) is clearly very fragile and easily hydrolysable. The time spent exposed to water needs to be minimized as much as possible. It is also very important to keep these compounds at a tightly buffered pH of 5 as much as possible by, using sodium phenyl phosphate in the extraction phase, adding EDTA to the water phases to chelate trace minerals, and to minimize the amount of water in the mobile phase of the RP-HPLC, and to keep all the subsequent fractions, that are obtained over time, dried frozen at in liquid nitrogen refrigerators at -196^{o}C, and minimum time exposed to room temperature. The N-dansyl amino-acyl phospho anhydrides and the N-dansyl amino-acyl-carboxy anhydride standard compounds will be very important to optimize the stability of the extraction and sample work up steps at a small scale before the large scale experiments are pursued. Each standard will be spiked into the extraction at different phases to test for stability and will be derivatized with PFB-Br to determine if the PFB-glycine (or PFB-amino acid) can be liberated.

We recently submitted an NIH R21 grant; if this gets funded we would work on the understanding the metabolism of these compounds. We would follow the changes in the metabolism of eight metabolically healthy volunteers, using oral stable isotope ^{13}C-glycine. This will be done by monitoring changes in the glycine-containing lipids during an oral glucose tolerance test (OGTT), as well as following the changes in the global metabolome by taking samples during the OGTT. We would also plan to follow the changes of these glycine-containing lipid compounds from eight volunteers who have been diagnosed with metabolic syndrome but have not yet been classified as having T2D.

As with the healthy volunteers, this will also be done by using the stable isotope ^{13}C-glycine during the OGTT. Again, by also following the changes in the full human plasma metabolome using global metabolomics by taking samples during the OGTT may reveal metabolic clues to the role of the glycine compounds on reducing insulin resistance.

By obtaining sufficient data, it is hoped that these results could then be validated by using a much larger cohort and be able to determine if these glycine-containing lipids can be used as early warning markers of the risk of developing IGT and T2D, and that simple dietary procedures could be developed to prevent and mitigate T2D.

REFERENCES CITED

Ahmed, M., Grapengiesser. E., Hellman, B. *Amino acid transformation of oscillatory Ca^{2+} signals in mouse pancraetic β-cells.* Journal of Endocrinology, 1999. **160**(2): p. 191-195.

American Diabetes Association, *Diabetes* Myths. http://www.diabetes.org/diabetes-basics/myths/.

American Diabetes Association, *Diagnosing Diabetes and Learning about Pre-diabetes.* http://www.diabetes.org/diabetes-basics/diagnosis/.

American Diabetes Association, *Statistics about diabetes*. http://www.diabetes.org/diabetes-basics/statistics/.

American Diabetes Association, *Type 2, http://www.diabetes.org/diabetes-basics/type-2/.*

American Heart Association, *About metabolic syndrome*. http://www.heart.org/HEARTORG/Conditions/More/MetabolicSyndrome/About-Metabolic-Syndrome_UCM_301920_Article.jsp.

Anguizola, J., Basiaga, S.B.G., Hage, D.S. *Effects of fatty acids and glycation on drug interactions with human serum albumin*. Current Metabolomics, 2013. **1**(3): p. 239-250.

Ansari, N.A., Dash, D. *Amadori glycated proteins : Role in production of autoantibodies in diabetes mellitus and effect of inhibitors on non-enzymatic glycation*. Aging and Disease, 2013. **4**(1): p. 50-56.

Ascenzi, P., *et al. Allosteric modulation of drug binding to human serum albumin*. Mini-Reviews in Medicinal Chemistry, 2006. **6**(4): p. 483-489.

Berger, S., Vongaray, N. *Insulin response to ingested protein in diabetes.* Diabetes, 1966. **15**(5): p. 303-306.

Boden, G., Laakso, M. *Lipids and glucose in type 2 diabetes*. Diabetes Care, 2004. **27**(9): p. 2253-2259.

Bowden, J. *Using chromatographic and mass spectrometry tools to probe albumin and its cargo: in search of understanding type 2 diabetes.* Montana State University, Bozeman, 2010. PhD Defense: p. 1-179.

Brunton, S.A. M.D. *The changing shape of type 2 diabetes*. The Medscape Journal of Medicine, 2008. **10**(6): p. 143.

Burns, T.W., Terry, B.E., Langley, P.E., Robison, G.A. *Insulin inhibition of lipolysis of human adipocytes*. Diabetes, 1979. **28**(11): p. 957-961.

Center for Disease Control, http://www.cdc.gov/diabetes/statistics/incidence/fig1.htm.

Choi, J. *et al. Interactions of very long-chain satruated fatty acids with serum albumin*. Journal of Lipid Research, 2002. **43**(7): p. 1000-1010.

Chuang, V.T.G., Otagiri, M. *How do fatty acids cause allosteric binding of drugs to human serum albumin?* Pharmaceutical Research, 2002. **19**(10): p. 1458-1464.

Dasarathy, S., *et al*., *Glycine and urea kinetics in nonalcoholic steatohepatitis in human: effect of intralipid infusion.* American Journal of Physiology Gastrointestinal and Liver Physiology, 2009. **297**(3): p. G567-G575.

Day, J.F., Thorpe, S.R., Baynes, J.W., *Nonenzymatically glucosylated albumin*. The Journal of Biological Chemistry, 1979. **254**(3): p. 595-597.

De Bowr, S.Y. *et al*. *Effect of intravenous glucose on intravenous amino acid-induced gallbladder contraction and CCK secretion*. Digestive Diseases and Sciences, 1994. **39**(2): p 268-274.

DeFronzo, R.A. *Dysfunctional fat cells, lipotoxicity, and type 2 diabetes*. International Journal of Clinical Practice, 2004. **58**(s143): p. 9-21.

Di Sabato, G, Jencks, W.P., *Mechanism and catalysis of reactions of acyl phosphates. 2. Hydrolysis*. Journal of American Chemical Society, 1961. **83**(21): p. 4400-4405.

Dockal, M., Chang, M., Carter, D.C., Ruker, F. *Five recombinant fragments of human serum albumin-Tools for the characterization of the warfarin binding site*. Protein Science, 2000. **9**(8): p. 1455-1465.

Donnelly, K.L. *et al. Sources of fatty acids stored in liver and secreted via lipoporoteins in patients with nonalcoholic fatty liver disease*. The Journal of Clinical Investigation, 2005. **115**(5): p. 1343-1351.

Fasano, M. *et al. The extraordinary ligand binding properties of human serum albumin.* Life, 2005. **57**(12): p. 787-796.

Fernàndez-Real, J.M., Lopez-Bermejo, A.L., Ricart, W. *Cross-talk between iron metabolism and diabetes.* Diabetes, 2002. **51**(8):p. 2348-2354.

Folch, J., Lee, M., Stanley, G.S. A simple method for the isolation and purification of total lipids from animal tissues. Journal of Biological Chemistry. 1957. **226**(1): p. 497-509.

Fujiwara, S., Amisaki, T. *Steric and allosteric effects of fatty acids on the binding of warfarin to human serum albumin revealed by molecular dynamics and free energy calculations*. Chemical and Pharmaceutical Bulletin, 2011. **59**(7): p 860-867.

Gall, W. E. *et al*. *α-Hydroxybutyrate is an early biomarker of insulin resistance and glucose intolerance in a nondiabetic population.* PLoS ONE, 2010. **5**(5): p. 1-10.

Gameiro, A., *et al*. *The neurotransmitters glycine and GABA stimulate glucagon-like peptide-1 release from the GLUTag cell line.* Journal of Physiology, 2005. **569**(3): p. 761-772.

Gannon, M.C., Nuttall, J.A., Nuttall, F.Q. *The metabolic response to ingested glycine.* American Journal of Clinical Nutrition, 2002. **76**(6): p. 1302-1307.

Glatt, H. *Sulfotransferases in the bioactivation of xenobiotics*. Chemico-Biological Interactions, 2000. **129**(1-2): p. 141-170.

Goldin, A. *et al. Advanced glycation end products: Sparking the development of diabetic vascular injury.* American Heart Association, 2006. **114**(6): p. 597-605.

Gonzàlez-Ortiz, M., Medina-Santillàn, R., Martínez-Abundis, E., Reynoso von Drateln, C. *Effect of glycine on insulin secretion and action in healthy first-degree relatives of type 2 diabetes mellitus patients.* Hormone and Metabolic Research, 2001. **33**(6): p. 358-360.

Harris, E.L. *Identification of N-terminal amino acids by high-performance liquid chromatography.* Methods in Molecular Biology, 1988. **3**: 49-55.

Heianza, Y. *et al. Screening for pre-diabetes to predict future diabetes using various cut-off points for HbA1c and impaired fasting glucose: the Toranomon Hospital Health Management Center Study 4 (TOPICS 4)*. Diabetic Medicine, 2012. **29**(9): p. e279-e285.

Hirsh, J., Fuster, V., Ansell, J. Halperin, J.L. *American heart association college of cardiology – Foundation guide to warfarin therapy.* Journal of the American College of Cardiology, 2003. **41**(9): p. 1633-1652.

Ikeda, Y. et al. *Identification of N-arachidonylglycine, U18666A, and 4-androstene-3,17-dione as novel insulin secretagogues.* Biochemical and Biophysical Research Communications, 2005. **333**(3): p. 778-786.

Jancova, P., Anzenbacker, P., Anzenbacherova, E. *Phase II drub metabolizing enzymes.* Biomedical Papers-Olomouc, 2010. **154**(2): p. 103-116.

Keller, W. *M. Keller on the conversion of benzoic acid to hippuric acid.* Provincial medical journal and retrospect of the medical sciences, 1842. **4**(92): p. 256-257.

Kendall, F.E. *Studies of human serum proteins II. Crystallization of human serum albumin*. The Journal of Biological Chemistry, 1941. **138**: p. 97-109.

Kikuchi, G. *The glycine cleavage system: Composition, reaction mechanism, and physiological significance.* Molecular and Cellular Biochemistry, 1973. **1**(2): p. 169-187.

Kluger, R., Grant, A.S., Bearne, S.L., Trachsel, M.R. *Dicarboxylic Acid Bis(methyl phosphates): Anionic biomimetic cross-linking reagents*. Journal of Organic Chemistry, 1990. ***55***(9): p. 2864-2868.

Kluger, R., Xianfeng Li, X., Loo, R. *1996 Bader award lecture aminoacyl ethyl phosphates. Biomimetically activated amino acids*. Canadian Journal of Chemistry, 1996. **74**(12): p. 2395-2400.

Kluger, R., Cameron, Cameron, L.L. *Activation of acyl phosphate monoesters by lanthanide ions: Enhanced reactivity of benzoyl methyl phosphate.* Journal of the American Chemical Society, 2002. **124**(13): p. 3303-3308.

Lamers, Y**.** *et al. Moderate dietary vitamin B-6 restriction raises plasma glycine and cystathionine concentrations while minimally affecting the rates of glycine turnover and glycine cleavage in healthy men and women***.** The Journal of Nutrition, 2009. **139**(3): p. 452-460.

Liska, D.J., *The detoxification enzyme systems*. Alternative Medicine Review, 1998. **3**(3): p. 187-198.

Lu, J. *et al. Albumin as a zinc carrier: properties of its high-affinity zinc-binding site.* Biochemical Society Transactions, 2008. **36**(6): p. 1317-1321.

Luevano-Contreras, C., Chapman-Novakofski, K. *Dietary Advanced Glycation End Products and Aging*. Nutrients, 2010. **2**(12): p. 1247-1256.

MacDonald, P.E., Willard, M.B. *Voltage-dependent K^+ channels in pancreatic beta cells: Role, regulation, and potential as therapeutic targets*. Diabetologia, 2003. **46**(8): p. 1046-1062.

Mandula, H., Parepally, J.M.R., Feng, R., Smith, Q.R., *Role of site-specific binding to plasma albumin in drug availability to brain.* Journal of Pharmacology and Experimental Therapeutics, 2006. **17**(2): p. 667-675.

Metlin: Metabolite and Tandem MS Database. http://metlin.scripps.edu/index.php

Murphy, R.C., Axelsen, P.H. *Mass spectrometric analysis of long-chain lipids.* Mass Spectrometry Reviews, 2010. **30**(4): p. 579-599.

Nathan, D.B. *et al*. *Impaired fasting glucose and impaired glucose tolerance*. Diabetes Care, 2007. **30**(3): p. 753-759.

Neish, A.S. *Microbes in gastrointestinal health and disease*. Gastroenterology, 2009. **136**(1): p. 65-80.

Newgard, C.B., *et al*. *A branched-chain amino acid-related metabolic signature that differentiates obese and lean humans and contributes to insulin resistance.* Cell Metabolism, 2009. **9**(4): p. 311-326.

Newgard, C.B. *Interplay between Lipids and Branched-Chain Amino Acids in Development of Insulin Resistance*. Cell Metabolism, 2012. **15**(5): p. 606-614.

Newsholme, P., Brennan, L., Bender, K. *Amino acid metabolism, B-cell function, and Diabetes.* Diabetes, 2006. **55**(2): p. S39-S47.

Nuttall, F.Q. *et al. Effect of protein ingestion on the glucose and insulin response to a standardized oral glucose load*, 1984. **7**(5): p. 465-470.

Okada. M., *et al*. *Effects of vitamin B-6 nutrition and diabetes on vitamin B-6 metabolism*. Nutritional Biochemistry, 1997. **8**(1): p. 44-48.

Omori, T. *et al*. *Identification of novel mammalian phospholipids containing threonine, aspartate, and glutamate as the base moiety*. Journal of Chromatography B-analytical Technologies in the Biomedical and Life Sciences, 2011. **879**(29): p. 3296-3302.

Pawloxky, R.J., Sprecher, H.W., Salem. N. *High sensitivity negative-ion GC-MS method for detection of desaturated and chain-elongated products of deuterated linoleic and linolenic acids.* Journal of Lipid Research, 1992. **33**(11): p. 1711-1717.

Perry, C. *et al. Effect of vitamin B6 availability on serine hydroxymethyltransferase in MCF-7 cells.* Archives of Biochemistry and Biophysics, 2007. **462**(1): p. 21-27.

Phillips, J.D., Kushner, J.P. *Fast track to the porphyrias.* Nature Medicine, 2005. **11**(10): p. 1049-1050.

Quinlan, G.J., Martin, G.S., Evans, T.W. *Albumin: Biochemcial properties and therapeutic potential*. Hepatology, 2005. **41**(6): p. 1211-1219.

Raal, F.J. *Pathogenesis and management of the dyslipidemia of the metabolic syndrome.* Metabolic Syndrome and Related Disorders, 2009. **7**(2): p. 83-88.

Reichling, D.B., Kyrozis, A., Wang, J., MacDermott, A.B. *Mechanisms of GABA and glycine depolarization-induced calcium transients in rat dorsal horn neurons.* Journal of Physiology, 1994. **476**(3): p. 411-421.

Rimmerman, N. *et al*. *N-Palmitoyl glycine, a novel endogenous lipid that acts as a modulator of calcium influx and nitric oxide production in sensory neurons.* Molecular Pharmacology, 2008. **74**(1): p. 213-224.

Roberts, L.D., Koulman, A., Griffin, J.L. *Towards metabolic biomarkers of insulin resistance and type 2 diabetes: progress from the metabolome.* Lancet Diabetes Endocrinology, 2014. **2**(1): p. 65-75.

Rudman, D., Bixler, T.J., Delrio, A.E. *Effect of free fatty acids on binding of drugs by bovine serum albumin, by human serum albumin and by rabbit serum.* Journal of Phamracology and Experimental Therapeutics, 1971. **176**(2): p. 261-272.

Sadler, P.J., Viles, J.H. *H-1 and Cd-113 NMR investigations of Cd2+ and Zn2+ binding sites on serum albumin: Competition with Ca2+, Ni2+, Cu2+, and Zn2+*. Inorganic Chemistry, 1996. **35**(15): p. 4490-4496.

Sekhar, R.V. *et al. Glutathione synthesis is diminished in patients with uncontrolled diabetes and restored by dietary supplementation with cysteine and glycine.* Diabetes Care, 2011. **34**(1): p. 162-167.

Selinger, Z., Lapidot, Y. *Synthesis of fatty acid anhydrides by reaction with dicyclohexylcarbodiimide*. Journal of Lipid Research, 1996. **7**(1): p. 174-175.

Sharifi, F., Nasab, N.M., Zadeh, H.J. *Elevated serum ferritin concentrations in prediabetic subjects.* Diabetes and Vascular Disease Research, 2008. **5**(1): p. 15-18

Simon, S.A., McIntosh, T.J. *Depth of water penetration into lipid bilayers.* Methods Enzymology, 1986. **127**: 511-521.

Song, F., Schmidt, A.M., *Glycation and insulin resistance: Novel mechanisms and unique targets.* Journal of the American Heart Association, 2012. **32**(8): p. 1760-1765.

Solerte, S.B. *et al. Metabolic effects of orally administered amino acid mixture in elderly subjects with poorly controlled type 2 diabetes mellitus.* American Journal of Cardiology, 2004. **93**(8A): p. 23A-29A.

Solerte, S.B. *et al. Improvement of blood glucose control and insulin sensitivity during a long-term (60 weeks) randomized study with amino acid dietary supplements in elderly subjects with type 2 diabetes mellitus*. American Journal of Cardiology, 2008. **101**(11A): p. 82E-88E.

Sparks, J.D., Sparks, C.E. *Insulin regulation of tri-acyl glycerol-rich lipoprotein synthesis and secretion*. Biochimica et Biophysica acta, 1994. **1215**(1-2): p. 9-32.

Spector, A.A. *Fatty acid binding to plasma albumin*. Journal of Lipid Research, 1975. **16**(3): p. 165-179.

Stec, D.E., Hosick, P.A., Granger, J.P. *Bilirubin, renal hemodynamics, and blood pressure*. Frontiers in Pharmacology, 2012. **3**: p. 1-7.

Sugio, S., *et al. Crystal structure of human serum albumin at 2.5 angstrom resolution*. Protein Engineering, 1999. **12**(6): p. 439-446.

Sudlow, G., Birkett, D.J., Wade, D.N. *The characterization of two specific drug binding sites on human serum albumin*. Molecular Pharmacology, 1975. **11**(6): p. 824-832.

Sudlow, G., Birkett, D.J., Wade, D.N. *Further characterization of specific drug binding sites on human serum albumin*. Molecular Pharmacology, 1976. **12**(6): p. 1052-1061.

Thiessen, H., Jacobsen, J., Brodersen, R. *Displacement of albumin-bound bilirubin by fatty acids.* Acta Paediatrica, 2008. **61**(3): p. 285-288.

Tripathi, A.S., Mazumder, P.M., Chandewar, A.V., *Changes in the pharmacokinetic of sildenafil citrate in rats with Streptozotocin-induced diabetic nephropathy*. Journal of Diabetes and Metabolic Disorders, 2014. **13**(18): p. 1-4.

Tzvetkova, S.K. *Biomimetic Aminoacylation.University of Toronto*, Toronto, 2008. PhD Defense: p. 1-104.

Van Kuijk, F.J.G.M., Thomas, D.W., Stephens, R.J., Dratz, E.A. *Gas chromatography-mass spectrometry method for determination of phospholipid peroxides II. Transesterification to form pentafluorobenzyl esters and detection with pictogram sensitivity*. Journal of free radicals in biology & medicine, 1985 **1**(5-6): p. 387.

Van Kuijk, F.J.G.M., Thomas, D.W., Konopelski, J.P., and Dratz, E.A. *Transesterification of phospholipids or triglycerides to fatty acid benzyl esters with simultaneous methylation of free fatty acids for gas-liquid chromatographic analysis*. Journal of Lipid Research, 1986. **27**(4): p. 452-456.

Van Loon, L.J.C., *et al*. *Amino acid ingestion strongly enhances insulin secretion in patients with long-term type 2 diabetes.* Diabetes Care, 2003. **26**(3): p. 625-630.

Waluk, D.P., Schultz, N., Hunt, M.C. *Identification of glycine N-acyltransferase-like 2 (GLYATL2) as a transferase that produces N-acyl glycines in humans.* FASEB Journal, 2010. **24**(8): p. 2795-2803.

Wang, T.J. *et al. 2-aminoadipic acid is a biomarker for diabetes risk*. Journal of Clinical Investigation, 2013a. **123**(10): p. 4309-4317.

Wang, W, Wu, Z, Dai, Z, et al, *Glycine metabolism in animals and humans: implications for nutrition and health*. Amino Acids, 2013b. **45**(3): p. 463-477.

Wang-Sattler, R. *et al*. *Novel biomarkers for pre-diabetes identified by metabolomics.* Molecular Systems Biology, 2012. **8**(615): p. 1-11.

Weir, G.C., Bonner-Weir, S. *Five states of evolving beta-cell dysfunction during progression to diabetes.* Diabetes, 2004. **53**(3): p. S16-S21.

Weisiner, R.A., *et al. Affinity of human serum albumin for bilirubin varies with albumin concentration and buffer composition - Results of a novel ultrafiltration method.* Journal of Biological Chemistry, 2001. **276**(32): p. 29953-2960.

Wikoff, W. R. *et al*. *Metabolomics analysis reveals large effects of gut microflora on mammalian blood metabolites.* Proceedings of the National Academy of Sciences of the United States of America, 2009. **106**(10): p. 3698-3703.

Wright, E., Scism-Bacon, J.L., Glass, L.C. *Oxidative stress in type 2 diabetes: the role of fasting and postprandial glycaemia.* International Journal of Clinical Practice, 2006. **60**(3): p. 308-314.

Xie, W. *et al. Genetic variants associated with glycine metabolism and their role in insulin sensitivity and type 2 diabetes.* Diabetes, 2013. **62**(6): p. 2141-2150.

Zervas, L., Dilaris, I. *Dealkylation and debenzylation of triesters of phosphoric acid-phosphorylation of hydroxyl and amino compounds*. Journal of the American Chemical Society, 1955. **77**(20): p. 5354-5357.